

The Zenith Program

Critical Design Review

FAMU-FSU College of Engineering

2525 Pottsdamer Street

Tallahassee, FL 32310

01/09/2023

Table of Contents

LIST OF TABLES	4
LIST OF FIGURES.....	5
1 SUMMARY	7
1.1 TEAM SUMMARY.....	7
1.1.1 Team Information	7
1.1.2 Mentor Information	7
1.1.3 Huntsville Travel Plans	8
1.1.4 CDR Completion Time	8
1.2 LAUNCH VEHICLE SUMMARY	8
1.2.1 Target Altitude	8
1.2.2 Final Motor Selection	8
1.2.3 Vehicle Sections	8
1.2.4 Vehicle Mass	8
1.2.5 Recovery System	9
1.2.6 Rail Size	9
1.3 PAYLOAD SUMMARY	9
2 MODIFICATIONS TO PROPOSAL	10
2.1 MODIFIED VEHICLE CRITERIA	10
2.2 CHANGES MADE TO PAYLOAD CRITERIA	11
2.3 CHANGES MADE TO PROJECT PLAN	11
3 VEHICLE CRITERIA	12
3.1 DESIGN AND VERIFICATION OF LAUNCH VEHICLE	12
3.1.1 Launch Vehicle Mission Statement	12
3.1.2 Launch Vehicle Success Criteria	12
3.1.3 Final Vehicle Design	13
3.1.4 Manufacturing and Assembly	44
3.1.5 Finite Element Analysis	62
3.1.6 Vehicle Weight Breakdown	66
3.1.7 Final Motor Choice	66
3.2 SUBSCALE CONSTRUCTION METHODS.....	68
3.3 SUBSCALE FLIGHT RESULTS.....	72
3.3.1 Flight Simulations and Prediction	72
3.3.2 Recovered Configuration	73
3.3.3 Flight Data and Timeline.....	74
3.3.4 Scaling Factors and Influence on Full-Scale Design.....	81
3.4 RECOVERY SYSTEM	82
3.4.1 Recovery System Summary	82
3.5 MISSION PERFORMANCE PREDICTIONS	83
3.5.1 Target Altitude	83
3.5.2 Updated Flight Profile	83

3.5.3	<i>Apogee Calculations</i>	84
3.5.4	<i>Stability Margin Calculations</i>	86
3.5.5	<i>Landing Kinetic Energy Calculations</i>	91
3.5.6	<i>Descent Time and Drift Calculations</i>	92
3.5.7	<i>Parachute Opening Shock Calculations</i>	93
4	PAYLOAD CRITERIA	94
4.1	PAYLOAD MISSION STATEMENT	94
4.2	PAYLOAD SUCCESS CRITERIA.....	94
4.3	PAYLOAD SYSTEM SUMMARY.....	94
4.3.1	<i>Component Integration</i>	96
4.3.2	<i>Vehicle integration</i>	103
5	SAFETY	104
5.1	VEHICLE ASSEMBLY AND OPERATION CHECKLISTS	104
5.1.1	<i>Vehicle Assembly Checklist</i>	105
5.1.2	<i>Pre-flight Checklist</i>	109
5.1.3	<i>Terminal Count and In-Flight Checklist</i>	110
5.1.4	<i>Post-Flight Checklist</i>	112
5.1.5	<i>Verify Notice Justifications</i>	113
5.2	HAZARD ANALYSIS.....	115
5.2.1	<i>Risk Matrix and Definitions</i>	115
5.2.2	<i>Vehicle Systems Failure Mode and Effects Analysis</i>	117
5.2.3	<i>Personnel Risk Assessment</i>	137
5.3	VERIFICATION STRATEGIES FOR PROPOSED MITIGATIONS	140
6	PROJECT PLAN	149
6.1	TESTING	149
6.2	REQUIREMENTS VERIFICATION	151
6.2.1	<i>Team Derived Requirements</i>	151
6.3	BUDGETING AND TIMELINE.....	155
6.3.1	<i>Budget</i>	155
6.3.2	<i>Funding and Material Acquisition</i>	155
6.3.3	<i>Project Timeline</i>	157
	APPENDIX A. REVISED BUDGET	A-1
	APPENDIX B. GANTT CHART	B-1
	APPENDIX C. STABILITY AND FLUTTER SPEED MATLAB CODE	C-1
	APPENDIX D. APOGEE CALCULATION MATLAB CODE	D-1
	APPENDIX E. RAFCO MISSION PRELIMINARY ARDUINO CODE	E-1

List of Tables

Table 1-1. Aerotech L850W Specifications	8
Table 1-2. Vehicle Masses.....	8
Table 1-3. Recovery System Components.....	9
Table 2-1. Vehicle Modifications.....	10
Table 2-2. Payload Modifications.....	11
Table 2-3. Project Modifications.....	11
Table 3-1. Fin Flutter Speed Parameters.....	37
Table 3-2. Fin Flutter Speed Results.....	37
Table 3-3. Vehicle Section Weights.....	66
Table 3-4. Sub-scale Flight Metrics	74
Table 3-5. Sub-scale Flight Error Analysis	74
Table 3-6. Event Outcomes.....	75
Table 3-7. Sub-scale Flight Timeline.....	75
Table 3-8. Sub-scale Vehicle Scaling Factors	81
Table 3-9. Nominal Flight Profile (No Wind, 5° Launch Angle).....	84
Table 3-10. Wind Speed vs. Stability for 5° Launch Angle.....	88
Table 3-11. Stability Parameters.....	90
Table 3-12. Stability Results	91
Table 3-13: Maximum Descent Velocity	91
Table 3-14. Descent Time and Drift	92
Table 3-15. Maximum Kinetic Energy	92
Table 3-16. Main Parachute Opening Shock	93
Table 5-1. Safety Verification(s) Rationale.....	113
Table 5-2. Risk Classification Matrix	115
Table 5-3. Severity Classification Definitions	116
Table 5-4. Likelihood Classification Definitions.....	116
Table 5-5. Avionics and Power Systems FMEA.....	117
Table 5-6. Avionics and Power Systems Risk Matrix	120
Table 5-7. Energetics and Pyrotechnics FMEA	121
Table 5-8. Energetics and Pyrotechnics Risk Matrix.....	125
Table 5-9. Recovery System FMEA.....	126
Table 5-10. Recovery System Risk Matrix	127
Table 5-11. Vehicle Structures FMEA.....	128
Table 5-12. Vehicle Structures Risk Matrix	130
Table 5-13. Payload FMEA	131
Table 5-14. Payload Risk Matrix.....	133
Table 5-15. Environment FMEA	134
Table 5-16. Environmental Risk Matrix.....	136
Table 5-17. Personnel FMEA.....	137
Table 5-18. Personnel Risk Matrix	139
Table 5-19. Risks, Mitigations, and Verifications	140
Table 6-1. Vehicle Component and Assembly Tests	149
Table 6-2: Safety Team Derived Verification Matrix	151
Table 6-3: Launch Vehicle Team Derived Verification Matrix	152
Table 6-4. Recovery Team Derived Requirements.....	153
Table 6-5. Payload Team-Derived Requirements.....	154
Table 6-6. Project Budget Summary	155
Table 6-7. Project Timeline Summary Sub-Scale through FRR.....	157

List of Figures

Figure 3-1. Launch Vehicle Assembly	13
Figure 3-2. Launch Vehicle Exploded/Transparent Assembly	13
Figure 3-3. Launch Vehicle Transparent Assembly	14
Figure 3-4. LD-Haack Series Nosecone Assembly	14
Figure 3-5. LD-Haack Nosecone Assembly CAD Drawing	15
Figure 3-6. Nosecone Shoulder CAD Drawing	16
Figure 3-7. Nosecone Lower Profile CAD Drawing	17
Figure 3-8. Nosecone Upper Profile CAD Drawing	18
Figure 3-9. Upper Payload Bay Assembly	19
Figure 3-10. Upper Payload Bay Assembly CAD Drawing	19
Figure 3-11. Upper Payload Bay Airframe CAD Drawing	20
Figure 3-12. Nosecone Bulkhead Assembly	21
Figure 3-13. Nosecone Bulkhead CAD Drawing	22
Figure 3-14. U-Bolt CAD Drawing	23
Figure 3-15. AV Bay Transparent Assembly	24
Figure 3-16. AV Bay Solid CAD Drawing	24
Figure 3-17. AV Bay Exploded Assembly	25
Figure 3-18. AV Bay CAD Drawing	26
Figure 3-19. AV Bay Outer Bulkhead CAD Drawing	27
Figure 3-20. AV Bay Inner Bulkhead CAD Drawing	28
Figure 3-21. Lower Payload Bay/Fin Can Transparent Assembly	29
Figure 3-22. Lower Payload Bay Airframe CAD Drawing	30
Figure 3-23. Lower Payload Bay Airframe w/ 1515 Rail Buttonhole	31
Figure 3-24. Labeled Fin Can Assembly	32
Figure 3-25. Lower Payload Bay/Fin Can Solid Assembly	33
Figure 3-26. Fin Can Assembly	34
Figure 3-27. Canted Clipped Delta Fin CAD Drawing Sheet 1 of 2	35
Figure 3-28. Canted Clipped Delta Fin CAD Drawing Sheet 2 of 2	36
Figure 3-29. Fin Can Assembly CAD Drawing 2	38
Figure 3-30. Forward Centering Ring CAD Drawing	39
Figure 3-31. Forward Fin Centering Ring CAD Drawing	40
Figure 3-32. Aft Fin Centering Ring CAD Drawing	41
Figure 3-33. Fin Can Assembly w/ Transparent Tail Cone	42
Figure 3-34. Tail Cone CAD Model	43
Figure 3-35. Tail Cone CAD Drawing	44
Figure 3-36. ABS Strength Characteristics	45
Figure 3-37. Subscale Launch Vehicle Nosecone	46
Figure 3-38. Subscale Launch Vehicle 3-D Printed LD-Haack Nosecone	47
Figure 3-39. Subscale Nosecone Assembly	48
Figure 3-40. Subscale Nosecone Shoulder	49
Figure 3-41. Full Scale Nosecone Cap	50
Figure 3-42. Full Scale Nosecone Midsection	51
Figure 3-43. Full Scale Nosecone Shoulder	52
Figure 3-44. 3-D Printed Subscale Fin	54
Figure 3-45. Subscale Fins Installed	55
Figure 3-46. Subscale Fin	56
Figure 3-47. Full Scale Fin	57
Figure 3-48. Integrated Thrust Plate and Tail Cone	59
Figure 3-49. Forward Bulkhead FEA	63
Figure 3-50. Avionics Bulkhead FEA	64
Figure 3-51. Integrated Thrust Plate & Tail Cone FEA	65

Figure 3-52. Fin Slots.....	68
Figure 3-53. Fin on 3D Print Bed	68
Figure 3-54. Avionics Sled	69
Figure 3-55. Avionics Bulkheads, Rods, and Ejection Charges	69
Figure 3-56. Ejection Test	70
Figure 3-57. Vehicle in Paint Process	70
Figure 3-58. The Zenith 0.5	71
Figure 3-59. Team Prepping Ejection Charges on Sub-scale Launch Day	71
Figure 3-60. Sub-scale OpenRocket Design.....	72
Figure 3-61. Sub-Scale Recovered Configuration	73
Figure 3-62. Detailed Section Views - Recovered Configuration.....	73
Figure 3-63. Altitude vs. Flight Time Plot	77
Figure 3-64. Event View, Altitude Plot	78
Figure 3-65. Velocity vs. Flight Time	79
Figure 3-66. Event View, Velocity Plot	80
Figure 3-67. CO2 Ejection Charge (Red) to Bulkhead Interface	82
Figure 3-68. Updated Flight Profile – 0 mph Winds	83
Figure 3-69. Stability vs. Flight Time	87
Figure 4-1. Payload design	95
Figure 4-2. Payload Internal View	95
Figure 4-3. Payload Internal Hardware	96
Figure 4-4. Payload Housing Drawing	97
Figure 4-5. Payload Housing Drawing Continued.....	98
Figure 4-6. Arduino/Motor Housing Drawing	99
Figure 4-9 Arduino/Motor Housing Drawing (Continued)	100
Figure 4-10 Camera Housing Drawing.....	101
Figure 4-11 Camera Housing Drawing (Continued).....	102
Figure 4-12. Lexan Camera Enclosure	103
Figure 6-1. Expenditure by Flight Milestone	156

1 Summary

1.1 Team Summary

1.1.1 Team Information

1.1.1.1 Team Name

This team has dedicated itself to laying the groundwork for continued yearly participation in NASA Student Launch and expansion into experimental liquid-fueled engine development by the parent AIAA chapter. To that end, the team has deemed itself the first year of FAMU-FSU AIAA's rocket development program, called the Zenith Program.

1.1.1.1 Mailing Address

Mail to:

FAMU-FSU AIAA
2525 Pottsdamer Street, Suite B111
Tallahassee, FL 32310

1.1.2 Mentor Information

1.1.2.1 Mr. Tom McKeown

- **Title:** Board Member, Spaceport Rocketry Association (NAR #342 / TRA #73)
- **Email:** mckeownt@ix.netcom.com
- **Phone:** 321-266-1928
- **NAR Flyer Number:** 57205
- **TRA Flyer Number:** 01922
- **NAR/TRA Certification Level:** Level 2

1.1.3 Huntsville Travel Plans

The team intends to attend launch week at NASA MSFC in Huntsville.

1.1.4 CDR Completion Time

The team spent approximately 200 hours working on the CDR document.

1.2 Launch Vehicle Summary

1.2.1 Target Altitude

The target altitude for the Zenith 1 is 4600 ft AGL.

1.2.2 Final Motor Selection

The final motor selected is the Aerotech L850W.

Table 1-1. Aerotech L850W Specifications

Motor Parameter	Value
Average Thrust	850 N
Initial Thrust	1,001 N
Maximum Thrust	1,866 N
Total Impulse	3,646 N-s
Burn Time	4.4 seconds

1.2.3 Vehicle Sections

The flight vehicle design is 99 inches in length with a body tube diameter of 6.18 inches and a total weight of 38.6 lbs. The static stability margin of the vehicle is 3.43 calibers and the max velocity the vehicle reaches is 545 ft/s. Section 3.1 expands further into the design of the vehicle, its subsections, and their weight distribution.

1.2.4 Vehicle Mass

Table 1-2. Vehicle Masses

Vehicle State	Mass (lbm)	Mass (g)
Dry Mass	33.671	15273
Wet Mass	38.625	17520

1.2.5 Recovery System

The recovery system consists of the TeleMega v4 dual-deployment flight computer which is capable of recording altimeter, GPS, and telemetry data. At apogee, a 24" high strength elliptical parachute will deploy. At around 550 feet above ground an 84" Iris Ultra elliptical main parachute will deploy. Ejection charges used are CO2 driven to avoid damaging the parachutes with hot gas produced by traditional black powder charges. The recovery system and all its relevant components are discussed further in Section 3.4.

Table 1-3. Recovery System Components

Component	Part Selected
Primary Flight Computer	TeleMega V4.0
Backup Altimeter	AIM4 USB
GPS Tracker/Locator 1	TeleMega V4.0
GPS Tracker/Locator 2	Apple AirTag
Ejection Charges	Tinder Rocketry Raptor CO2 Ejection Charge
Drogue Parachute	Fruity Chutes Classic Elliptical 24"
Main Parachute	Fruity Chutes Iris Ultra Standard 84"

1.2.6 Rail Size

The launch vehicle will utilize 1515 rails.

1.3 Payload Summary

The payload design has been greatly simplified since PDR to allow for more emphasis on the actual scored portion of the payload competition. Rather than deploying a mobile rover, the team has opted to create a static 3D printed camera housing, which will contain an Arduino Mega microcontroller, ArduCam mini camera, and stepper motor to drive the rotation of the camera. The camera housing has been designed as a pyramid, with a wide flat base to prevent tipping or rolling as it sets down on the ground under parachute. The microcontroller and camera are mounted to a 3D printed turret, driven by the stepper motor, with the camera protruding from the top of the pyramid into a protective plexiglass case.

2 Modifications to Proposal

2.1 Modified vehicle criteria

Table 2-1. Vehicle Modifications

Description of Change	Reason for the Change
LEXAN nose cone camera housing removed. Nose cone will now be a completely ABS.	Reduce manufacturing/assembly complexity and prevent adhesive connection points between dislike materials
Nose cone bulkhead and shoulder now fixed in place and non-removable after epoxying.	No need for nose cone entry point due to determination of camera and camera housing.
Forged eye bolt connection to motor case in substitution of U-bolt/bulkhead configuration above the motor.	Decreases weight, increases lower payload bay cabin space, and shaves a few steps off of assembly process.
Centering rings cut to hold fin tabs.	Prevents fin tab connection via threaded rods and decreases compression acting on threaded rods.
Threaded rods shortened to run from aft end of vehicle to forward fin-cut centering ring.	Decreases compression on rods, decreases overall vehicle weight, and improves ease of assembly/disassembly.
Forward fin-cut centering ring epoxied into airframe while after centering ring is held in place via threaded rods.	Optimizes thrust distribution to airframe while maintaining modularity in removability of the aft centering ring.
Thrust Plate and Tail Cone will be printed as one component and held in via threaded rods.	Reduces weight, allows personal modifications, shortens build time, and allows motor retainer to be completely removed.

2.2 Changes made to payload criteria

Table 2-2. Payload Modifications

Description of Change	Reason for the Change
FULL REDESIGN: Rover concept replaced with static pyramid housing camera system	Reduce complexity. Focus solely on the assembly of the camera turret and coding of the microcontroller to receive and execute command string. Allow 2023/24 team to improve payload with knowledge gained.
Lens on ArduCam switched for fisheye wide angle	Initial lens did not meet NASA FOV requirement

2.3 Changes made to project plan

Table 2-3. Project Modifications

Description of Change	Reason for the Change
STEM Engagement delayed. Planning begins in January. Execution in February	More difficulty in finding points of contact and planning events than was initially anticipated
Full-scale manufacturing brought forward into early January	Parts list by vendor created and waiting for submission to ME department. Can begin ordering/building early for a test flight in early/mid-February. Gives margin for re-flight if any off-nominal event occurs
Payload manufacturing brought forward into early January	Payload requires more time for code debugging. Need to test receiving, decoding, executing commands over VHF. 3D print times for housing are longer than expected
Full-scale test flight brought forward into mid-February	Sub-scale flight had little to no margin for re-flight. Want 100% nominal full-scale so early first flight and backup dates are scheduled.

3 Vehicle Criteria

3.1 Design and Verification of Launch Vehicle

3.1.1 Launch Vehicle Mission Statement

The mission of the Zenith Program's launch vehicle, the Zenith 1, is to reach within 5% margin of error of the targeted 4600 ft AGL apogee, safely recover the vehicle, and deploy a payload with a nominal dual deployment recovery while employing a modular and highly reusable design for future iteration and re-flight.

3.1.2 Launch Vehicle Success Criteria

- 1) The launch vehicle meets NASA requirements for starting static stability between 2-5 calibers, and simulations show the vehicle stays within the stability margin of 2-5 during the flight, regardless of launch angle or wind conditions.
- 2) The launch vehicle can be assembled and made launch-ready in under 2 hours.
- 3) The vehicle can remain launch-ready on the pad for a hold of up to 2 hours.
- 4) The motor ignites when the launch command is given and the 12V igniter initiates.
- 5) The launch vehicle achieves over 52 ft/s at rail exit to comply with NASA requirements.
- 6) The vehicle does not go supersonic.
- 7) Maximum velocity is within +/- 5% of OpenRocket prediction.
- 8) The vehicle apogee is within +/- 5% of 4600 ft AGL target.
- 9) The lower half of the rocket separates at apogee, deploying the drogue parachute while the upper payload bay remains pinned to the avionics bay.
- 10) The upper half of the rocket separates at 550ft, deploying the main parachute and payload.
- 11) All 4 independent ejection charges fire during the flight. The vehicle is not recovered with live charges endangering the team.
- 12) No section of the vehicle is ever jettisoned. All sections remain tethered together under parachute by the nylon recovery harnesses.
- 13) The vehicle impacts the ground inside a 2500 ft radius of the launch pad.
- 14) The descent from apogee occurs in under 90 seconds.
- 15) The vehicle impacts with KE of the heaviest section being under 75 ft-lb to comply with NASA requirements.
- 16) Ground impact causes no damage to the airframe, fins, internal structures, avionics, or payload.
- 17) Flight data can be extracted from the flight computers. Data is sampled across the entire flight profile.

3.1.3 Final Vehicle Design

The final design chosen for the Zenith Program will be 100 inches long with an estimated loaded weight of 38.23 pounds (17,485 grams) and an unloaded weight of 33.67 pounds (15,273 grams).

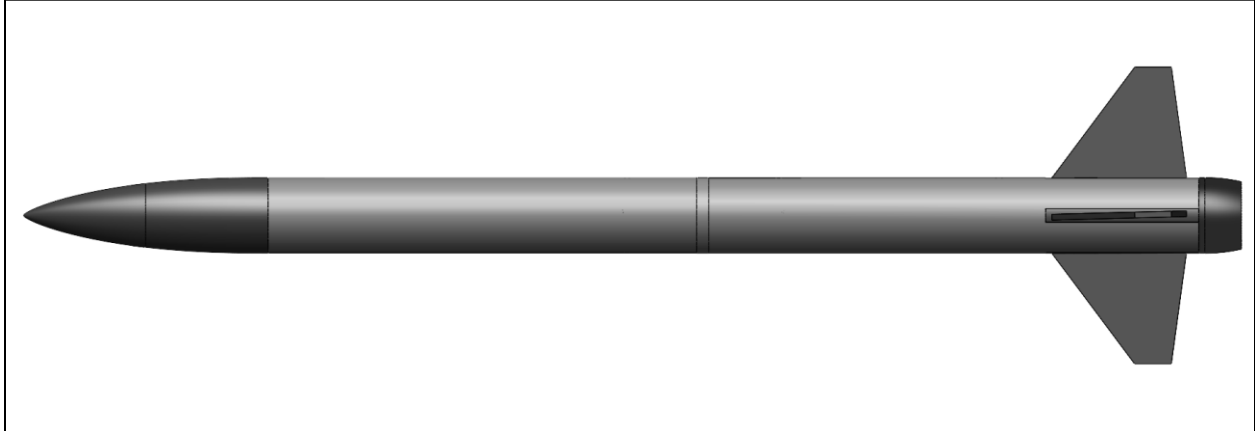


Figure 3-1. Launch Vehicle Assembly

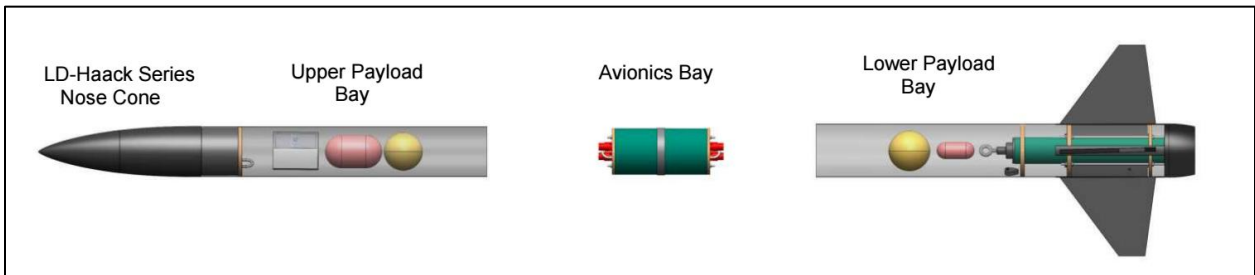


Figure 3-2. Launch Vehicle Exploded/Transparent Assembly

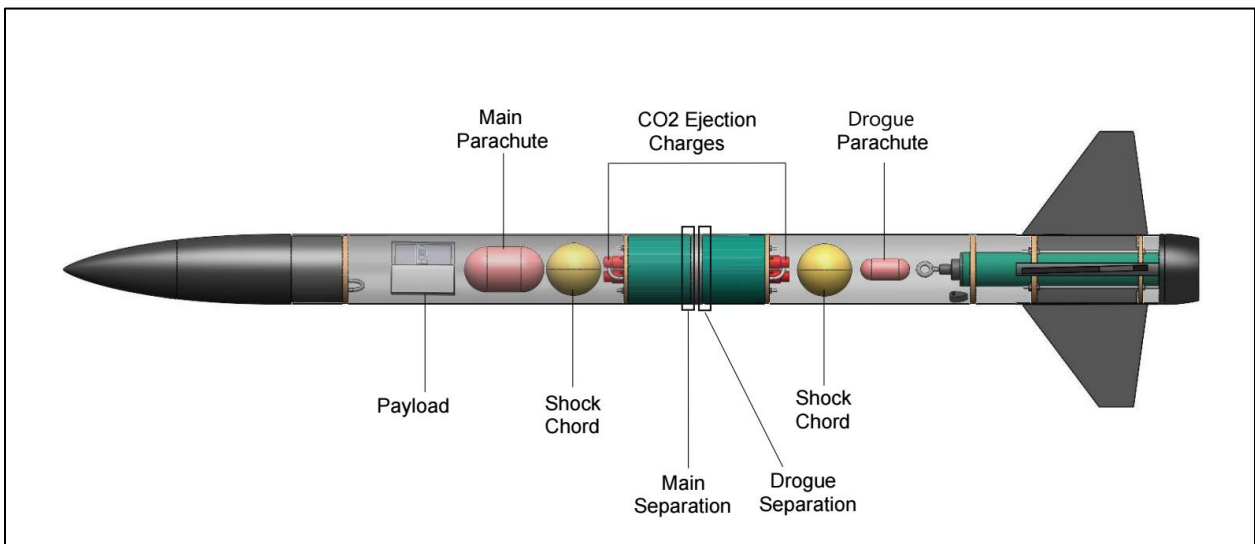


Figure 3-3. Launch Vehicle Transparent Assembly

3.1.3.1 Nosecone Configuration

The final design for the nosecone configuration will be an LD-Haack Series with threaded shoulder attachment. The leading design presented in PDR included a nosecone with a camera housing unit to satisfy our faculty advisor's request of capturing the flight through video recording from inside the vehicle. However, after further discussion with our faculty advisor, it has been decided to leave out the camera housing due to manufacturing complexity and potential failure points. The nosecone will be printed from acrylonitrile butadiene styrene (ABS) and the camera housing was supposed to be made of LEXAN glass. Attempting to connect the two different materials raised concerns in terms of flight performance and structural integrity as the vehicle enters large speeds during flight. As the nosecone is positioned at the front of the vehicle, it will be undergoing many aerodynamic forces during flight, interrupting the structural integrity of the nosecone's profile could cause the nosecone to break during flight. Instead, the whole nosecone profile will be made of ABS material without any camera house.

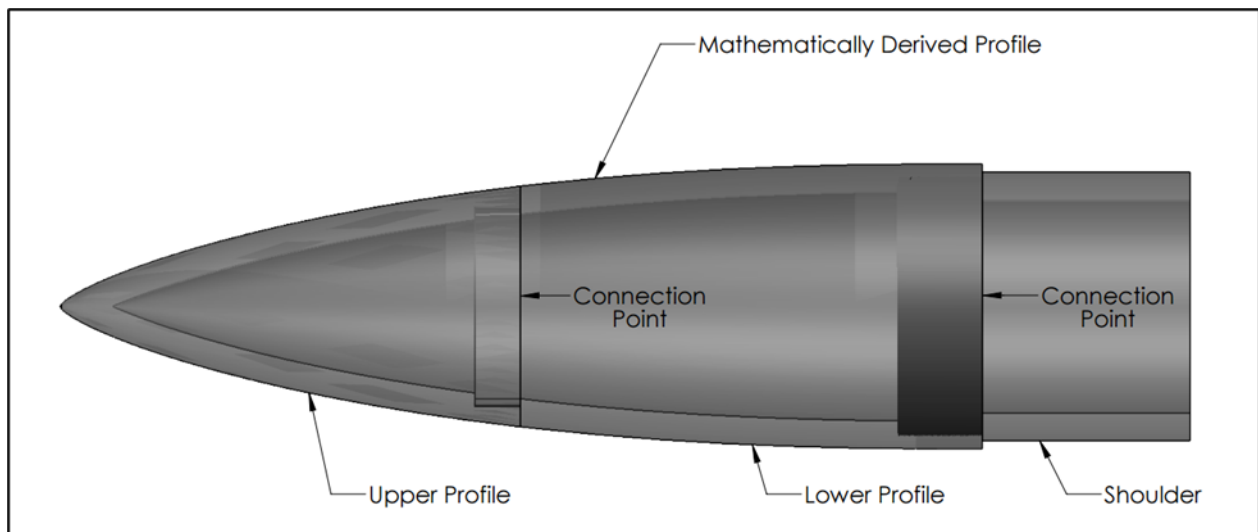


Figure 3-4. LD-Haack Series Nosecone Assembly

The nosecone configuration is separated into three sections: upper profile, lower profile, and shoulder. The configuration of the nosecone was ultimately separated into three sections for ease of manufacturing. The upper profile is connected to the lower profile by a cylindrical shoulder. The shoulder, receiving end, and connection faces between the two sections will be epoxied together. The lower profile is connected to the shoulder by a threaded cylindrical shoulder and the two sections will also be epoxied together. Shown below are dimensioned CAD drawings of each component and the full nosecone assembly. 3D printing specifications and notes have also been included in the drawings included in the drawings.

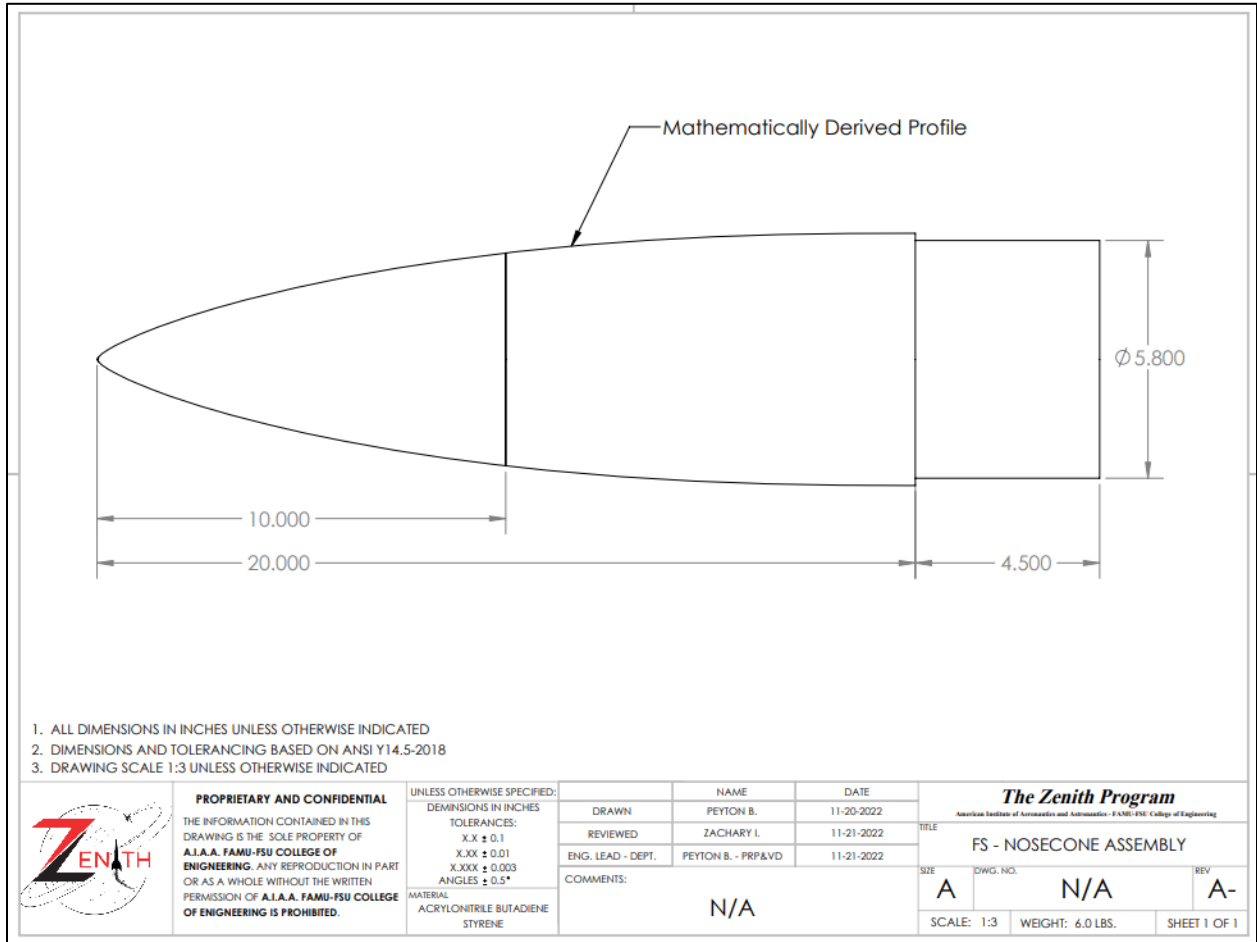


Figure 3-5. LD-Haack Nosecone Assembly CAD Drawing

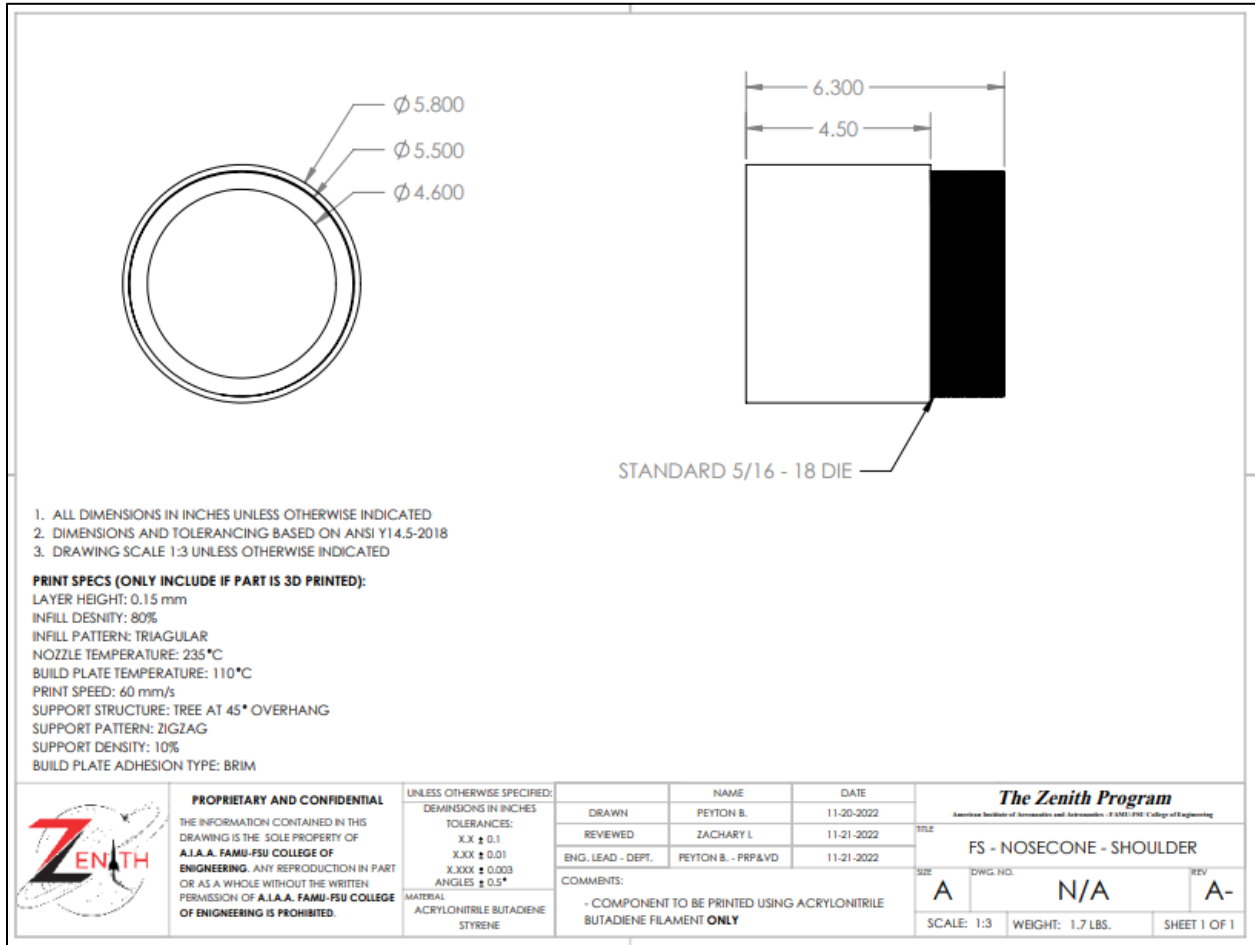


Figure 3-6. Nosecone Shoulder CAD Drawing

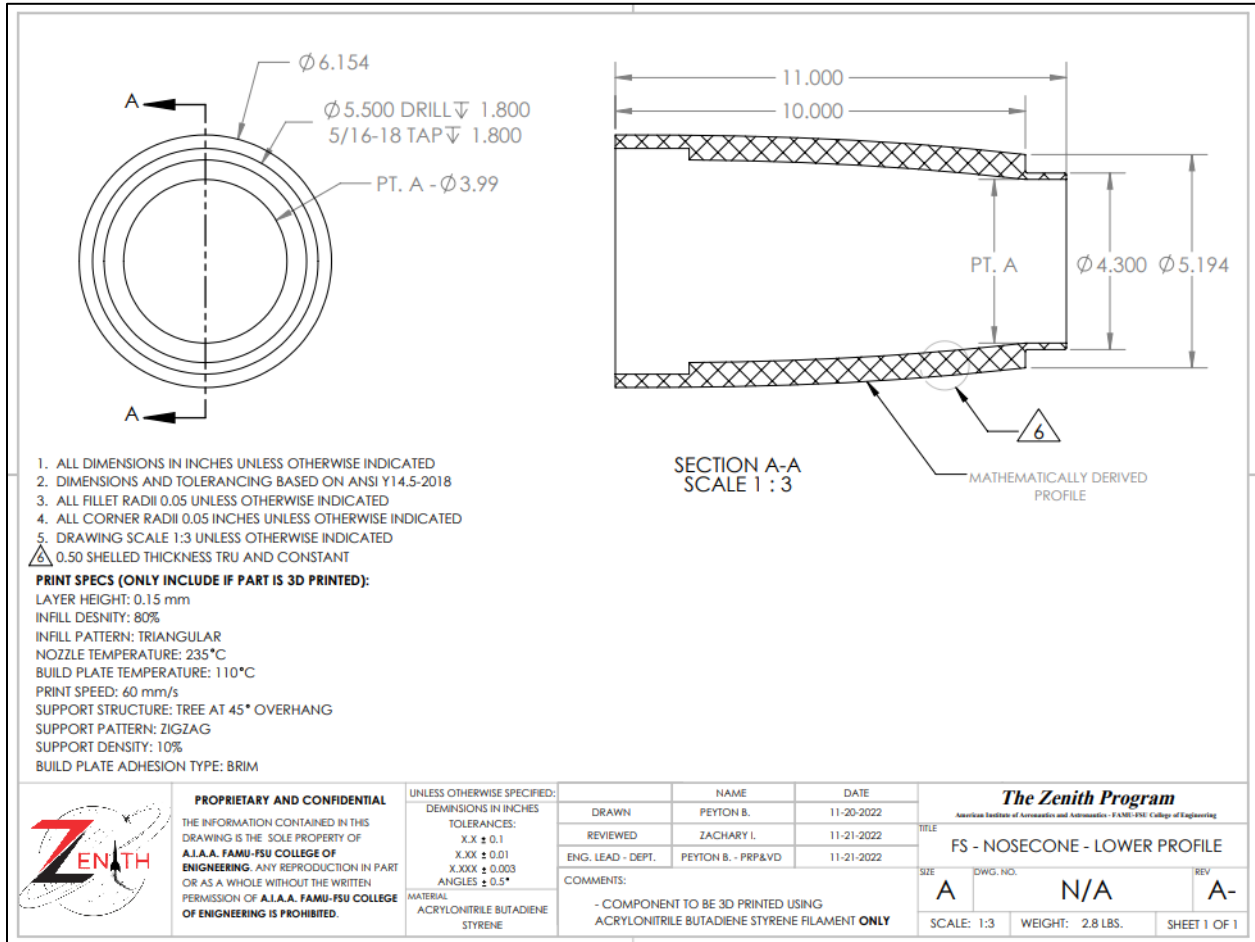


Figure 3-7. Nosecone Lower Profile CAD Drawing

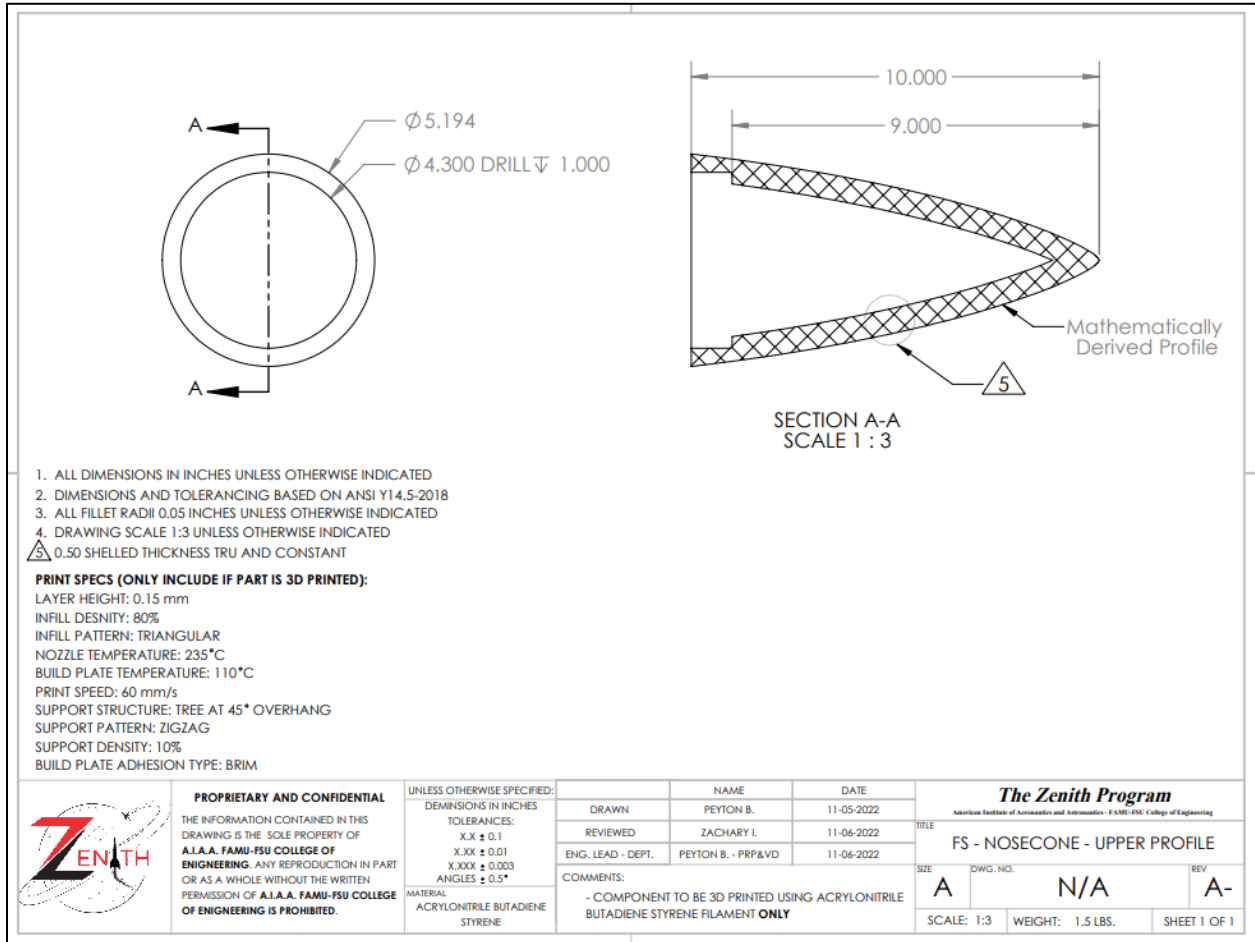


Figure 3-8. Nosecone Upper Profile CAD Drawing

3.1.3.2 Upper Payload Bay

The upper payload bay consists of a 35-inch-long blue tube airframe with a forward bulkhead that sits flush against the nosecone shoulder.

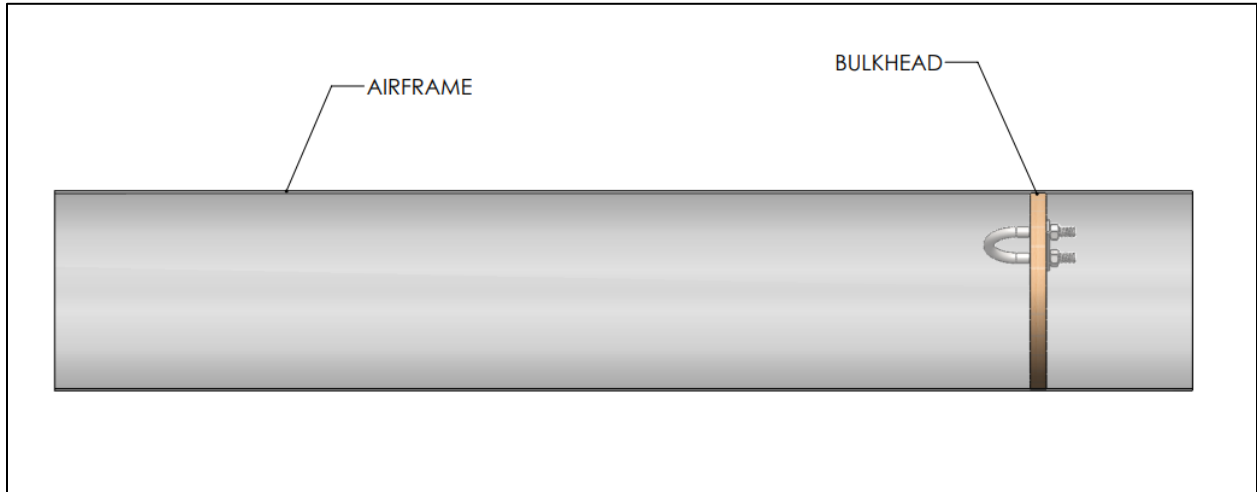


Figure 3-9. Upper Payload Bay Assembly

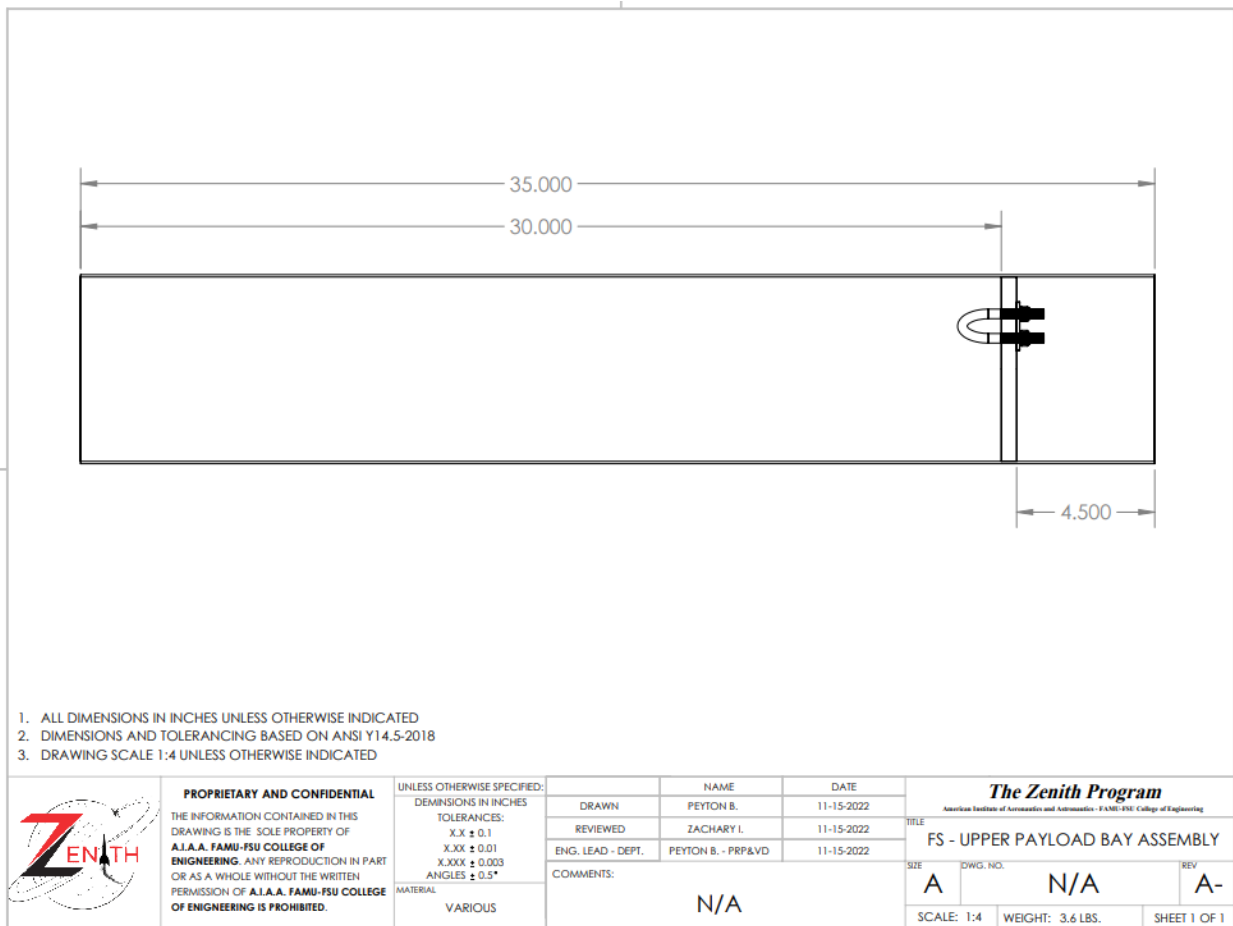


Figure 3-10. Upper Payload Bay Assembly CAD Drawing

(a) Upper Payload Bay Airframe

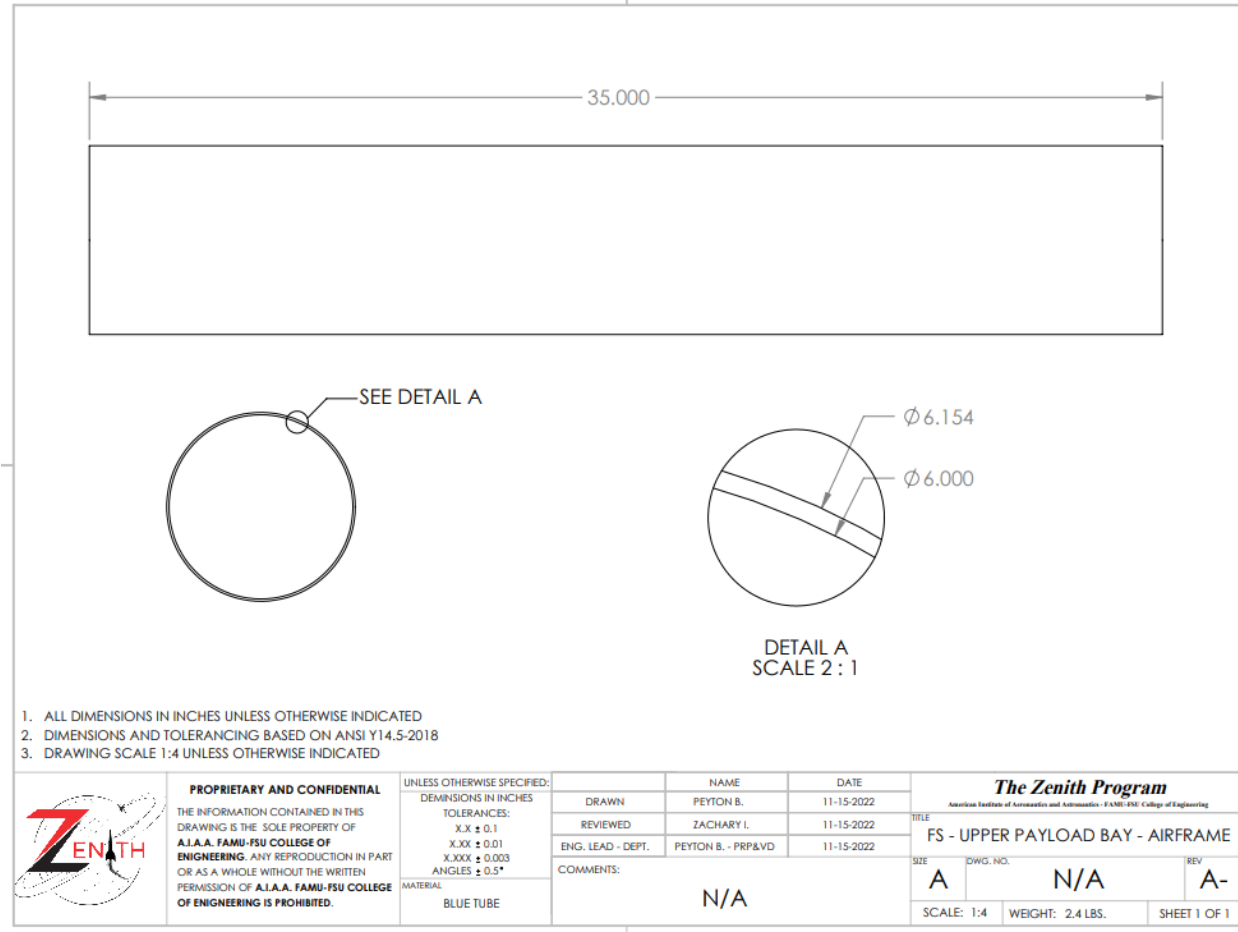


Figure 3-11. Upper Payload Bay Airframe CAD Drawing

(b) Updated Nose Cone Bulkhead

Originally, the nosecone bulkhead was designed with two holes for a bolted connection to the nosecone shoulder. However, now that the nosecone camera housing has been eliminated from the vehicle’s design, bolted connection (which allowed access to the nosecone) is not needed. All other design aspects of the nosecone bulkhead have remained the same with a 5/16” U-Bolt and fastener plate configuration attached to the bulkhead for main parachute shock chord connection purposes. The ½” bulkhead is fabricated from Baltic Birch Plywood. Shown below are dimensioned CAD drawings of the nosecone bulkhead design and each of its components.

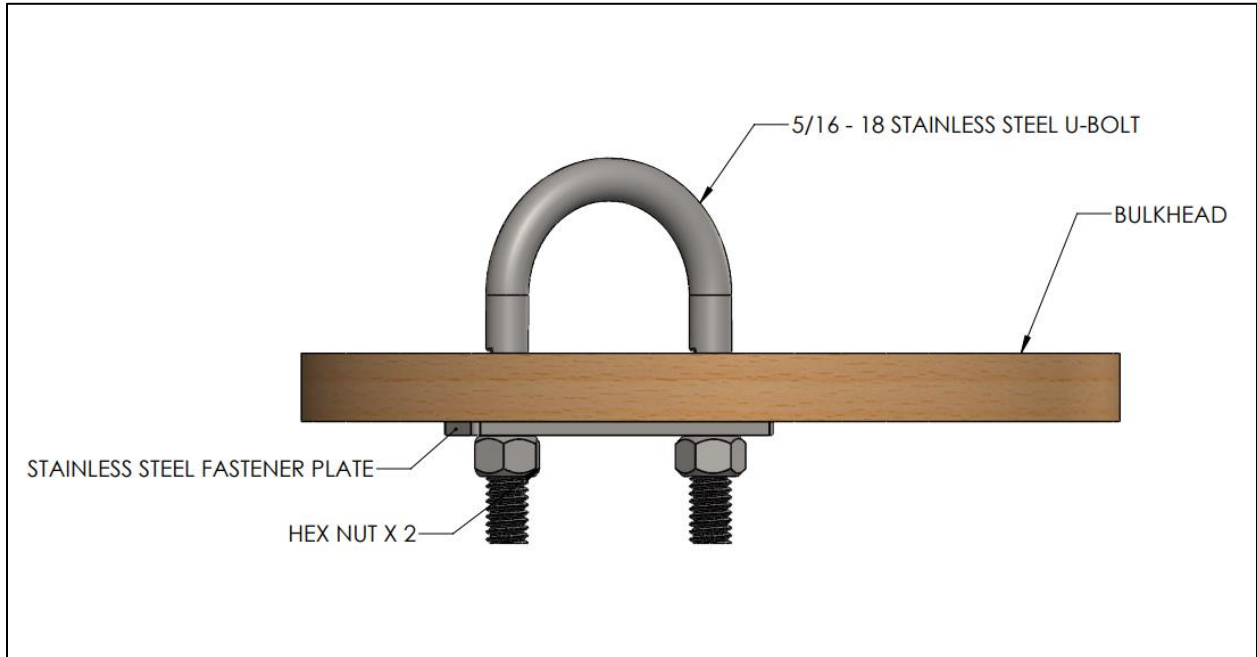


Figure 3-12. Nosecone Bulkhead Assembly

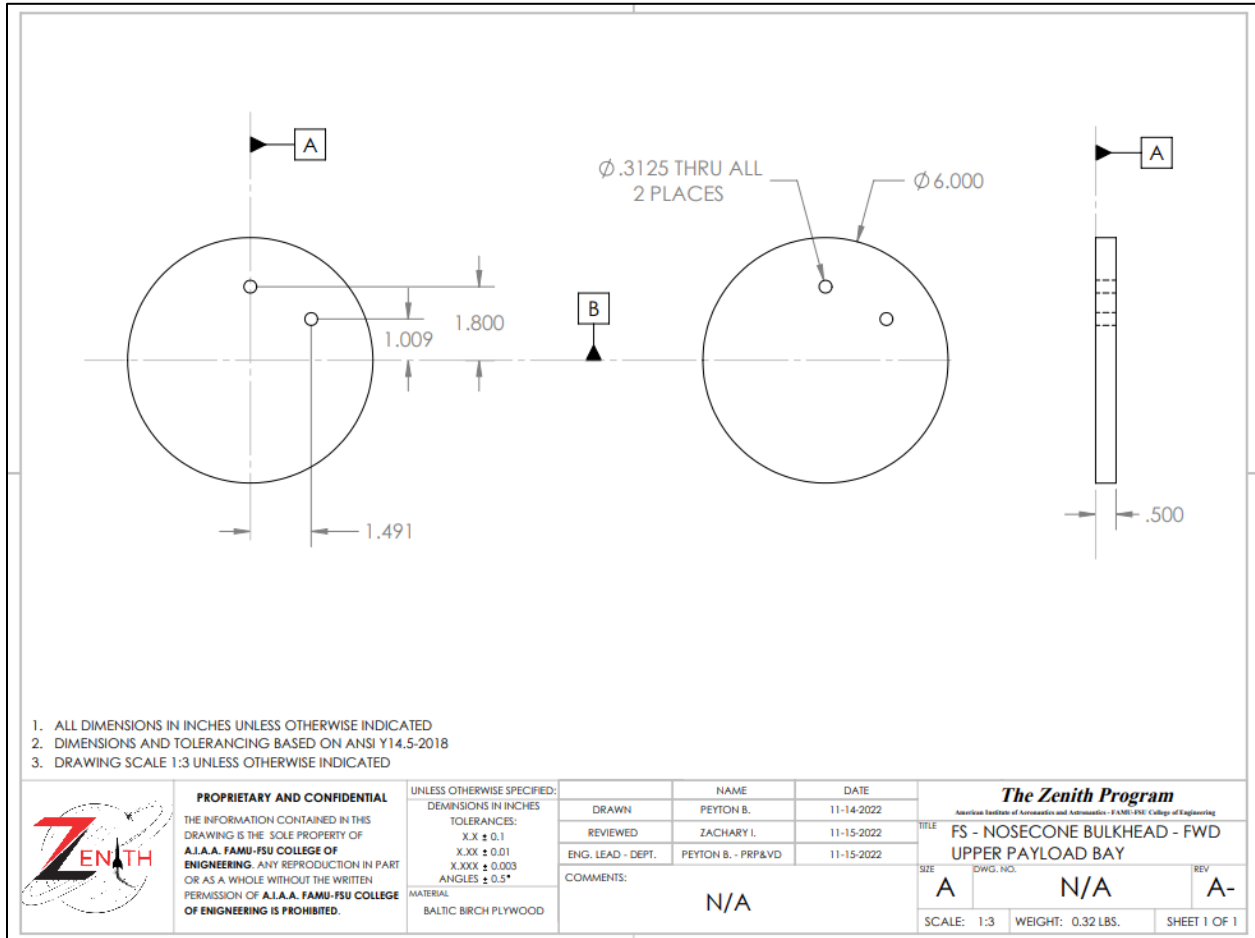


Figure 3-13. Nosecone Bulkhead CAD Drawing

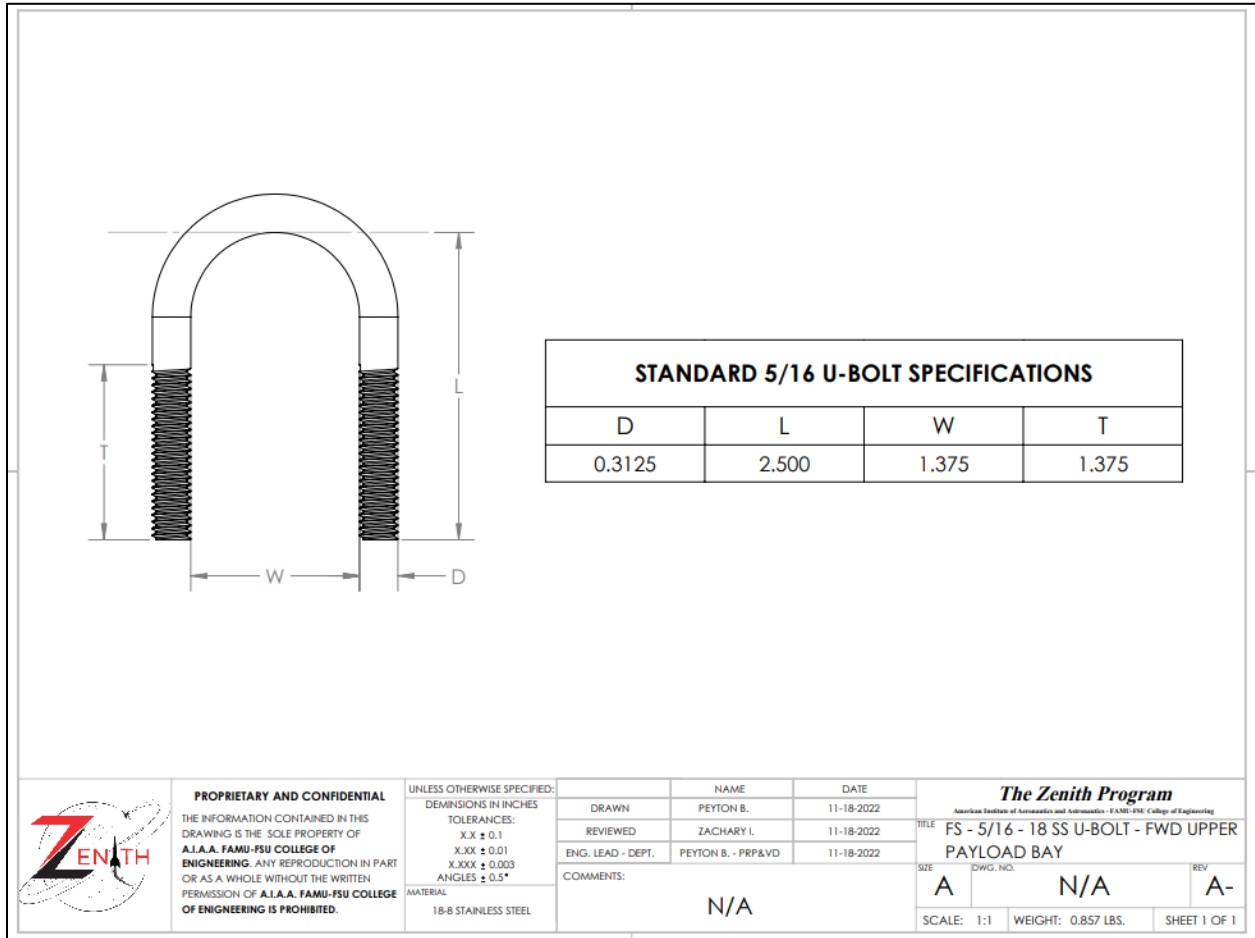


Figure 3-14. U-Bolt CAD Drawing

3.1.3.3 Avionics Bay

The avionics bay will be located between the upper and lower payload bays to not only act as a coupler connection point between the two airframe sections, but also house the avionics equipment. The avionics coupler is 12 inches in length and made from blue tube with a 1-inch-long outer airframe ring hugging the external surface of the coupler to provide a flush connection point between the coupler and the vehicle’s airframe. The avionics bay as a whole is expected to weigh 3.71 lbs.

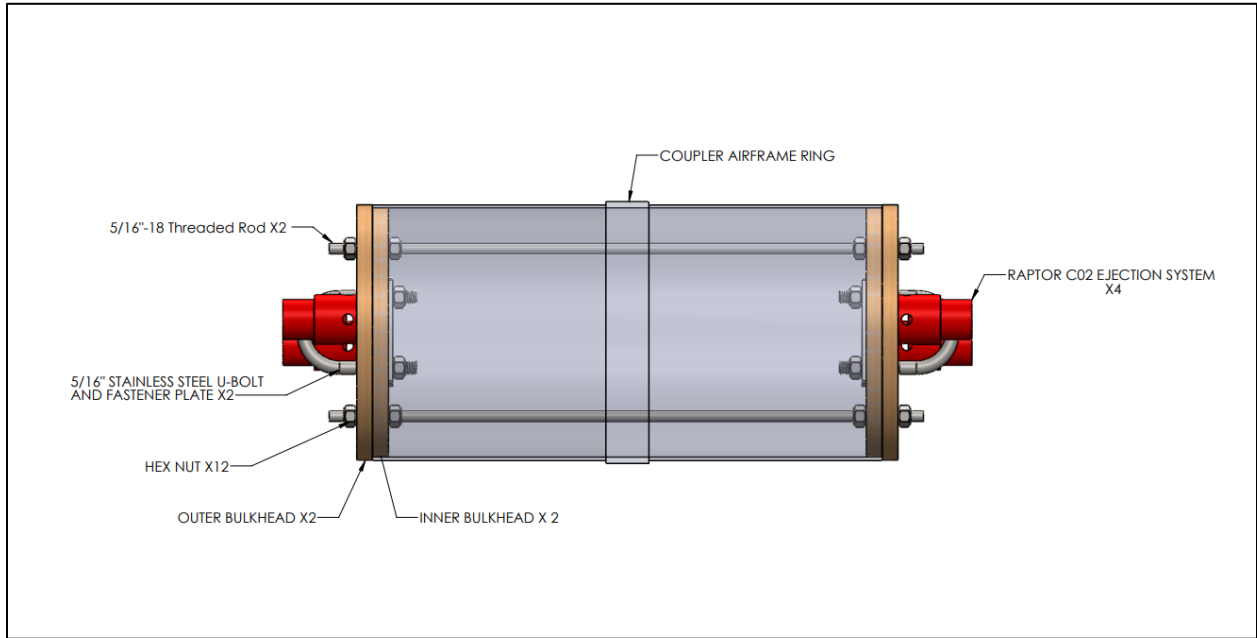


Figure 3-15. AV Bay Transparent Assembly

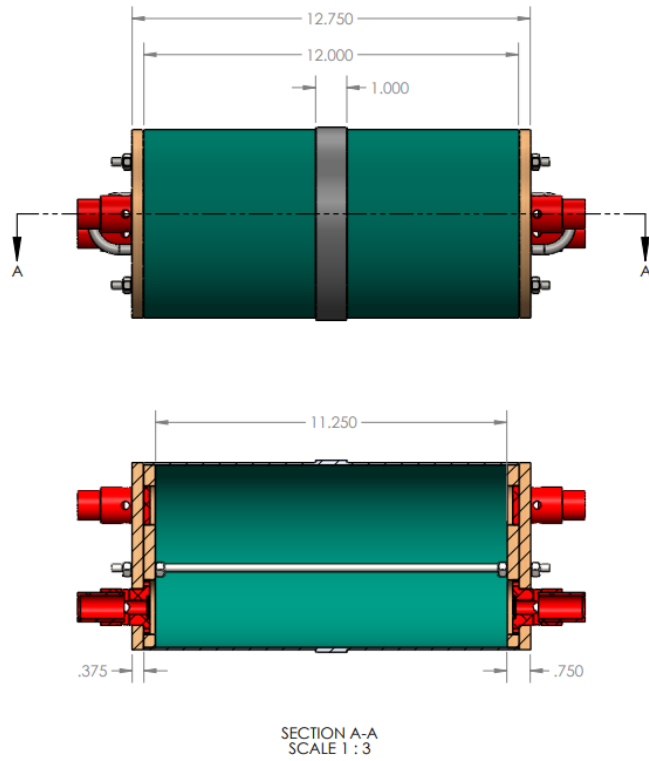


Figure 3-16. AV Bay Solid CAD Drawing

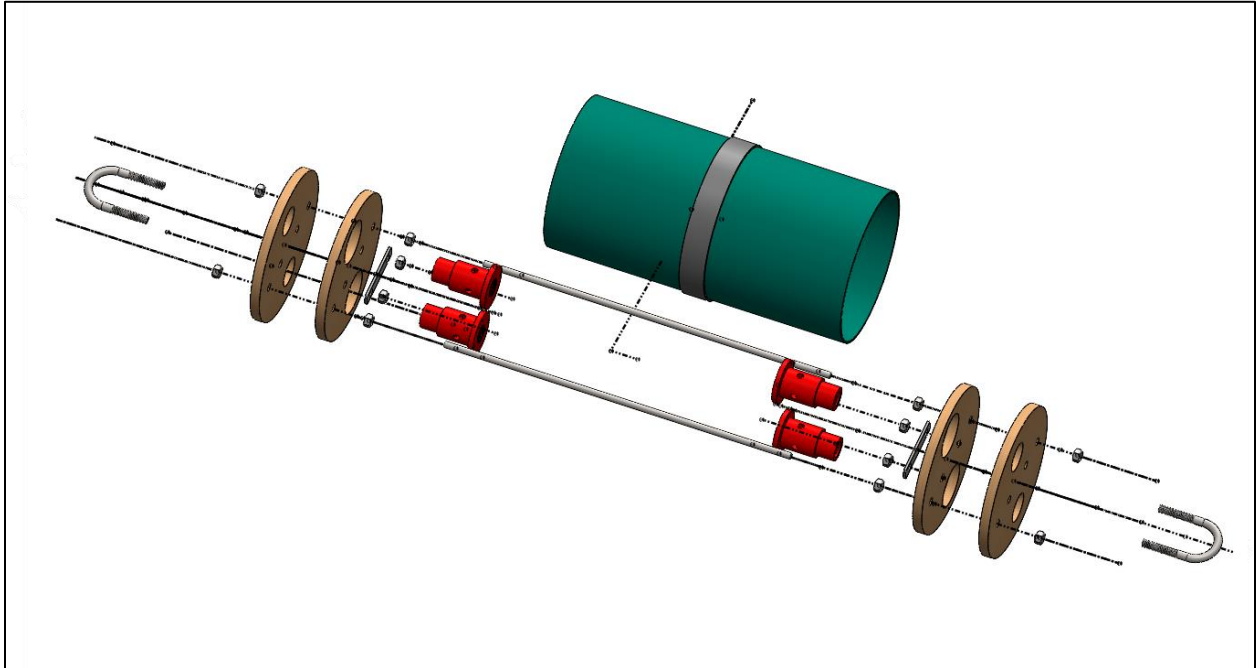


Figure 3-17. AV Bay Exploded Assembly

The coupler will have 4 bulkheads, 2 inner bulkhead and 2 outer bulkheads both 0.375" thick. The inner bulkheads, located inside the coupler, sit coincident against the outer flat face of the coupler and the outer bulkheads sit, located outside of the coupler, sit coincident against the outer flat face of the coupler. To account for modularity, the avionics bay has been designed to allow for a quick disassembly if any parts need to be modified or replaced. The RAPTOR CO2 Ejection Systems will be located at the inner and outer bulkheads of each side. The bulkheads will be modified to allow the ejection systems to be inserted through the two bulkheads and fixed in place via screws. Shown below are dimensioned CAD drawings of the avionics bay assembly and each of its components.

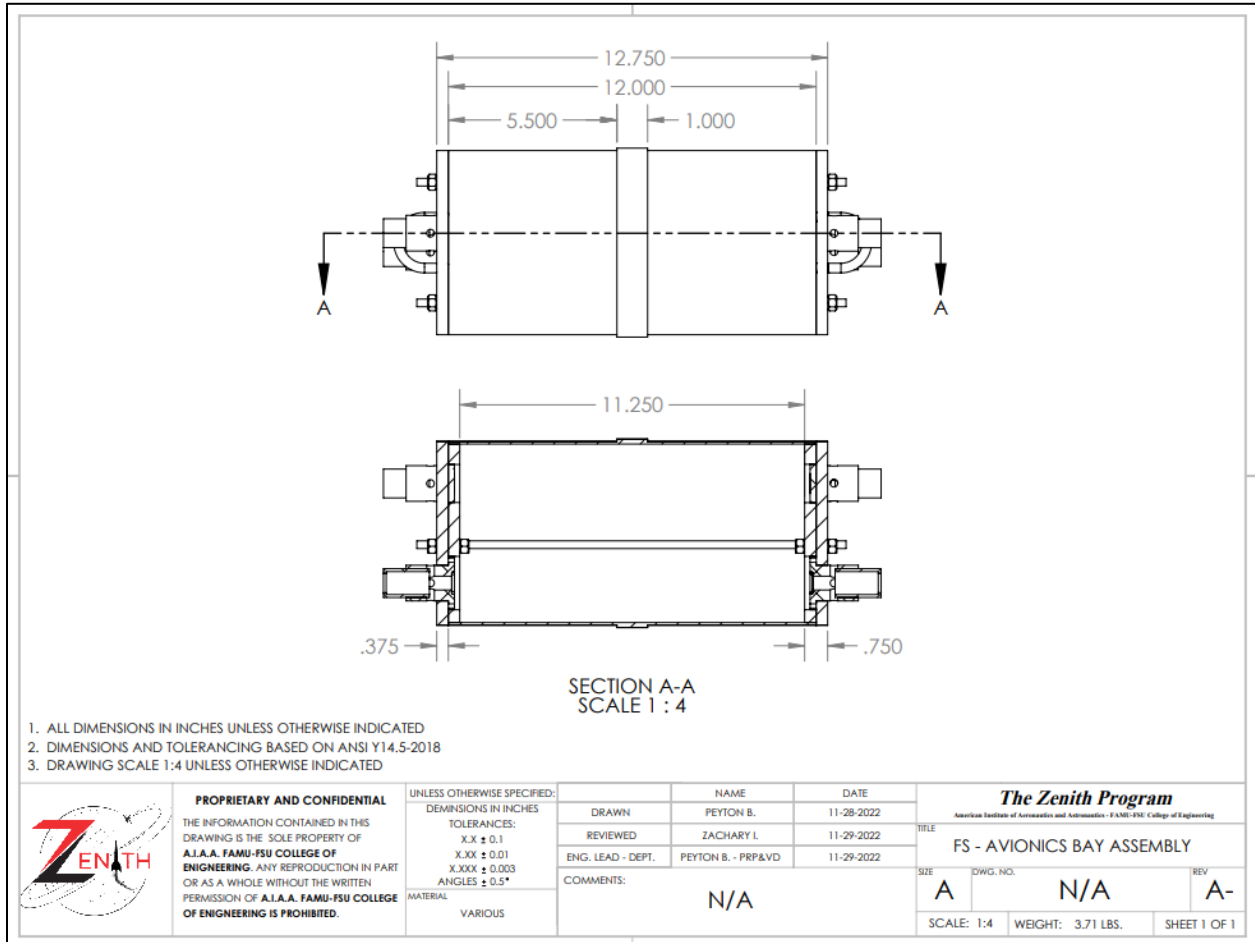


Figure 3-18. AV Bay CAD Drawing

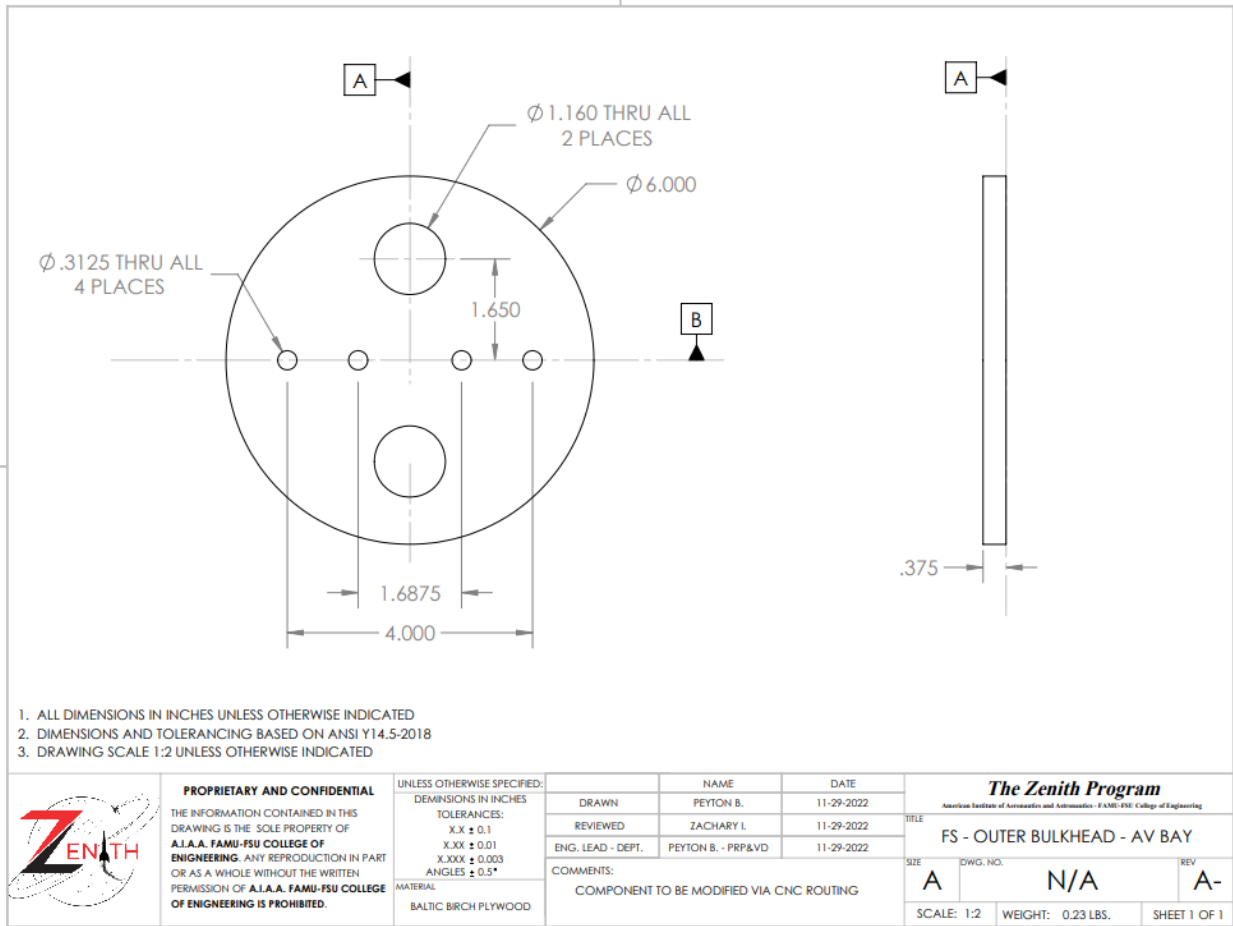


Figure 3-19. AV Bay Outer Bulkhead CAD Drawing

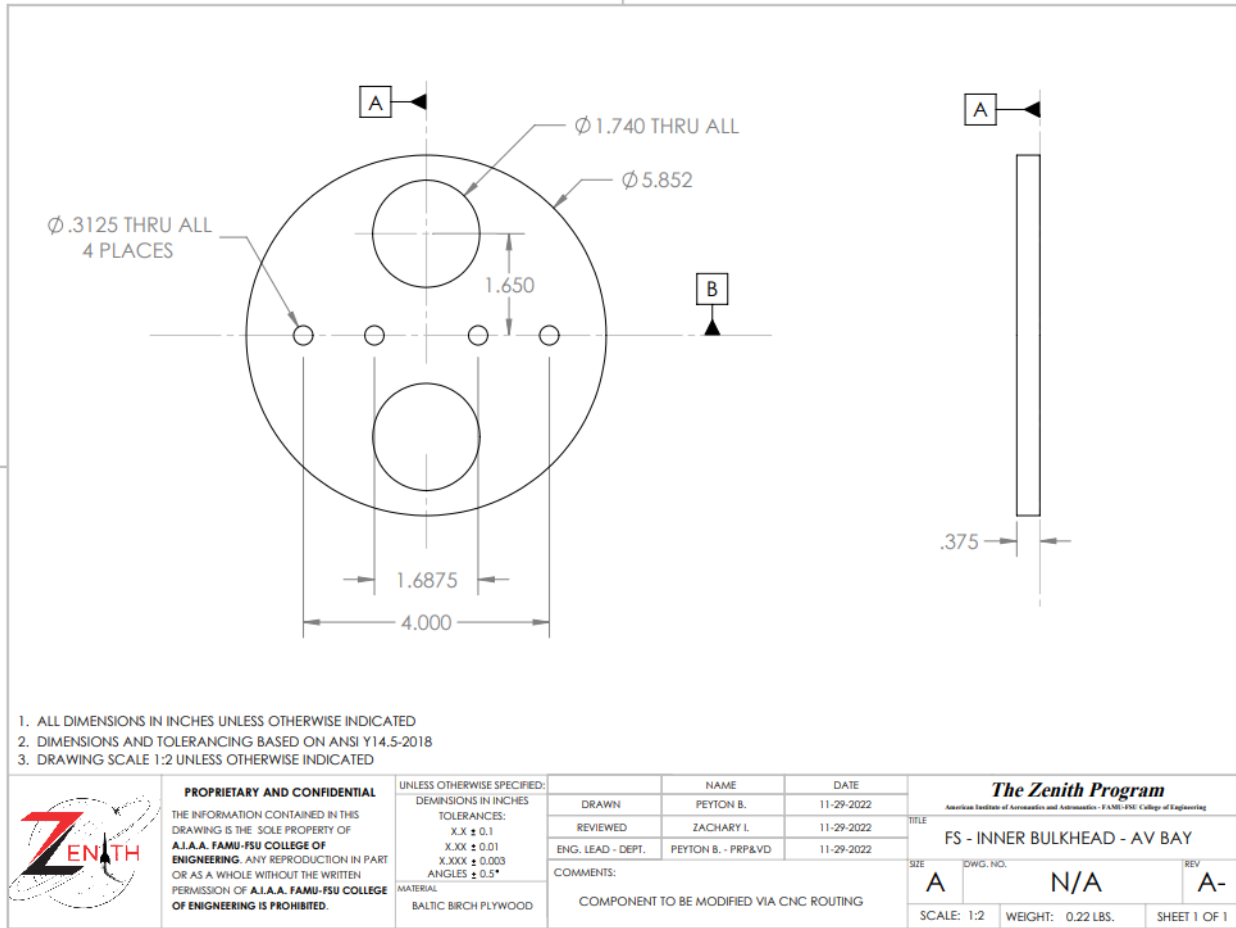


Figure 3-20. AV Bay Inner Bulkhead CAD Drawing

3.1.3.4 Lower Payload Bay and Thrust Structure

The lower payload bay as a whole is 43.50 inches in length.

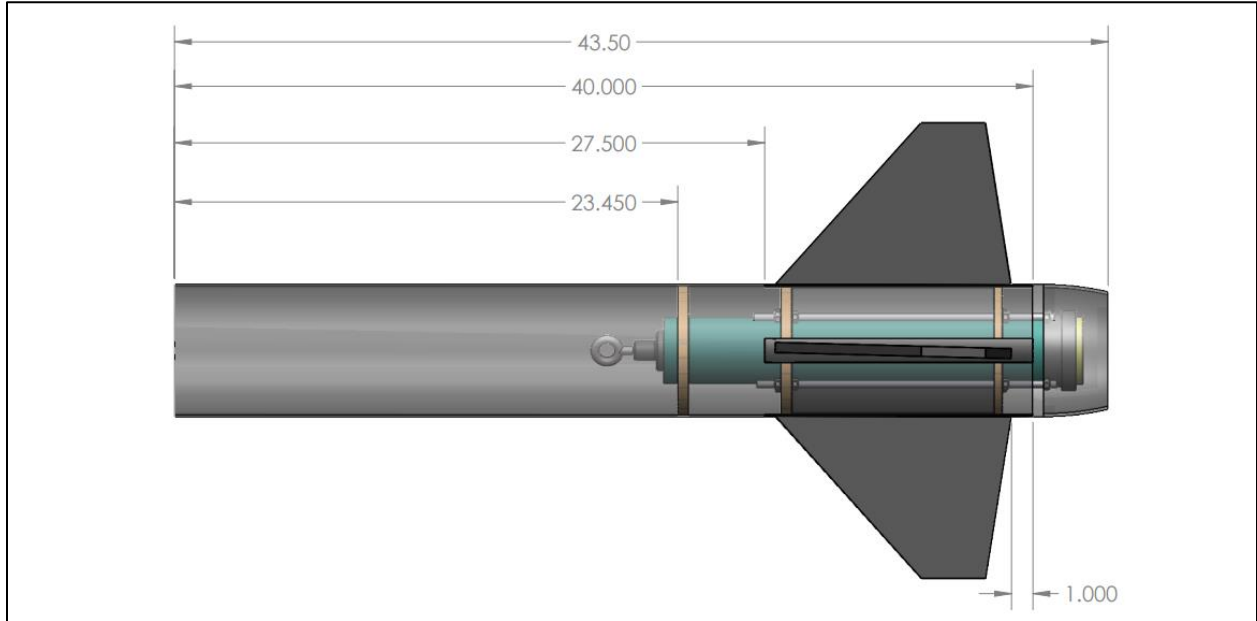


Figure 3-21. Lower Payload Bay/Fin Can Transparent Assembly

(a) Lower Payload Bay Airframe

The airframe of the lower payload bay will be 40 inches in length and made of blue tube material. The fin slots in the airframe will be CNC machined at our in-house manufacturing shop by certified personnel. The fins are designed to slide into the fin slots, with the fin base having the same curvature as the airframe for a flush and tangent surface fit.

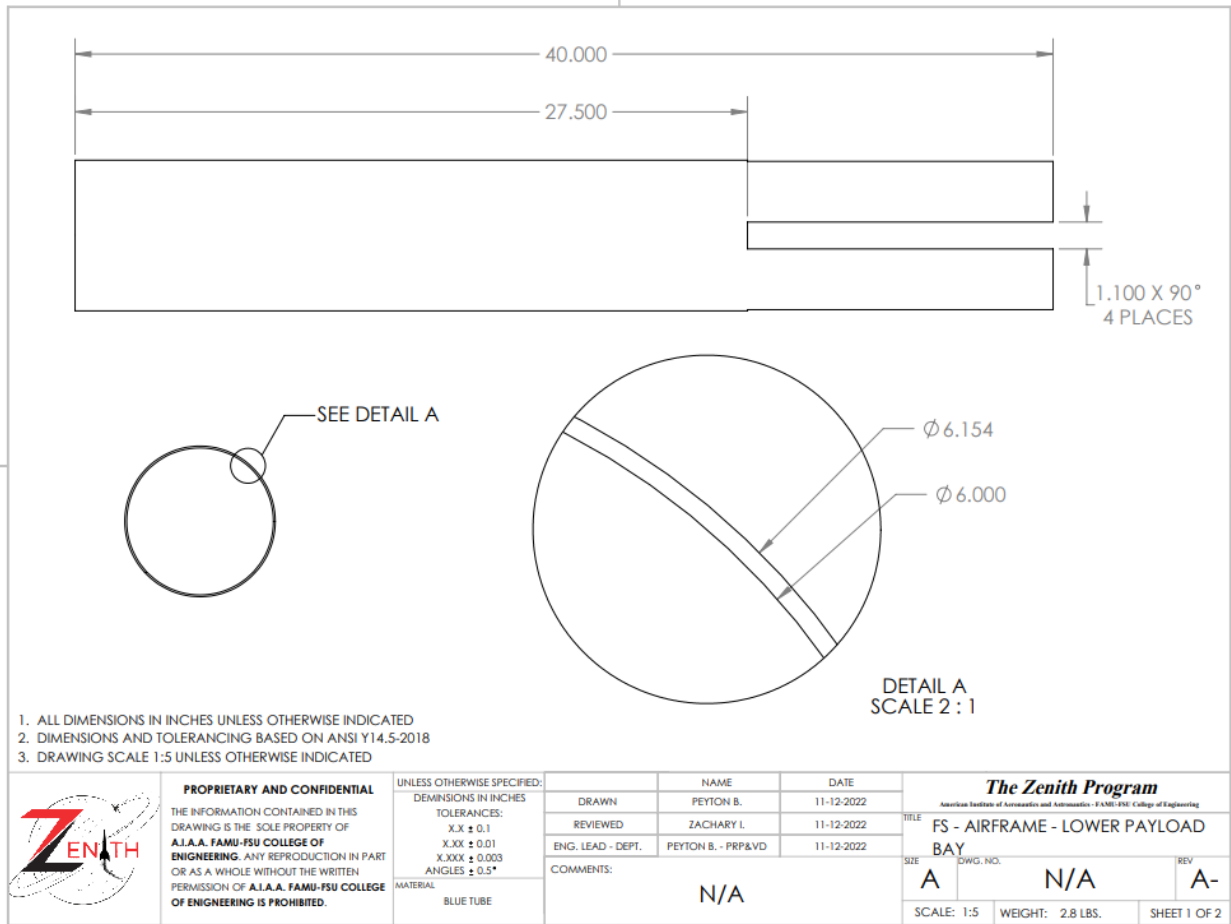


Figure 3-22. Lower Payload Bay Airframe CAD Drawing

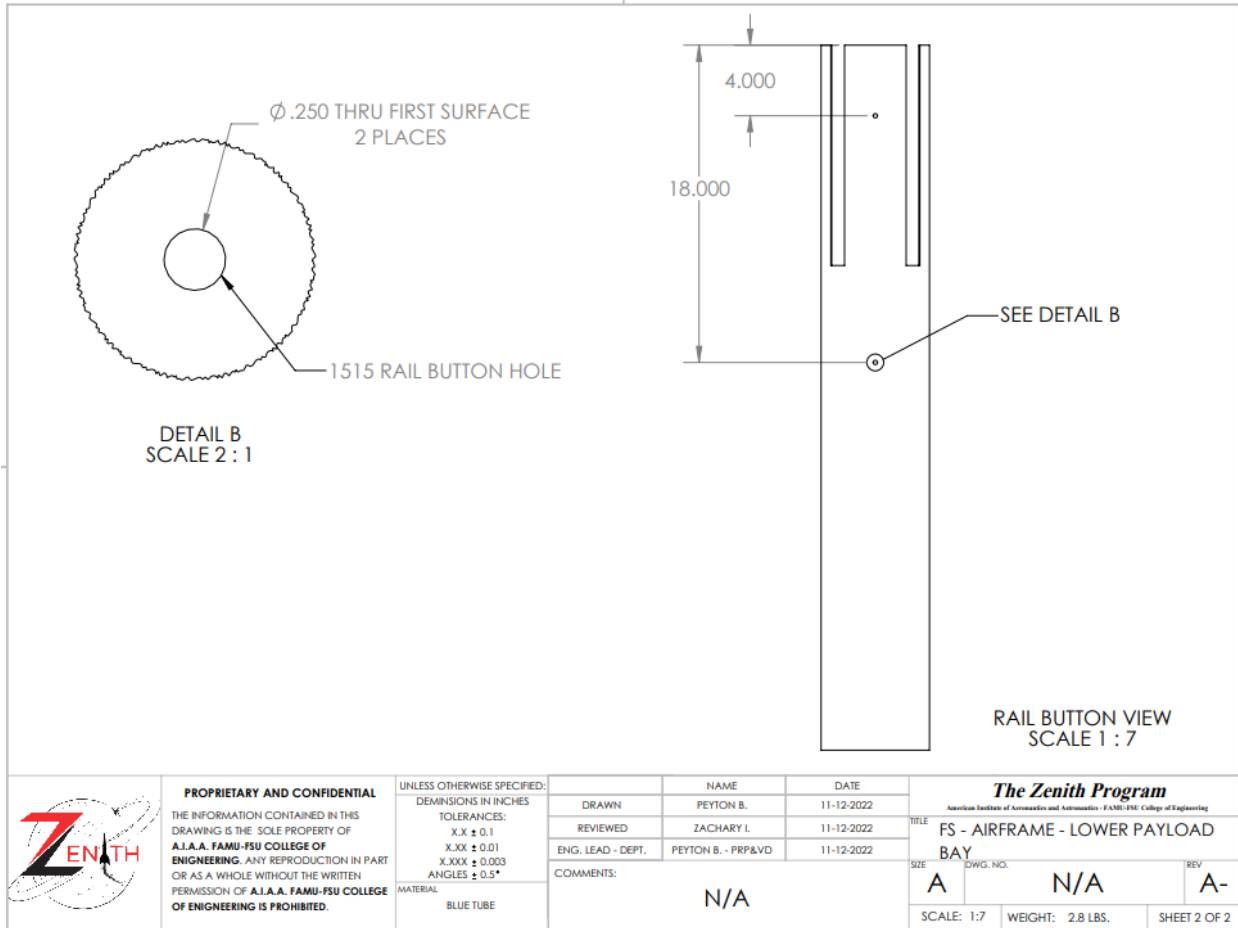


Figure 3-23. Lower Payload Bay Airframe w/ 1515 Rail Buttonhole

(b) Updated Thrust Structure

The thrust structure presented in PDR is relatively similar to the updated design, but with a few small changes.

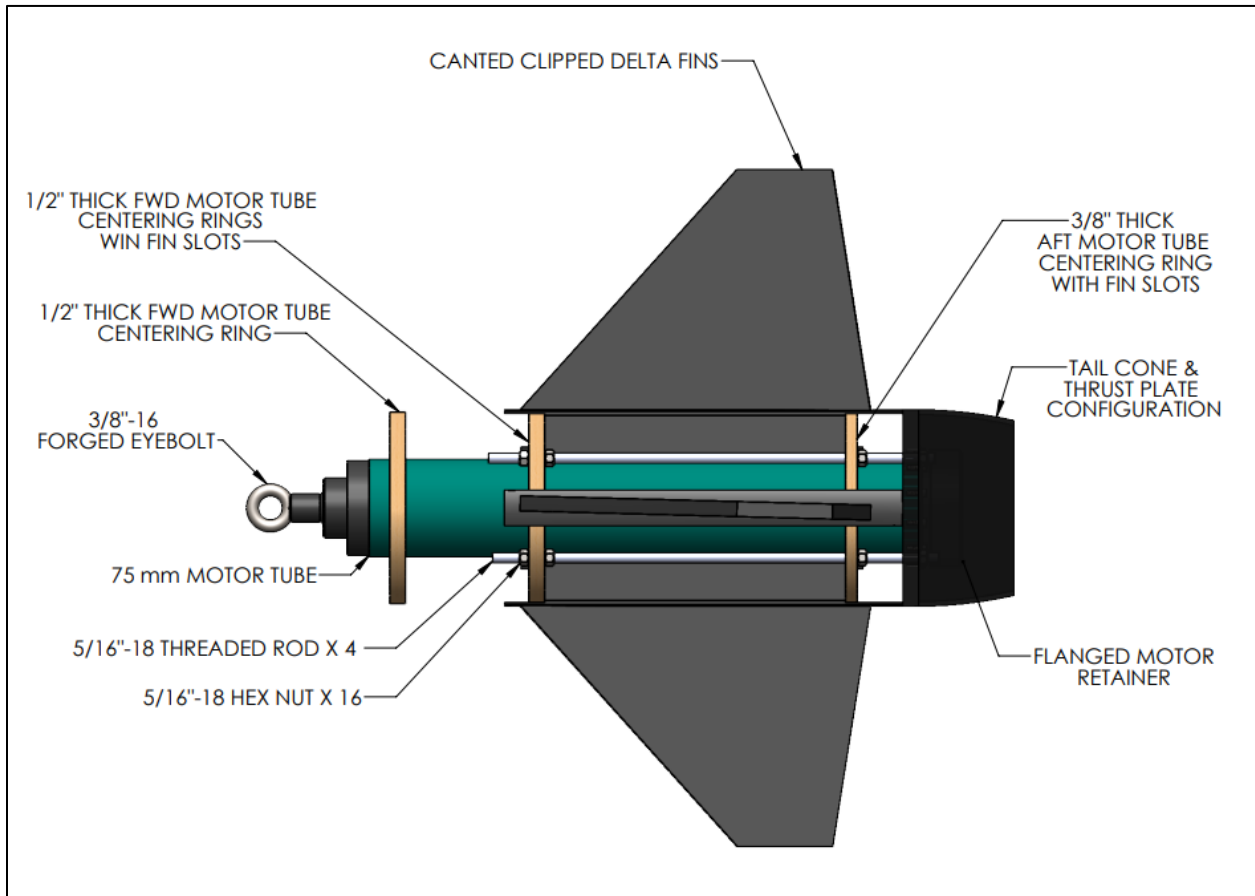


Figure 3-24. Labeled Fin Can Assembly

The fin tabs have been designed differently to fit into slots that were cut in the centering rings. Originally, the threaded rods ran through the fin tabs up to the forward bulkhead above the motor case (as shown in Figure 3-12 of PDR). However, the leading concerns with the design was the amount of compression acting on the threaded rods. The original design used 22-inch long 3/8"-24 threaded rods whereas the new design uses 14.5-inch long 1/4"-20 threaded rods. The threaded rods now only serve to hold the fins and the thrust plate/tail cone configuration in place. This modification decreases the amount of compression acting on the threaded rods and drastically lowered the vehicle's weight, increasing the stability margin. The final fin design chosen for the vehicle will be the clipped delta fin shape. The large surface area of the clipped delta fin decreases wing loads and increases the stability of the fins. The fins will be canted 1.5 degrees clockwise off vertical to introduce spinning stabilization to the vehicle during flight. The

base plate of the fin has the same thickness and radial curvature as the airframe for a flush surface fit.

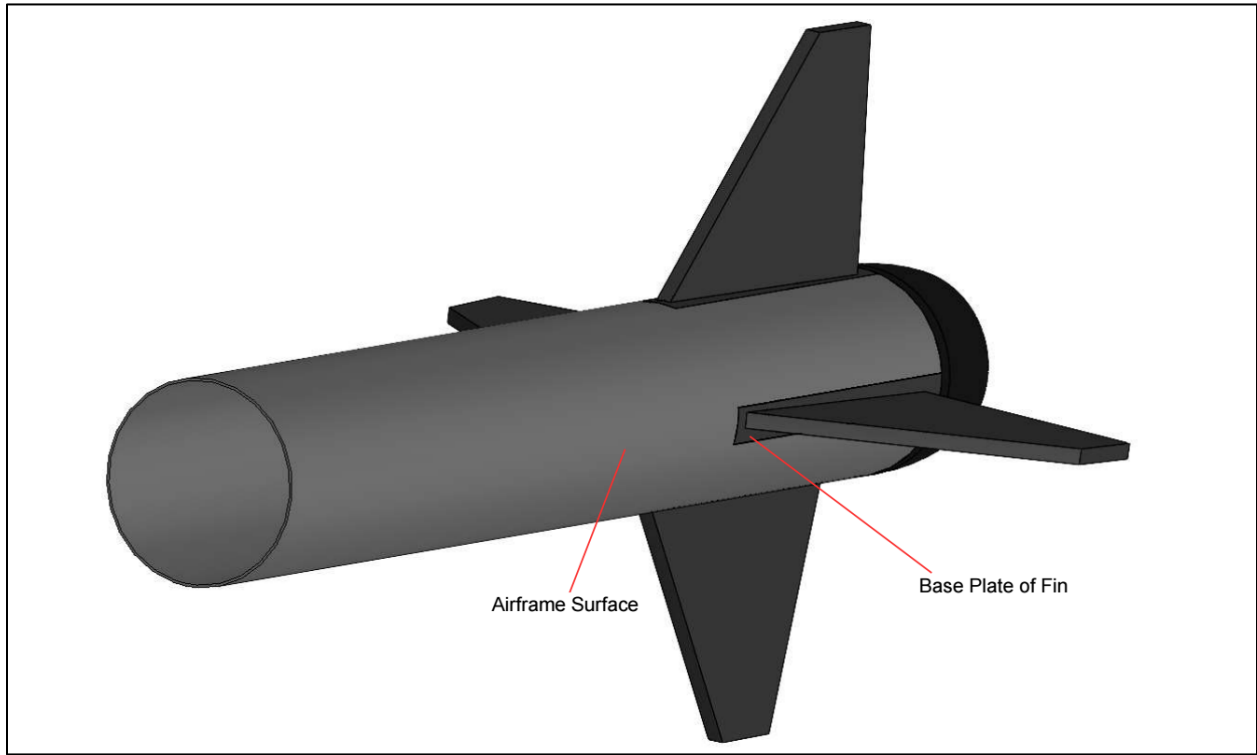


Figure 3-25. Lower Payload Bay/Fin Can Solid Assembly

The fins slide into the slots in the centering rings and the threaded rods sandwich the fin tabs between the two centering rings to keep the fins fixed in place. The fin tabs extend to the motor tube for extra structural stabilization and to transfer thrust loads to the centering rings.

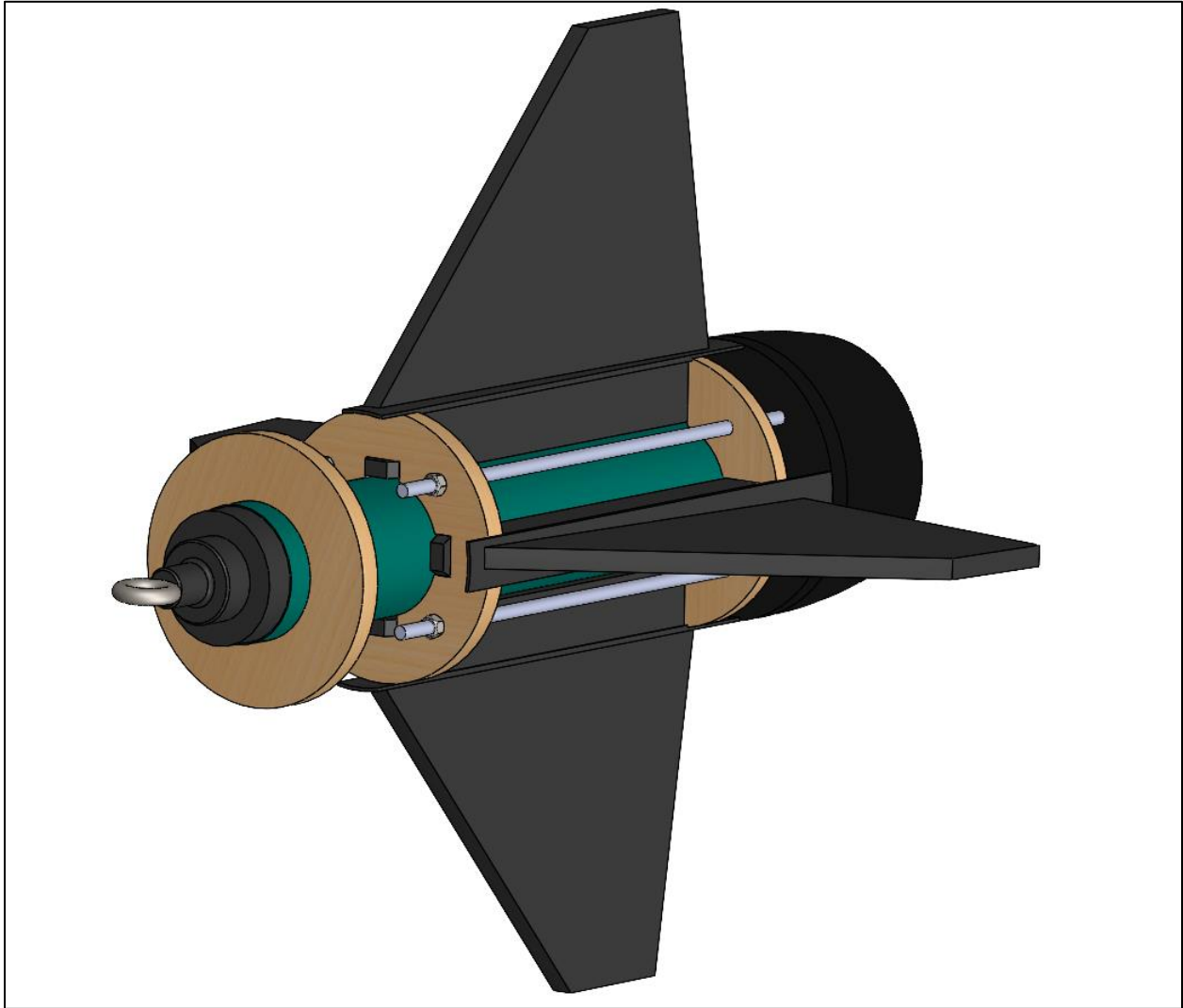


Figure 3-26. Fin Can Assembly

The fin assembly shown above was replicated in the subscale vehicle and had great success. The slots in the centering rings prevent the fins from rotating and each end of the fin tabs the slide into the centering rings are chamfered for ease of fitment. The fins will be 3D printed using ABS filament and have an estimated weight of 1.3 pounds each (608 grams). Shown below are dimensioned CAD drawings of the clipped delta fins.

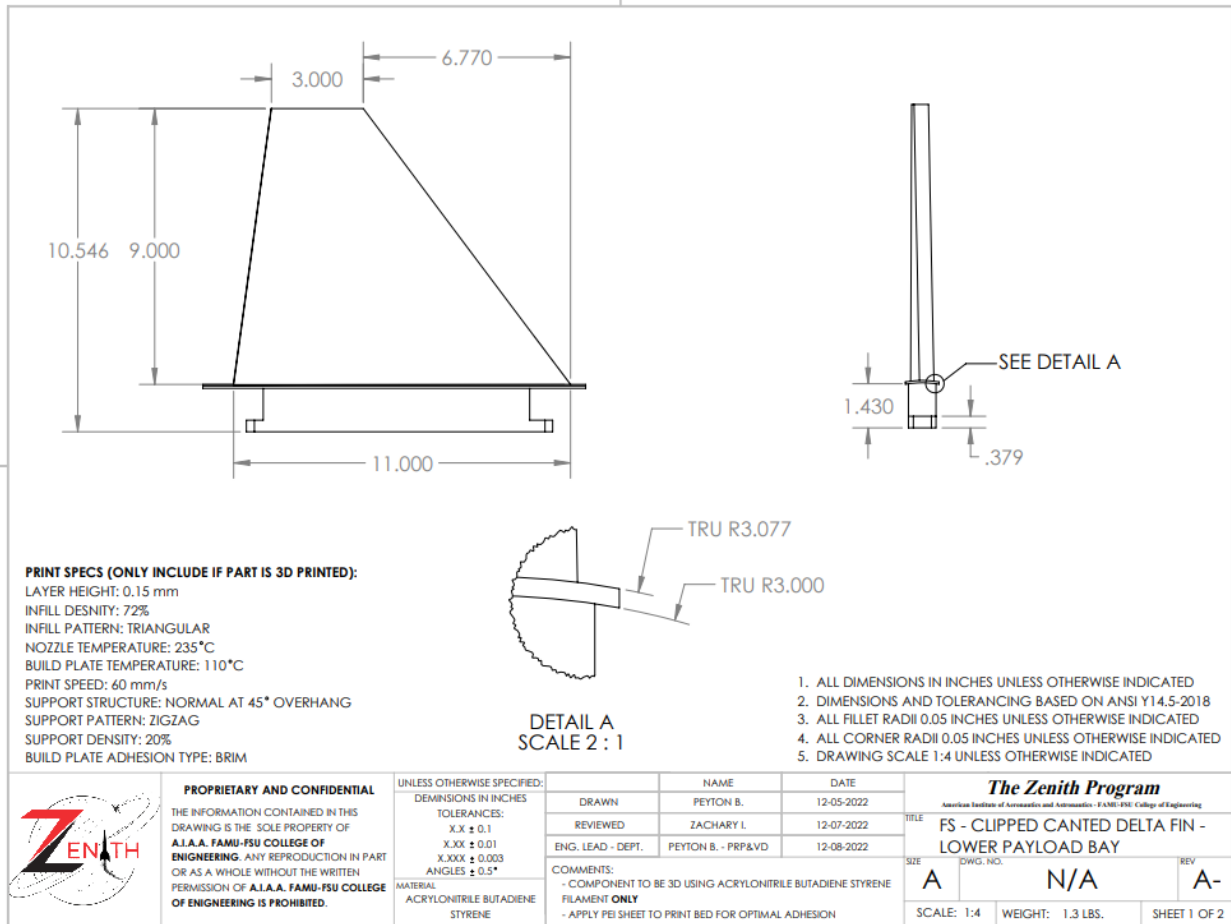


Figure 3-27. Canted Clipped Delta Fin CAD Drawing Sheet 1 of 2

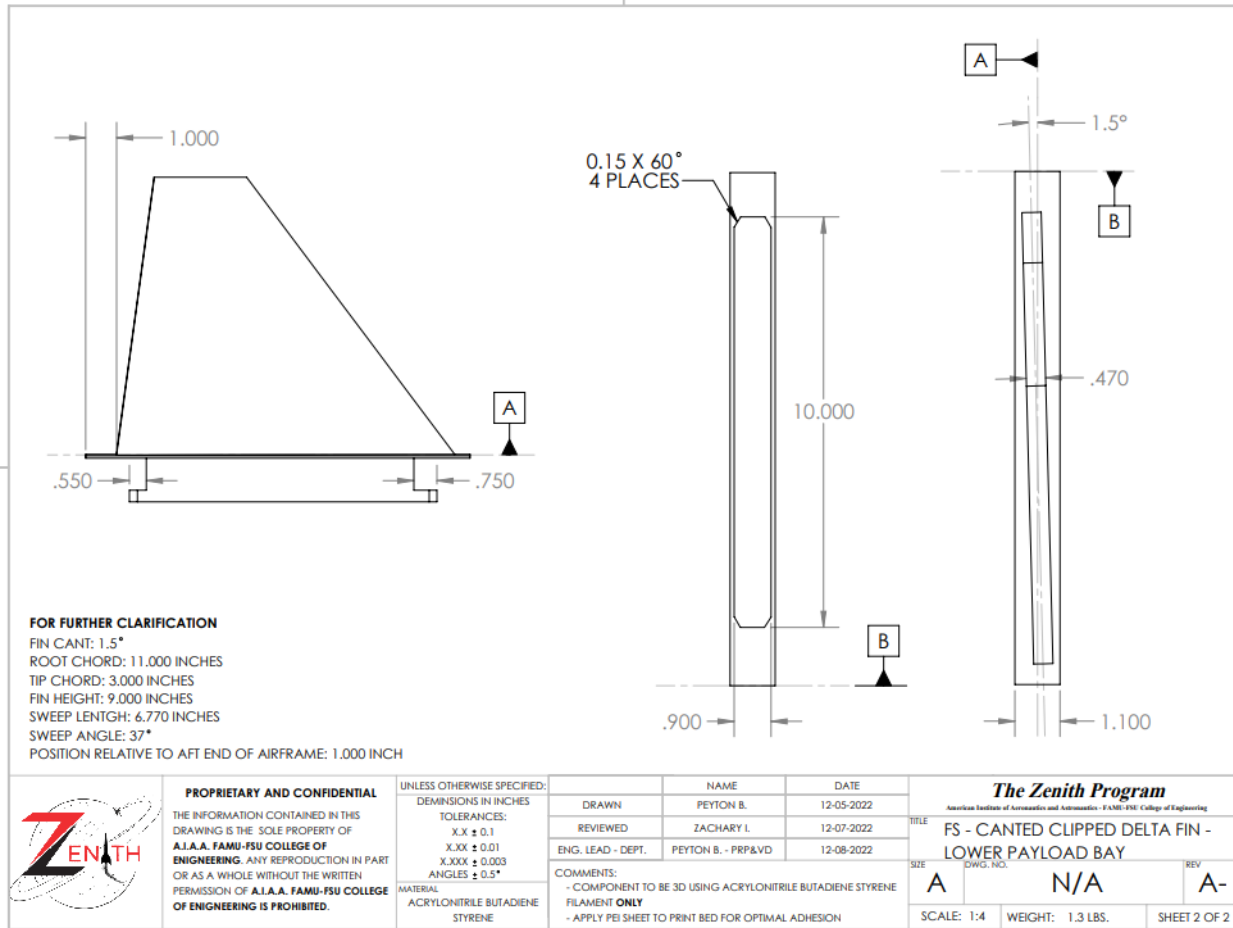


Figure 3-28. Canted Clipped Delta Fin CAD Drawing Sheet 2 of 2

Previously mentioned in PDR, a rising concern with using ABS as the material of choice was the fin flutter speed. To triple check our fin design for the final vehicle design, the fin flutter speed was calculated again. Shown below is the equation used to find the fin flutter speed, along with the variables and their calculated values.

$$V_f = a \sqrt{\frac{G}{\frac{1.337AR^3P(l+1)}{2(AR+2)\left(\frac{t}{c}\right)^3}}$$

The variables in the equation are defined below along with their calculated values. The MATLAB code used to calculate these values and the flutter speed is attached as Appendix C.

Table 3-1. Fin Flutter Speed Parameters

Fin Flutter Speed			
Parameter	Symbol	Value	Unit
Speed of Sound	a	1098.9	ft/s
Shear Modulus	G	151920	lb/in ²
Aspect Ratio	AR	1.0714	
Pressure	P	12.44	lb/in ²
Taper Ratio	l	0.2727	
Fin Thickness	t	0.47	inches
Root Chord	c	11	inches
Fin Flutter Speed	V_f	1446.3	ft/s

Table 3-2. Fin Flutter Speed Results

Max Vehicle Speed:	545 ft/s
Fin Flutter Speed:	1446.3 ft/s
Percent Flutter Speed Achieved:	38%
Factor of Safety:	2.65

The centering rings used for the thrust structure will be fabricated from Baltic Birch plywood. The two forwards are 0.5 inches thick and the aft centering rings is 0.375 inches thick. Both forward centering rings are epoxied to the motor tube and the inner airframe while the aft centering ring is held in place by the threaded rods. Shown below is a labeled image of the thrust structure showing which centering rings are epoxied for further clarification.

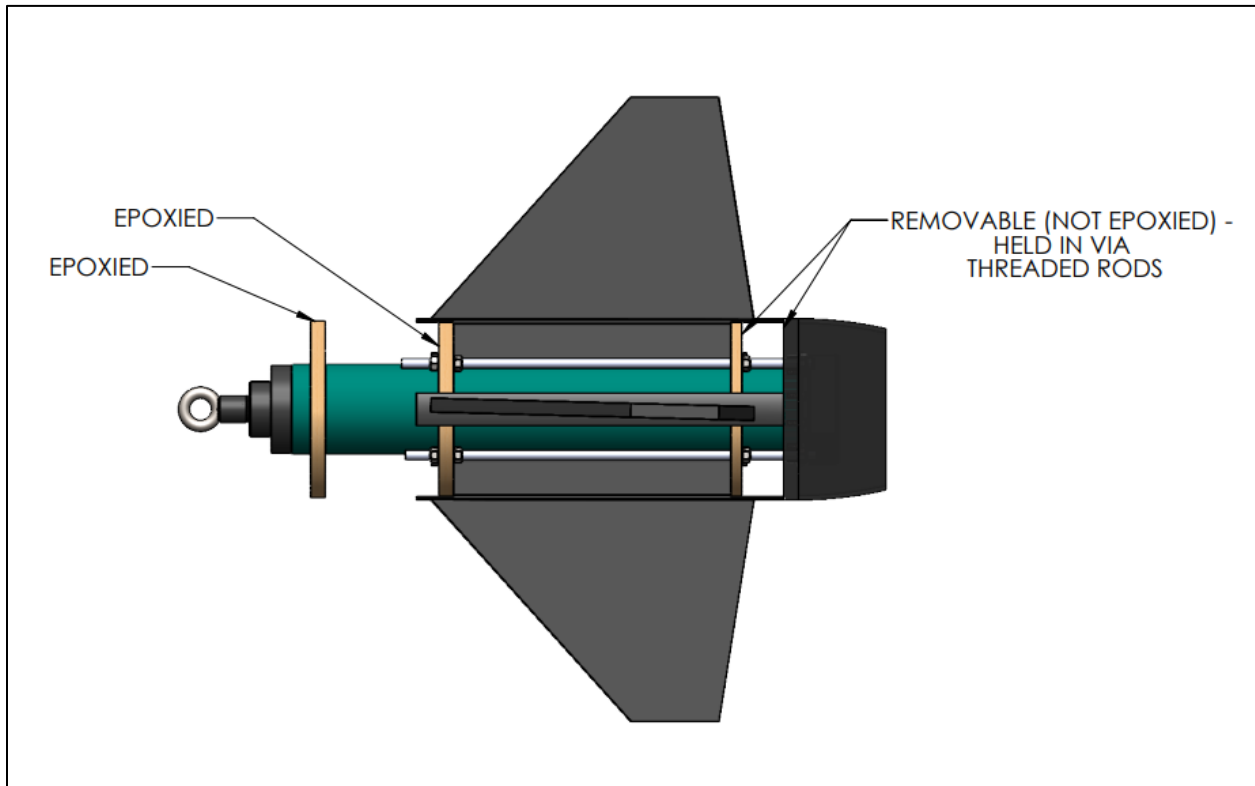


Figure 3-29. Fin Can Assembly CAD Drawing 2

The aft centering ring and the thrust plate/tail cone configuration were designed to be removable to allow the fins to slide out of the vehicle for modularity purposes. Simply remove the threaded rods from vehicle and the thrust plate will no longer be attached to the vehicle, allowing the aft centering ring to slide out of the vehicle. This will enable the fins to be removed from the vehicle and quickly replaced in the case of fin failure during assembly or testing.

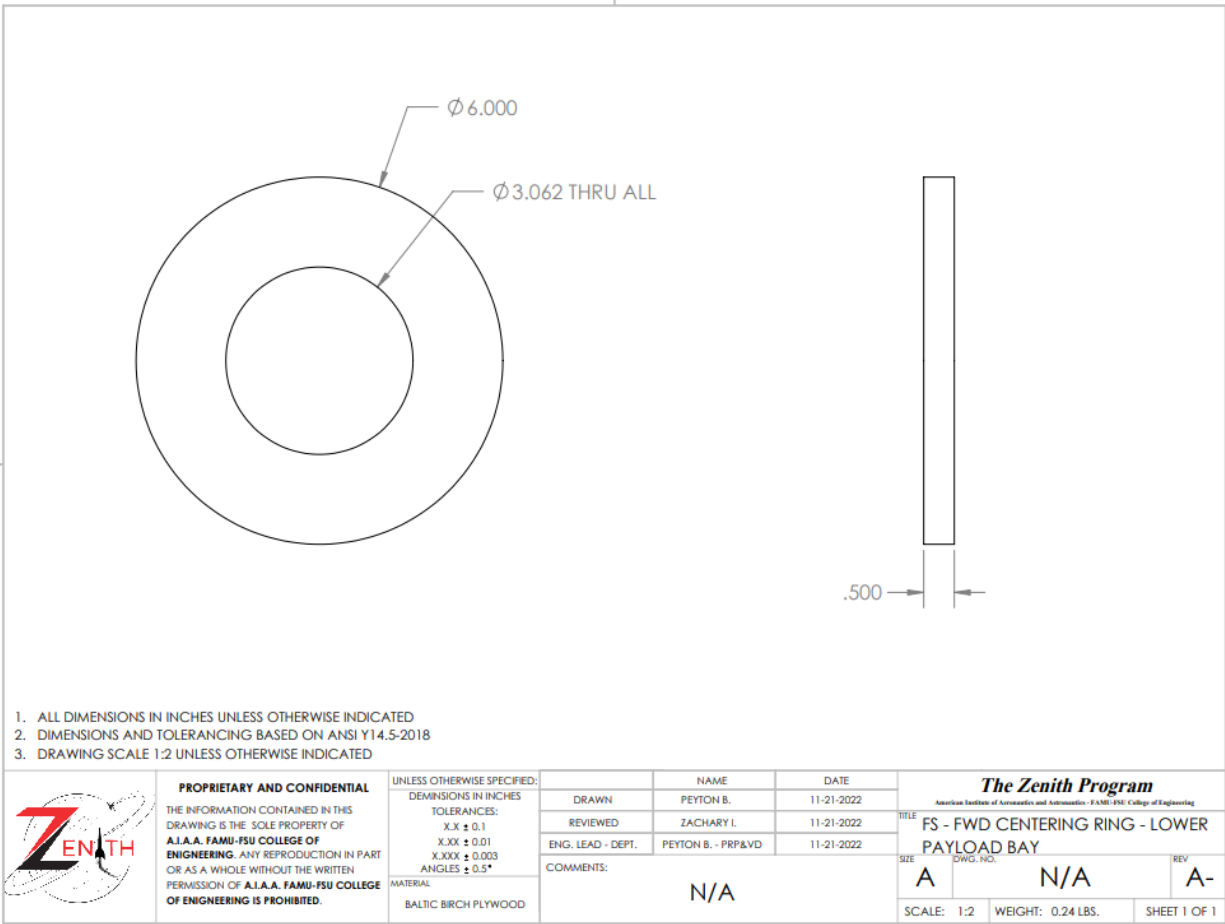


Figure 3-30. Forward Centering Ring CAD Drawing

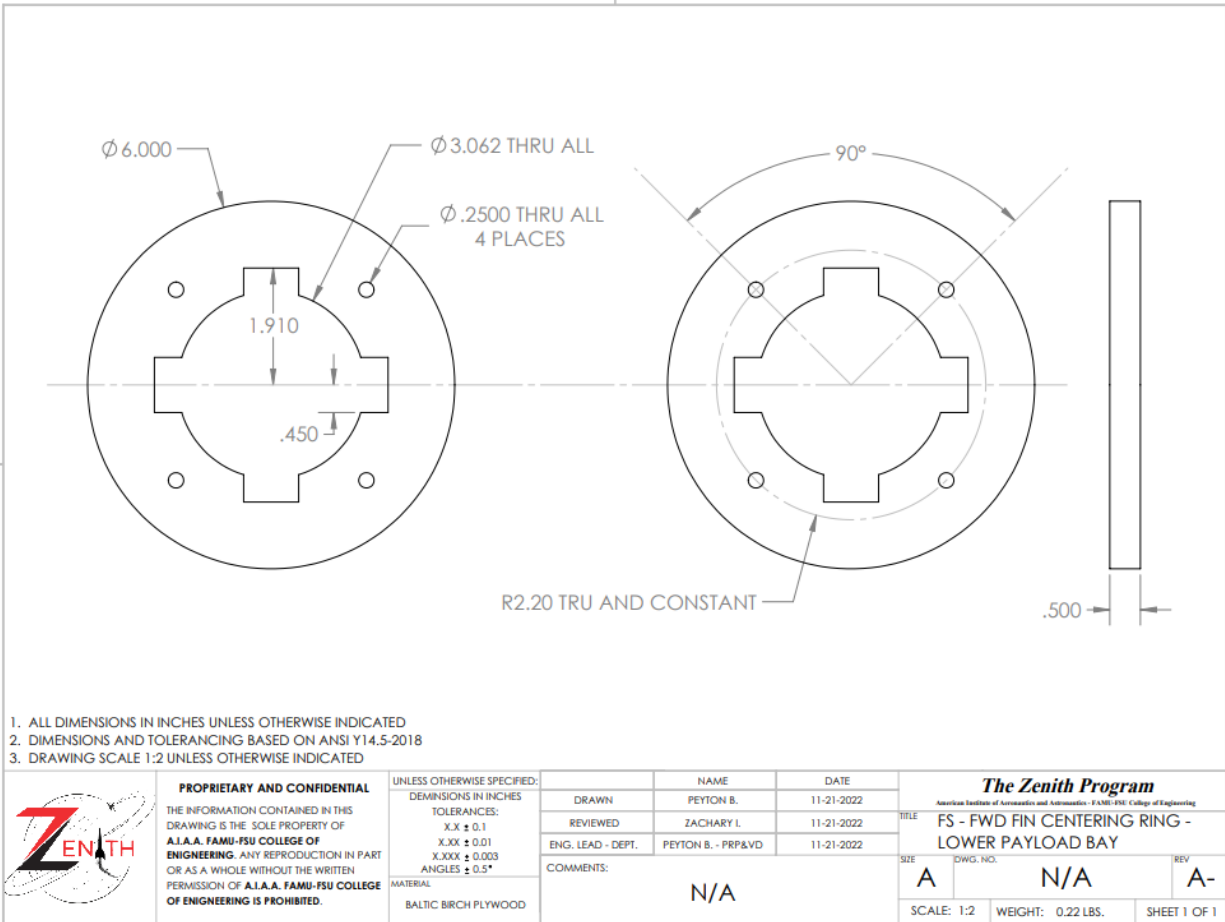


Figure 3-31. Forward Fin Centering Ring CAD Drawing

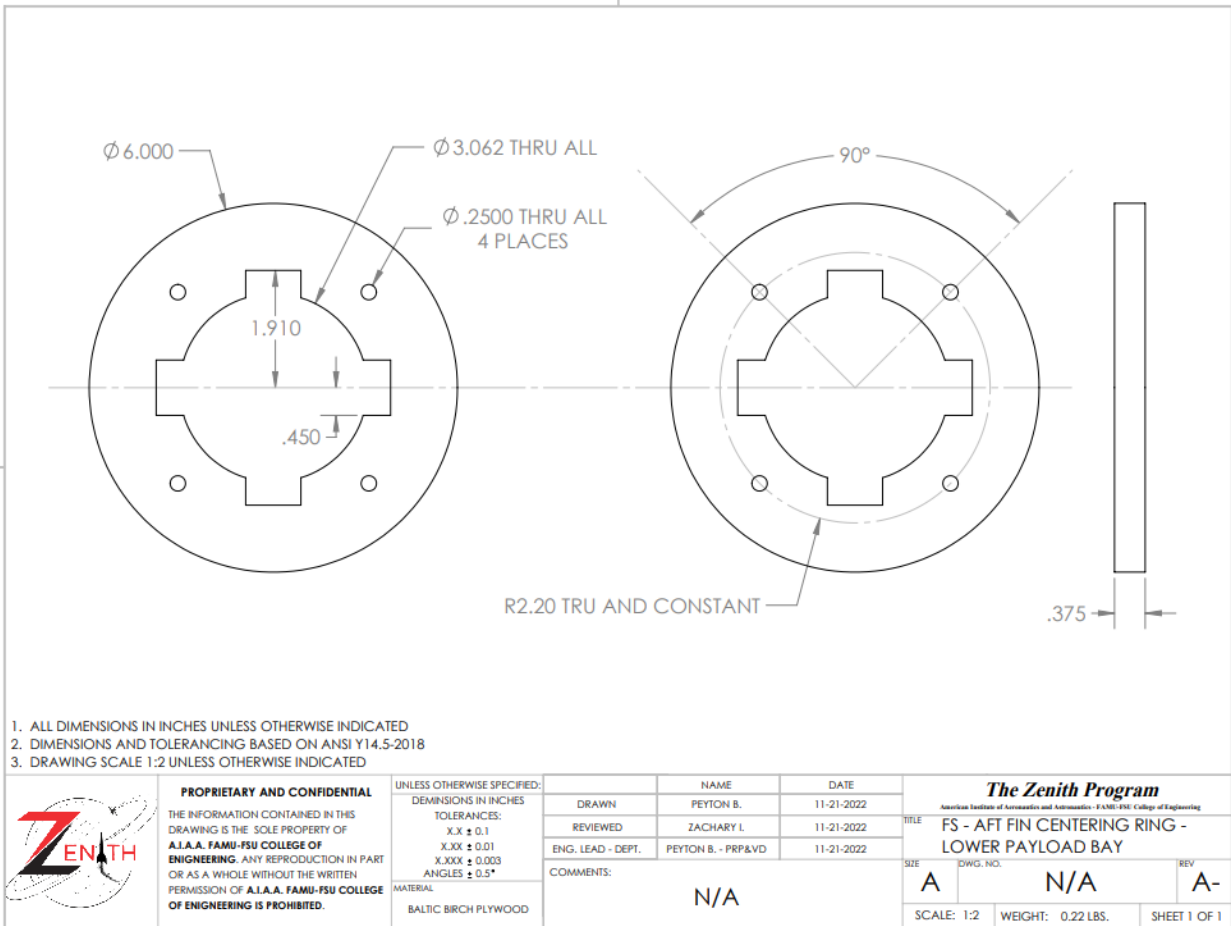


Figure 3-32. Aft Fin Centering Ring CAD Drawing

As previously mentioned, the thrust plate and tail cone configuration will be removable. The thrust plate and tail cone will be 3D printed as a whole component using ABS and will be held to the vehicle by the threaded rods. The flanged motor retainer body will be screwed to the 3D printed thrust plate using twelve 6# - 32 x 1/2" socket head cap screws.

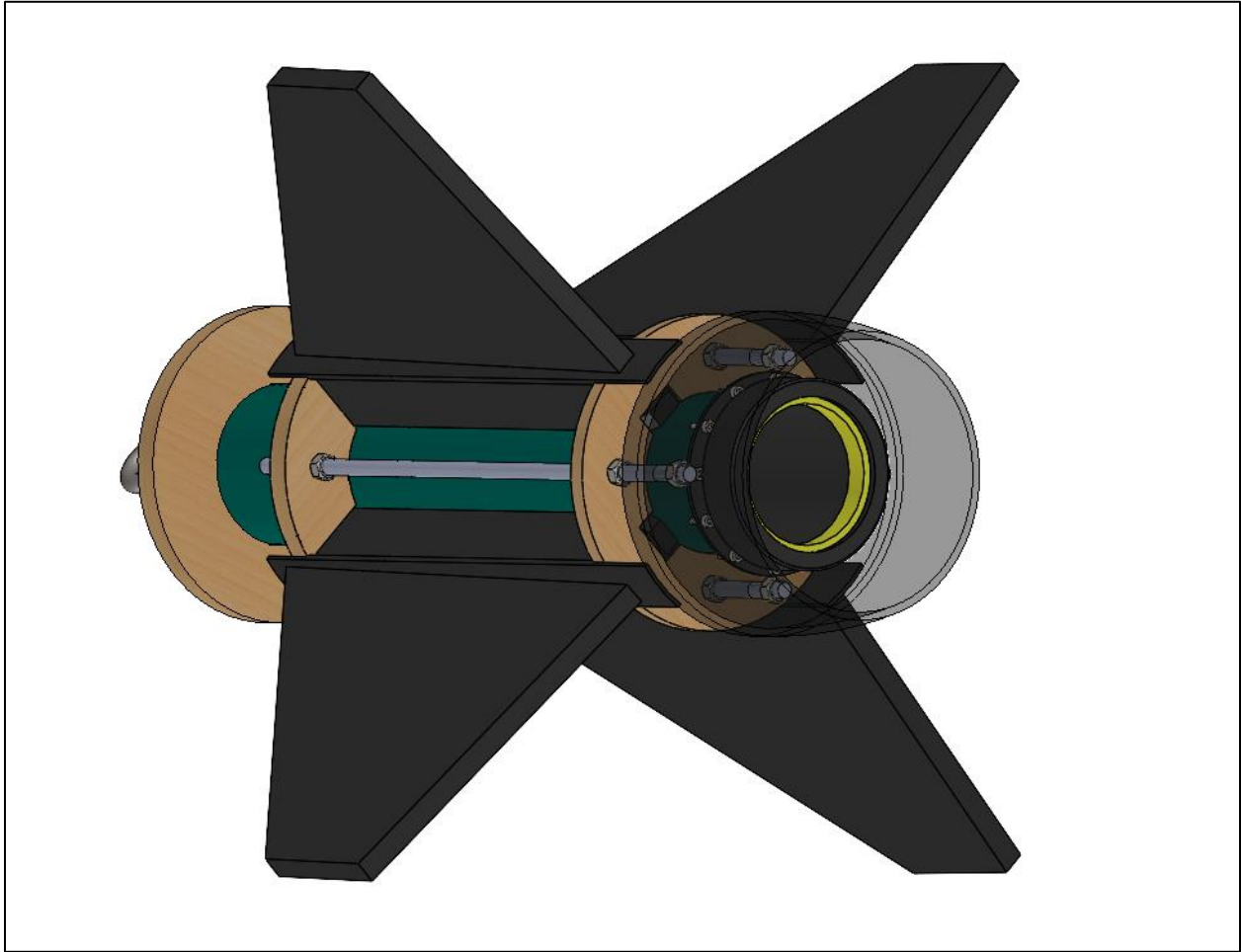


Figure 3-33. Fin Can Assembly w/ Transparent Tail Cone

The original leading design alternative discussed in PDR used an aluminum thrust plate and the team was considering using a tail cone to reduce the wake drag at the aft end of the vehicle. However, the weight of using an aluminum thrust plate is much heavier than a thrust plate printed from ABS. The aluminum thrust plate weighed 0.83 lb (380 g) at a thickness of 0.375 inches versus the ABS thrust plate weighing 0.43 lb (197 g) at a thickness of 0.5 inches. The decrease in weight raised the vehicle's stability margin and ultimately saved our team money on material and manufacturing costs. The newest and final design for the thrust plate and tail cone configuration shown below (not including the flanged motor retainer) and 3D printed at a 90% infill density weighs 0.73 lb (330 g). The thickness of the thrust plate is 0.5 inches, and the length of the tail cone is 3 inches.

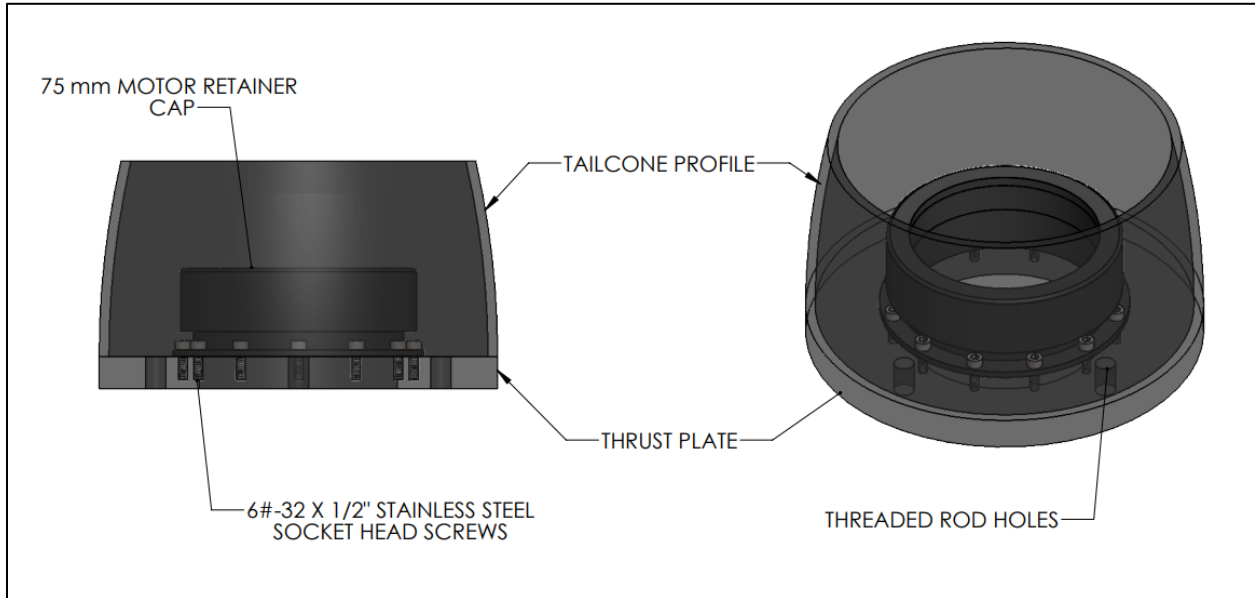


Figure 3-34. Tail Cone CAD Model

In traditional tail cone designs, the tail cone profile is much longer in order to act as a motor retainer. The length of the tail cone for our final design has been shortened and will not act as a motor retainer. The tail cone was implemented into the vehicle's designed to prevent the aft end wake of the vehicle and enhance the overall aesthetic. The length was shortened to prevent any direct contact to the exhaust flame during flight that could cause the ABS to melt. To take extra precaution, fiberglass sheets will be formed around the inner surface of the tail cone to reduce the amount of heat transfer to the ABS. The diameter of the thrust plate is the same diameter as the outer diameter of the vehicle's airframe and the tail cone's curvature is tangent to the vehicle's outer airframe surface. As the vehicle is launched, the thrust load will be transferred to the airframe as the thrust plate pushes against the aft end of the airframe.

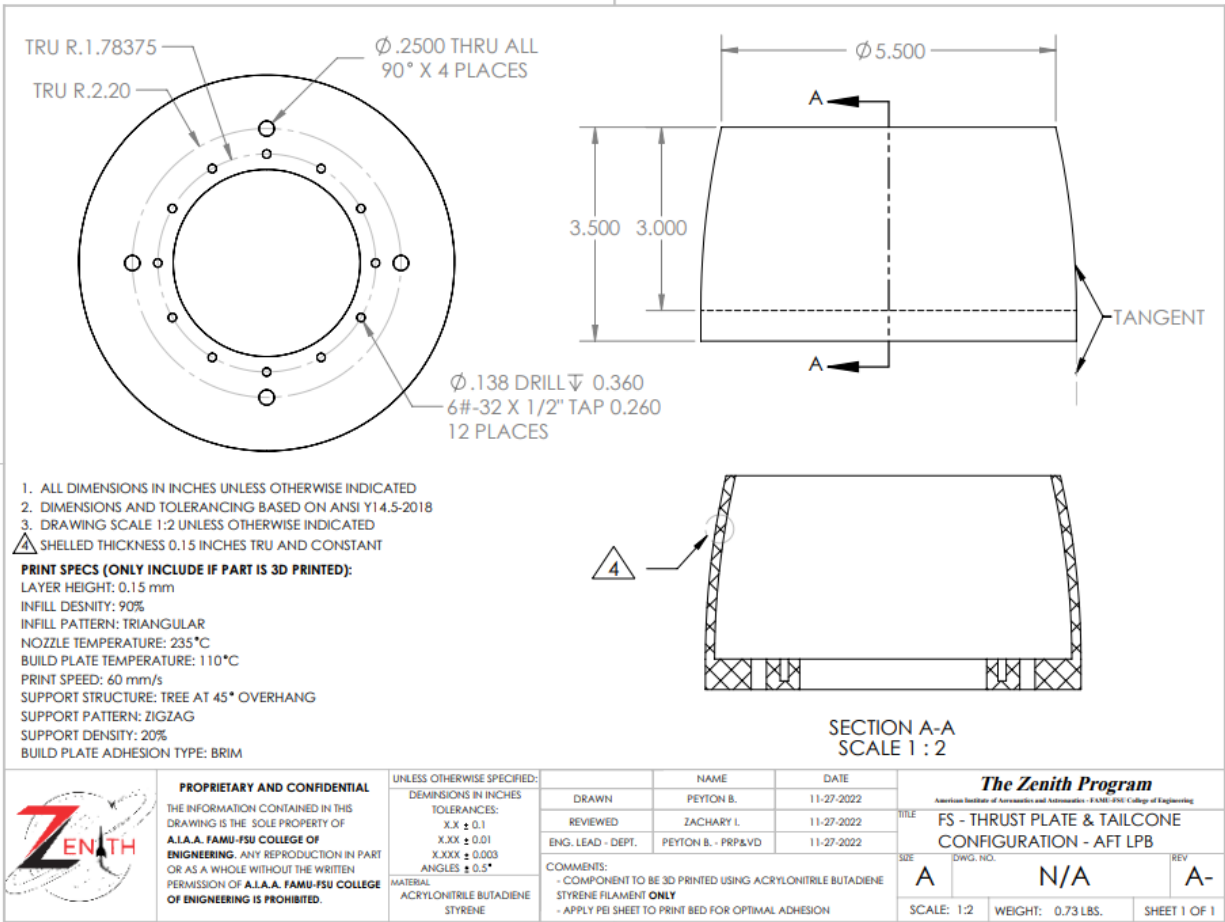


Figure 3-35. Tail Cone CAD Drawing

3.1.4 Manufacturing and Assembly

3.1.4.1 3D Printed Components

One of the considerations that must be made when creating a part with additive manufacturing (especially FDM 3D printing) is the orientation in which the part is printed. The print orientation is important because it will determine which plane the layers of a part are built up in. A majority of printed parts on this vehicle will be made of ABS plastic. When ABS is 3D printed, the bonds that hold layers to each other are weaker in tension than the material itself, therefore 3D printed ABS components will be the strongest when force is applied parallel to the print planes.

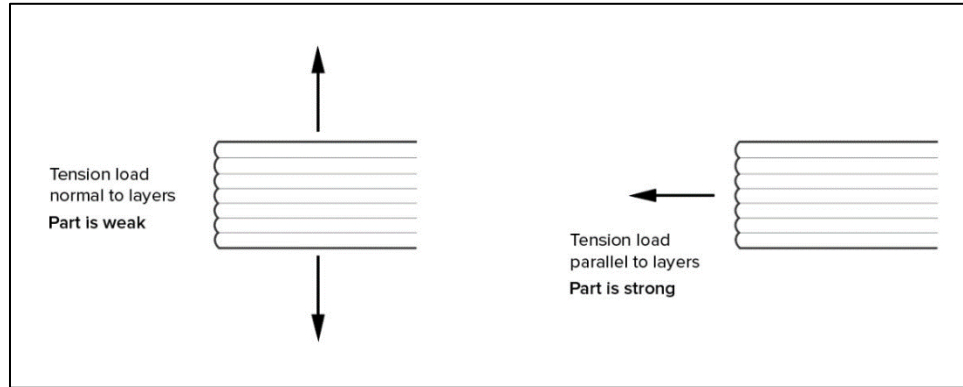


Figure 3-36. ABS Strength Characteristics

Printed ABS parts are strong and will maintain all desired dimensions if printed correctly, but some components will require post-processing to function properly. Because the prints are weakest perpendicular to the layer planes, post-processing can strengthen the connection between layers, normalizing the strength of the part. ABS melts when exposed to acetone, so immersing parts in an acetone vapor bath can fuse the outermost layers together. In addition to acetone smoothing, printed components can be coated with a thin layer of epoxy resin to build a hard outer shell to parts.

In order to quantify the effects that layer orientation and post-processing hardening methods have on the strength of the parts, a number of tests will be run. These tests will include a Short Beam Shear (SBS) test, an Izod hardness test, and applying measured forces on full scale parts. The SBS test will involve a small sample cuboid (8mm x 24mm x 4mm) being held between 2 notches, then applying a measured shear load to the sample. The SBS test is expected to provide helpful results as to how print orientation affects shear strength, but the small size of the samples limits the ability to test how different infill patterns and density will affect the parts. In order to learn about the factors not accounted for in the SBS test, an Izod hardness test will be conducted. The Izod hardness test involves impacting a notched specimen to observe fracture. Results from the SBS test will be considered when interpreting Izod data, to verify if results are due to layer orientation or infill qualities.

Testing of full-scale parts will be done by adding hanging weights to a part, and hopefully with a wind tunnel. Applying weight to a print allows for the part to be mounted in a similar fashion to how it will be on the vehicle, and the limits of each component will be accurately assessed. The wind tunnel (if tests are able to be completed) will allow for a better understanding of flow properties than could be secured with CFD. The use of a wind tunnel will also allow for testing of components to see if uncoated prints will “peel” layers away at high velocities, as well as if coated prints will flake off surface ABS or any epoxy resin coat. The nosecone, fins, and thrust plate/tail cone will be printed on a BIQU BE SE Plus 3D printer using ABS filament. To account for ABS deformation during the print, polyetherimide (PEI) adhesive sheets will be placed on

the printing bed for optimal adhesion. PEI sheets were used for the subscale components and will be replicated in printing the full-scale components.

(a) Nosecone

The subscale nosecone was printed as two parts: the nosecone profile, and the shoulder. The shoulder piece is 2.25 inches in length and had a threaded coupling end to screw into the receiving end of the nosecone component. The nosecone profile was 10 inches in length and is shown below.

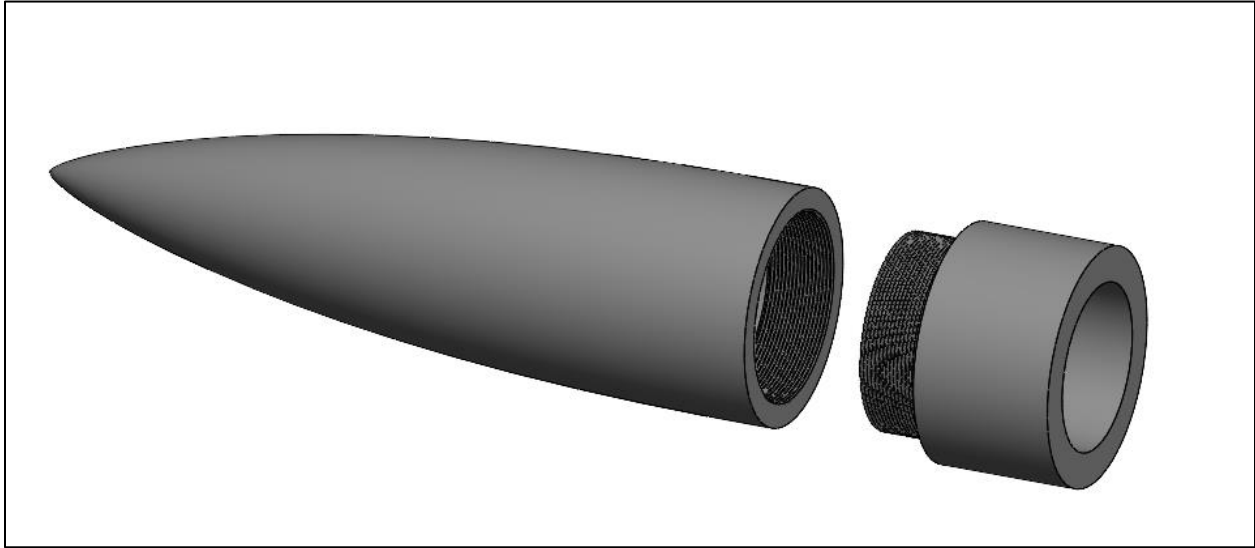


Figure 3-37. Subscale Launch Vehicle Nosecone

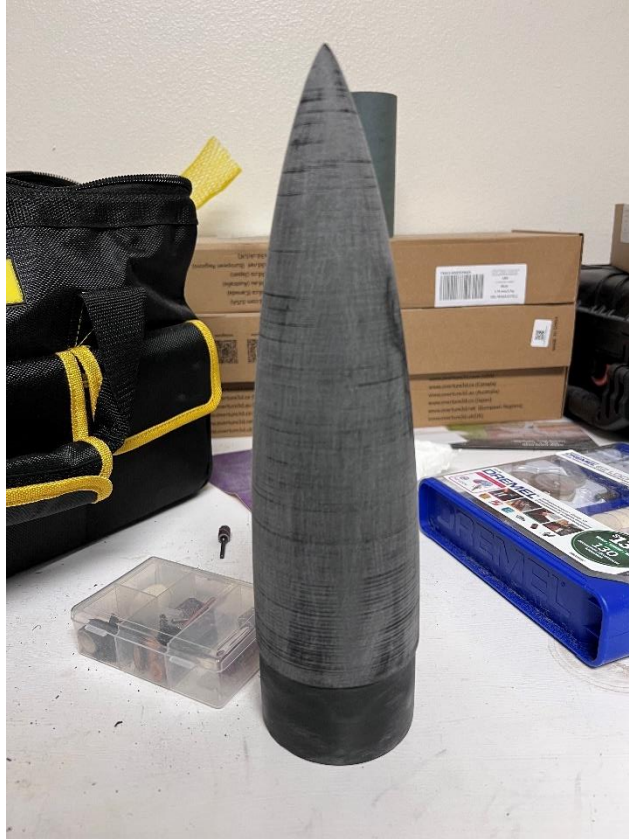


Figure 3-38. Subscale Launch Vehicle 3-D Printed LD-Haack Nosecone

The printing orientation plays a big role in the performance of the print, the nose cone for both the subscale and the full-scale vehicle are printed vertically. With printing ABS, there will more than likely be some deformation regardless of how insulated the machine is or how much adhesion is provided to the part. To account for this, the base of the nosecone shoulder and the profile was printed $3/8''$ longer than the actual model so that the team could sand down the base to ensure a smooth and flat base at the exact length simulated in OpenRocket and modeled in SolidWorks. Shown below is the orientation and print specifications for the subscale and full-scale nosecone using Ultimaker Cura software.

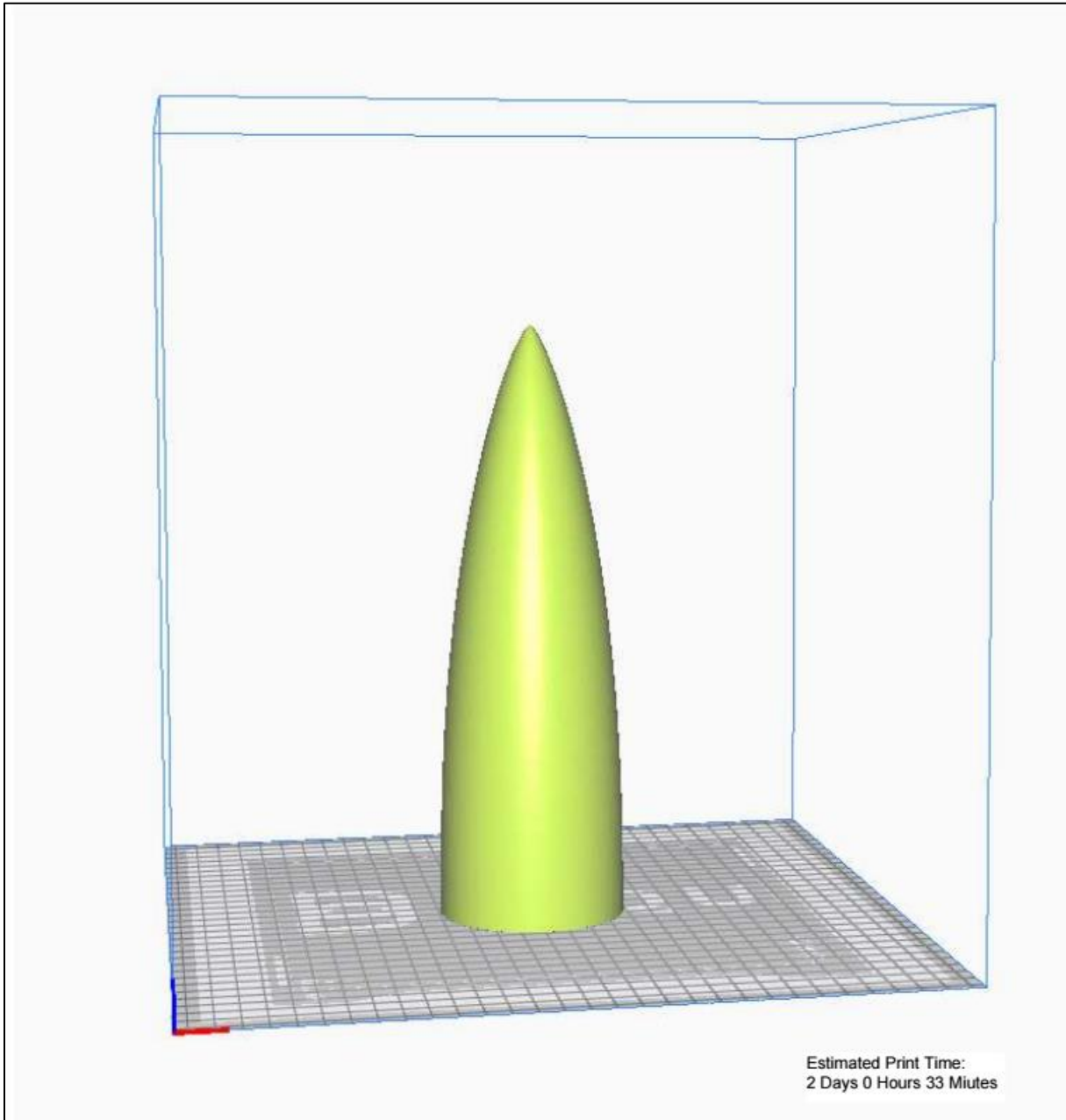


Figure 3-39. Subscale Nosecone Assembly

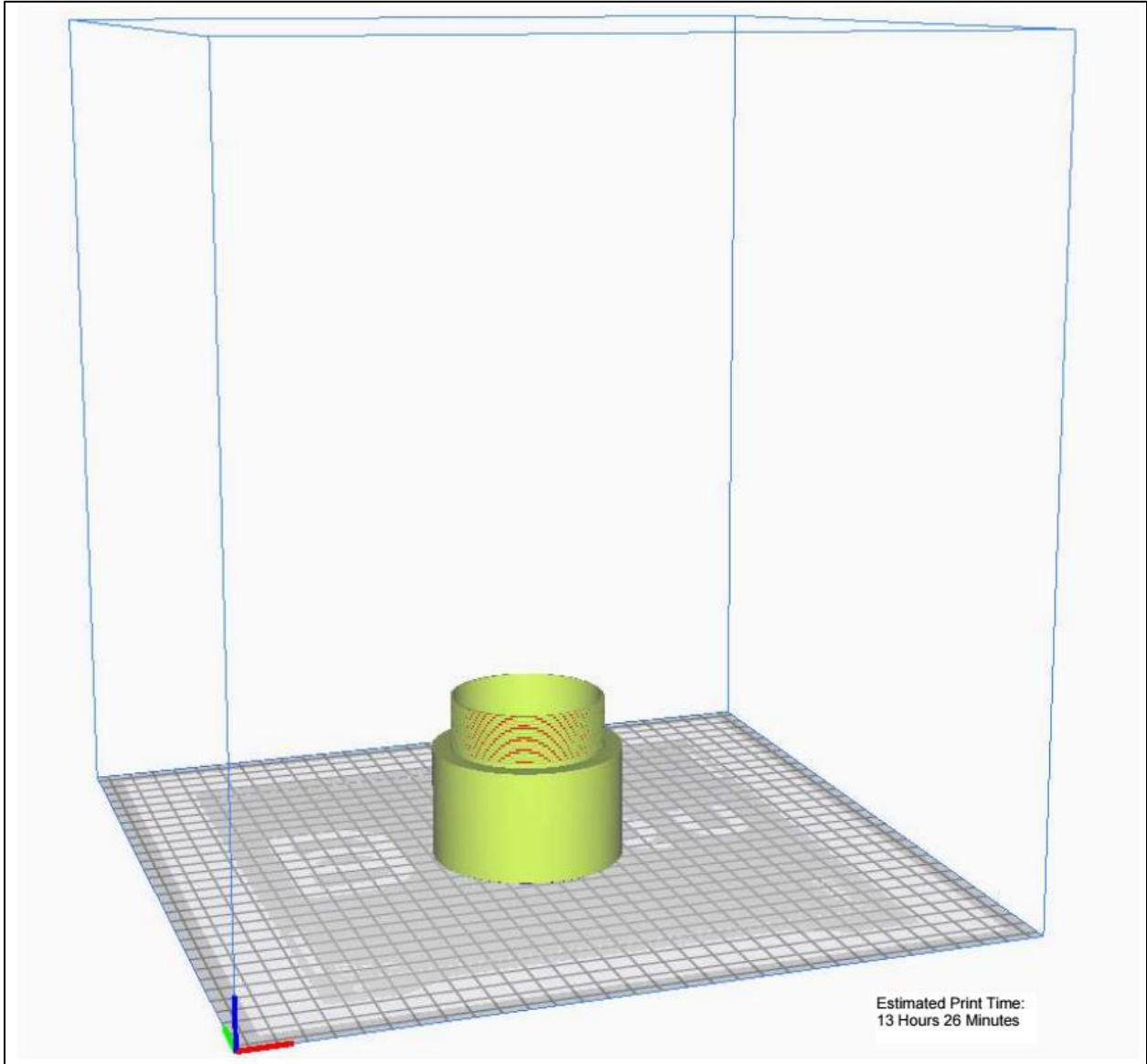


Figure 3-40. Subscale Nosecone Shoulder

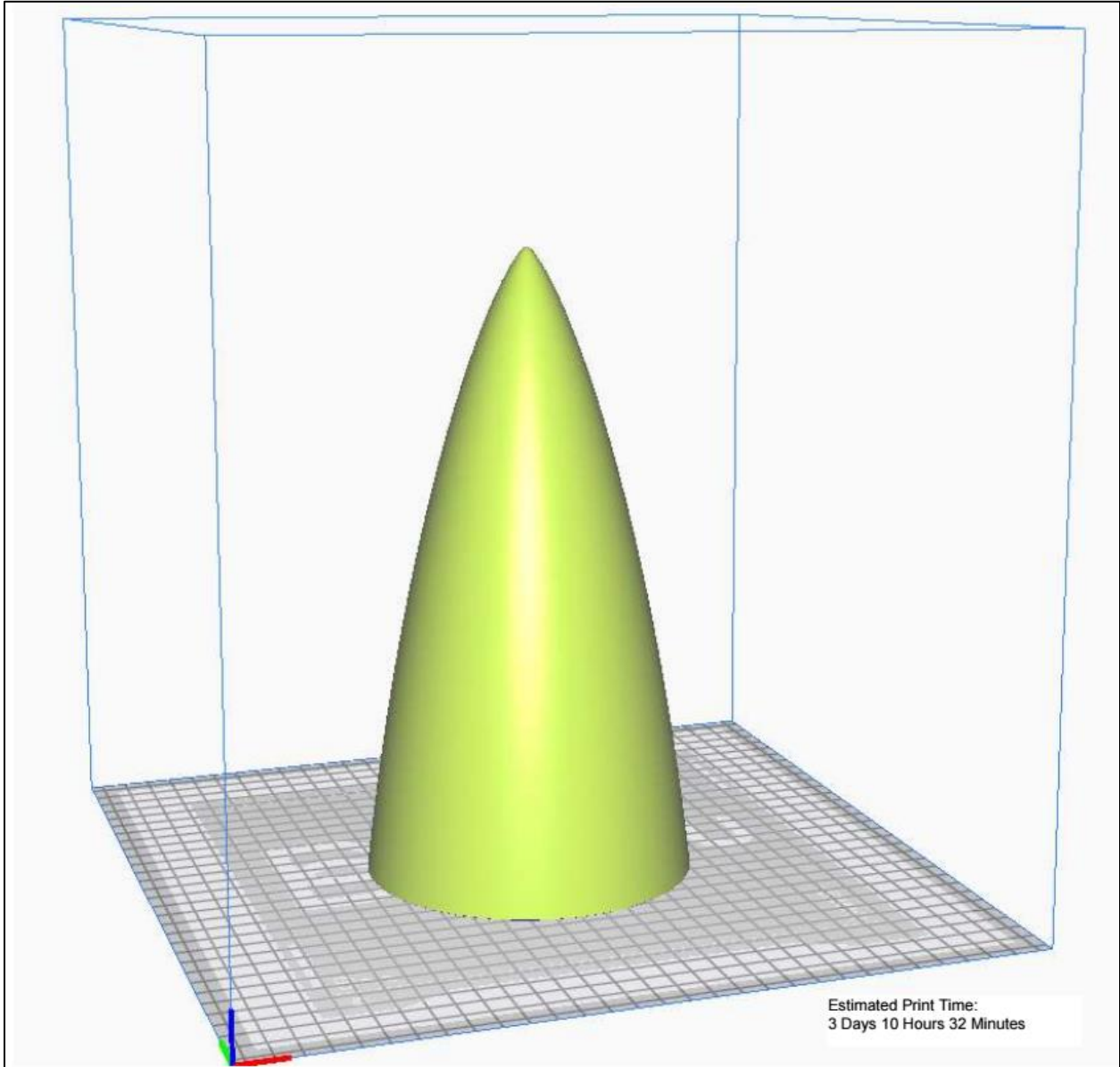


Figure 3-41. Full Scale Nosecone Cap

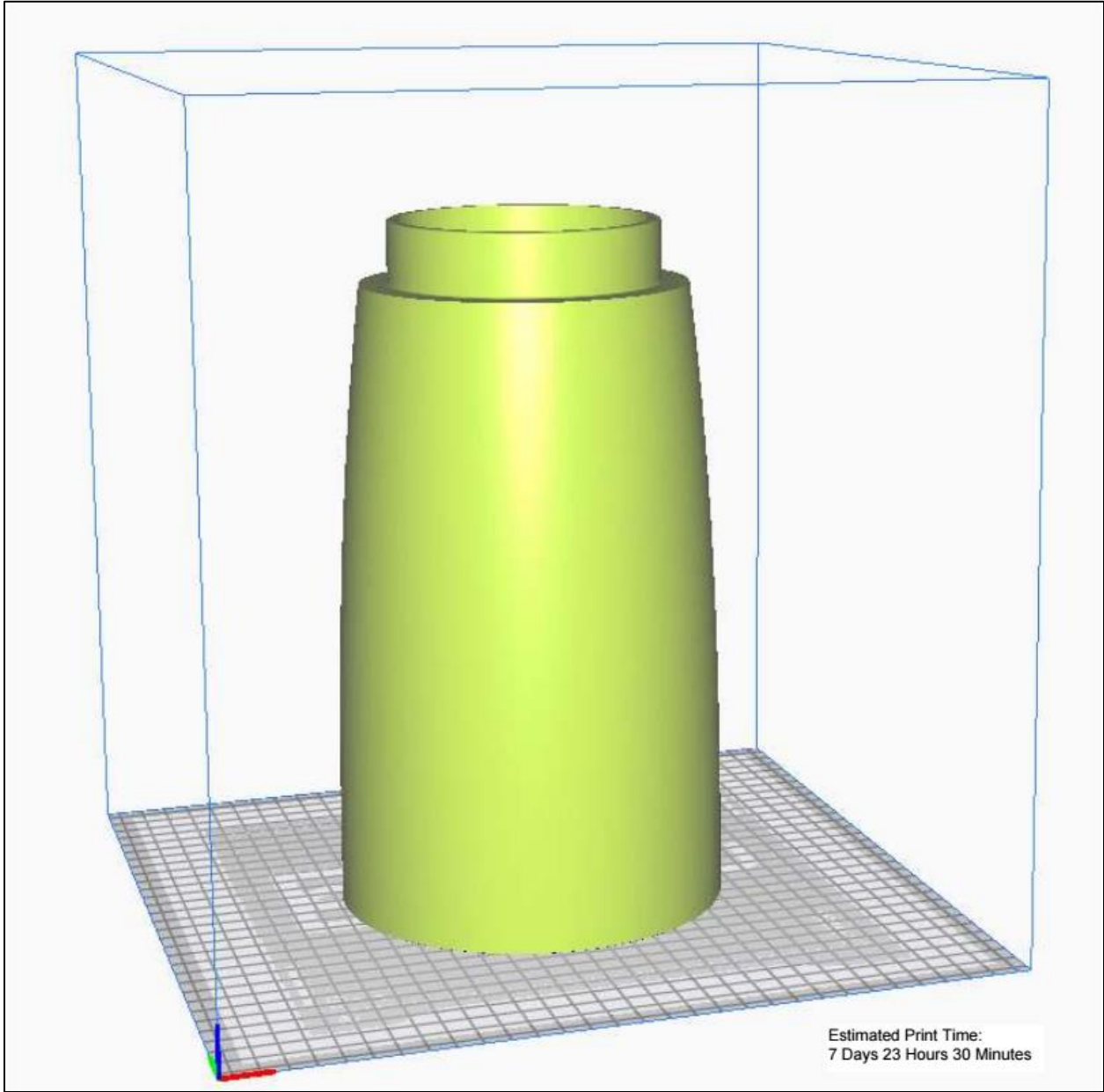


Figure 3-42. Full Scale Nosecone Midsection

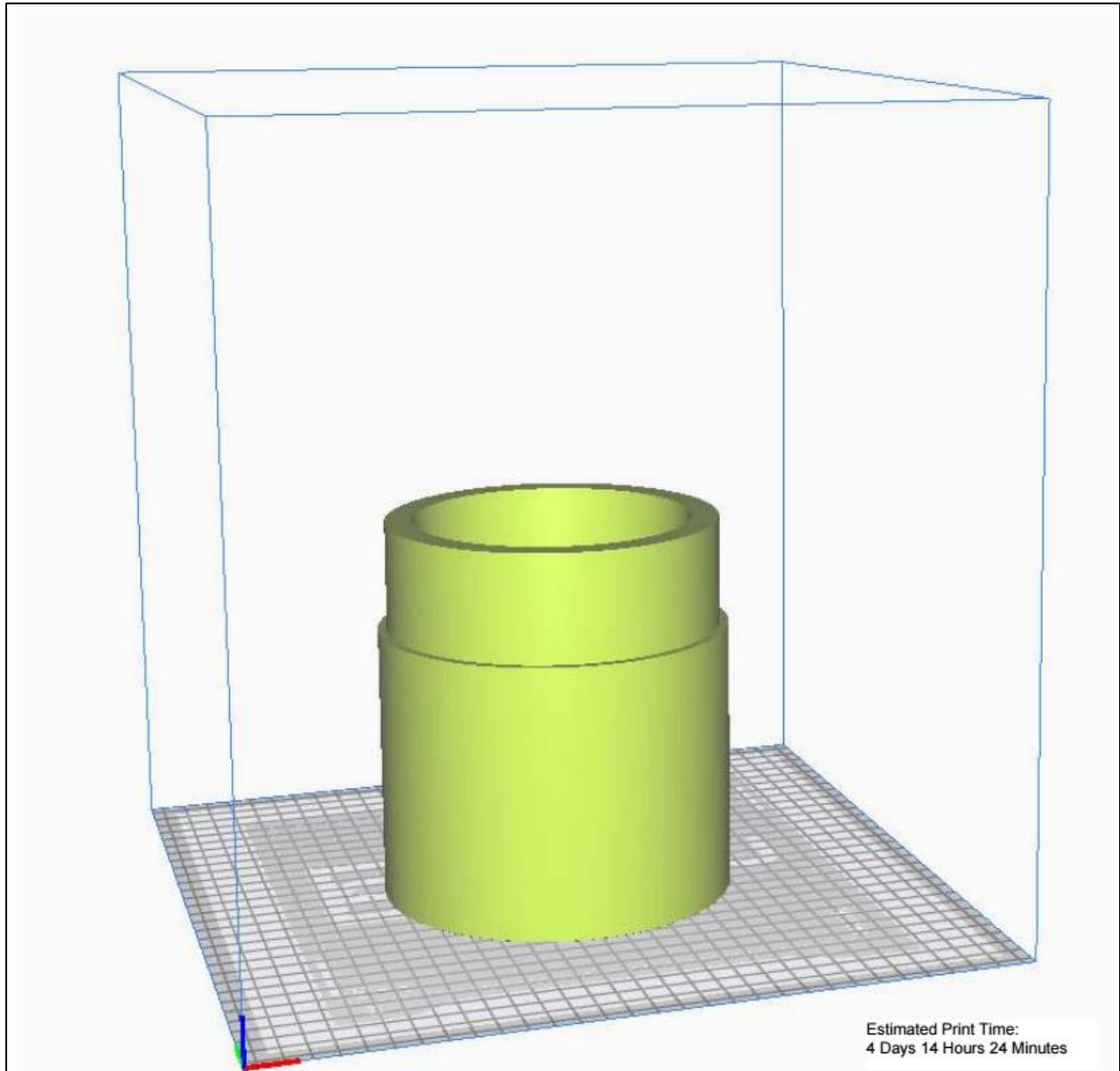


Figure 3-43. Full Scale Nosecone Shoulder

NOTE: The printing specifications shown below will be used for the full-scale vehicle nose cone due to successful subscale print.

Ultimaker Cura Printing Specifications	
Layer Height	0.15 mm
Infill Density	85%
Infill Pattern	Triangular
Nozzle Temperature	235°C
Build Plate Temperature	110°C
Print Speed	60 mm/s
Support Structure	Tree Structure at 45° Overhang
Support Pattern	Zigzag
Support Density	10%
Build Plate Adhesion Type	10 mm thick Brim

(b) Fins

The subscale fin shown below represents a ½ scale of the full-scale fin.



Figure 3-44. 3-D Printed Subscale Fin

Looking at the image above, the subscale fin experienced a small amount of deformation at the fin tab base and the fin root chord base. Many different printing methods were used to try and counteract the deformation such as PEI adhesion printing sheets, different printing structural supports, and different print speeds. Figure 3-44 shows the best print of the many attempts. So, the printing specifications used for the 3D printed fin show in figure 3-44 were the print specifications used for the rest of the fins. PETG will be ordered and printed to compare fin prints between ABS and PETG to further our 3D printing study. Shown below is the fin assembly used for the subscale flight.



Figure 3-45. Subscale Fins Installed

Looking at the image above, electrical tape was put in the base of the fins and the airframe to form a flush surface between the fin base and the outer surface of the airframe. The electrical tape provided successful results in terms of fin performance; however, the full-scale 3D printed fins will guarantee a non-deformed, flush fit with the fins into the fin slots. Shown below is the orientation and print specifications for the subscale and full-scale fins using Ultimaker Cura software.

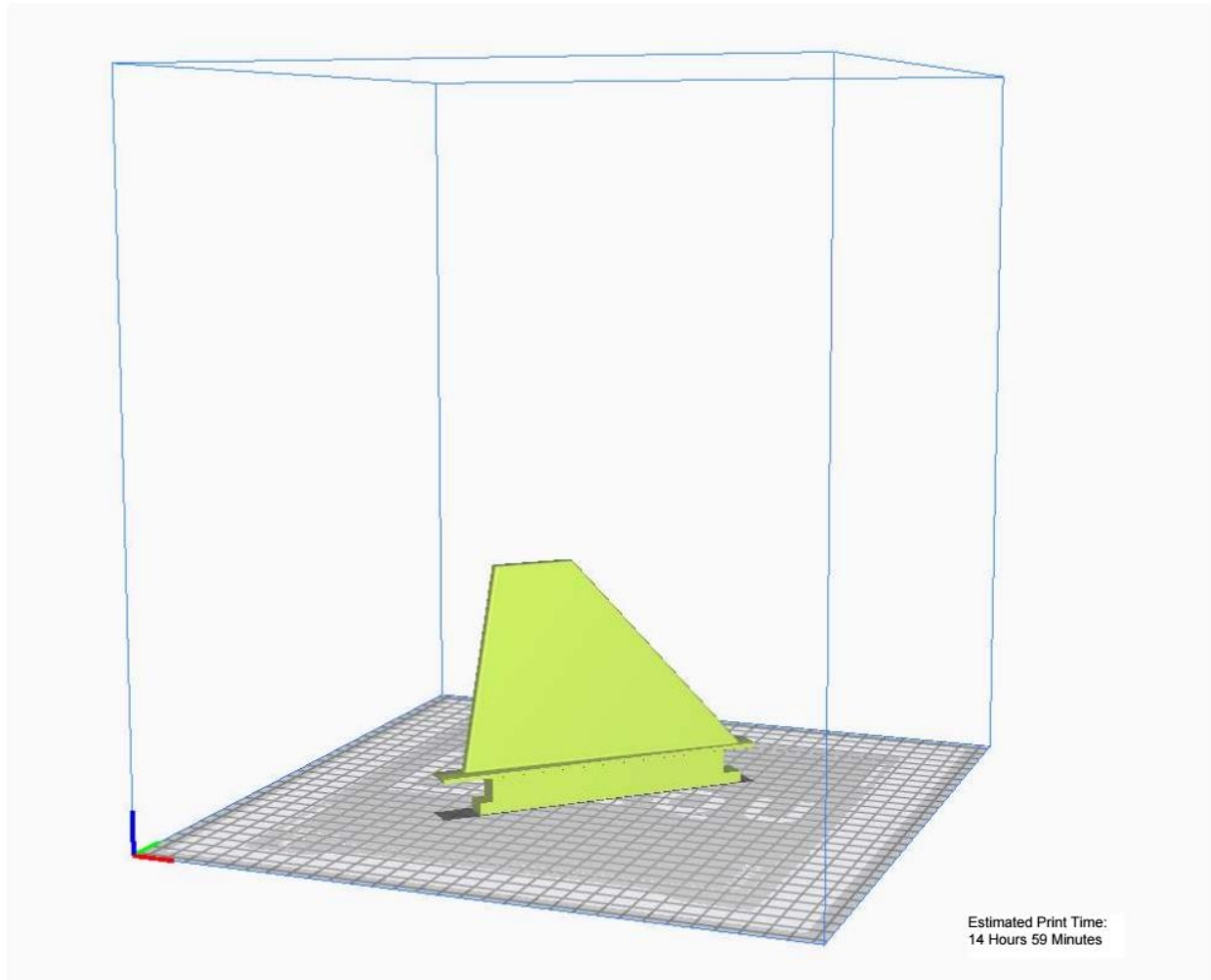


Figure 3-46. Subscale Fin

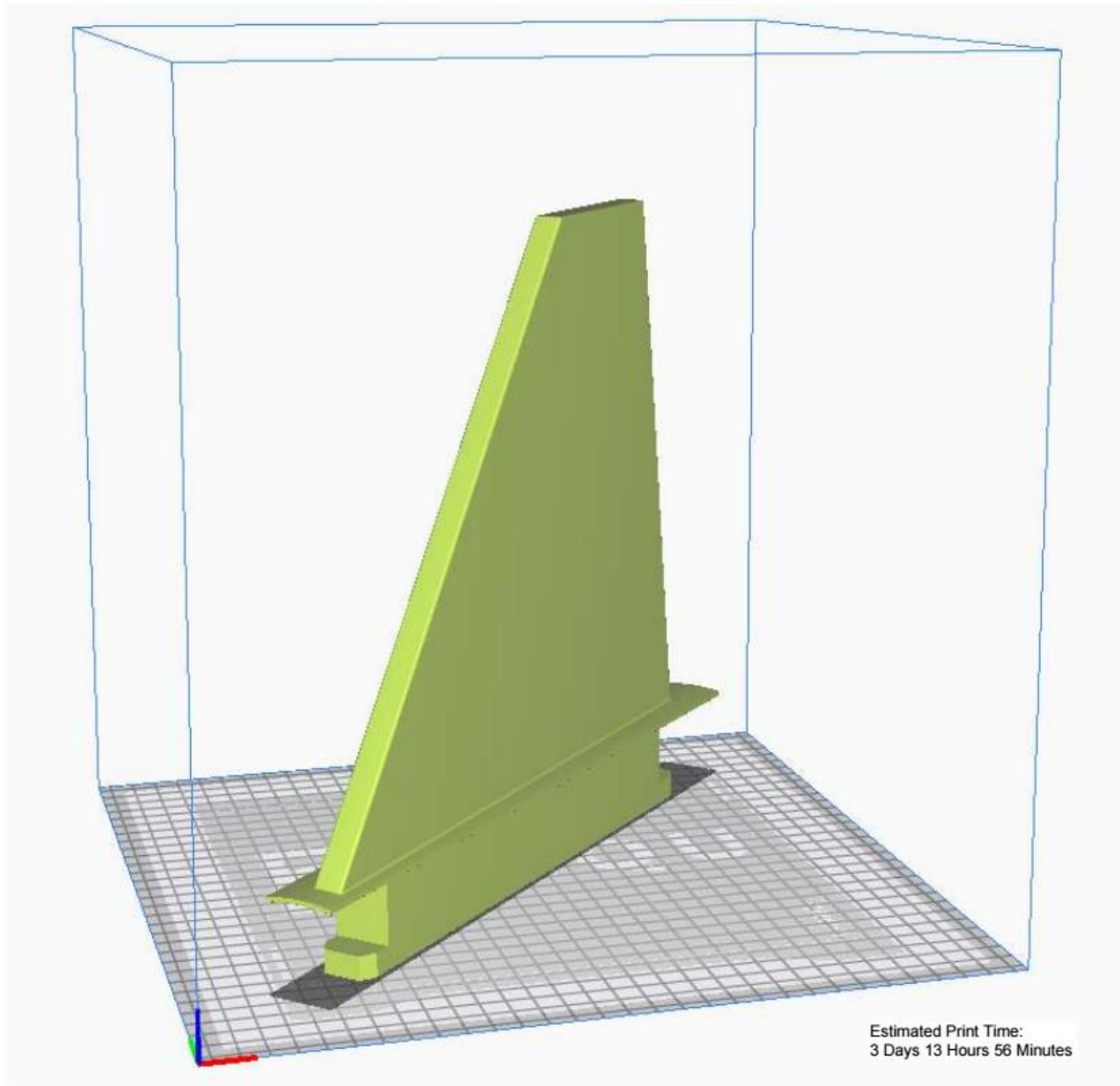


Figure 3-47. Full Scale Fin

Ultimaker Cura Printing Specifications – SUBSCALE VEHICLE	
Layer Height	0.15 mm
Infill Density	85%
Infill Pattern	Triangular
Nozzle Temperature	235°C
Build Plate Temperature	110°C
Print Speed	60 mm/s
Support Structure	Normal Structure at 45° Overhang
Support Pattern	Zigzag
Support Density	10%
Build Plate Adhesion Type	10 mm thick Brim

The infill density for the full-scale fins will be less than the subscale. The infill density was lowered to improve the stability margin during the OpenRocket simulation phase of the final full-scale design.

Ultimaker Cura Printing Specifications – FULL-SCALE VEHICLE	
Layer Height	0.15 mm
Infill Density	72%
Infill Pattern	Triangular
Nozzle Temperature	235°C
Build Plate Temperature	110°C
Print Speed	60 mm/s
Support Structure	Normal Structure at 45° Overhang
Support Pattern	Zigzag
Support Density	20%
Build Plate Adhesion Type	10 mm thick Brim

(c) Tail Cone and Thrust Plate Configuration

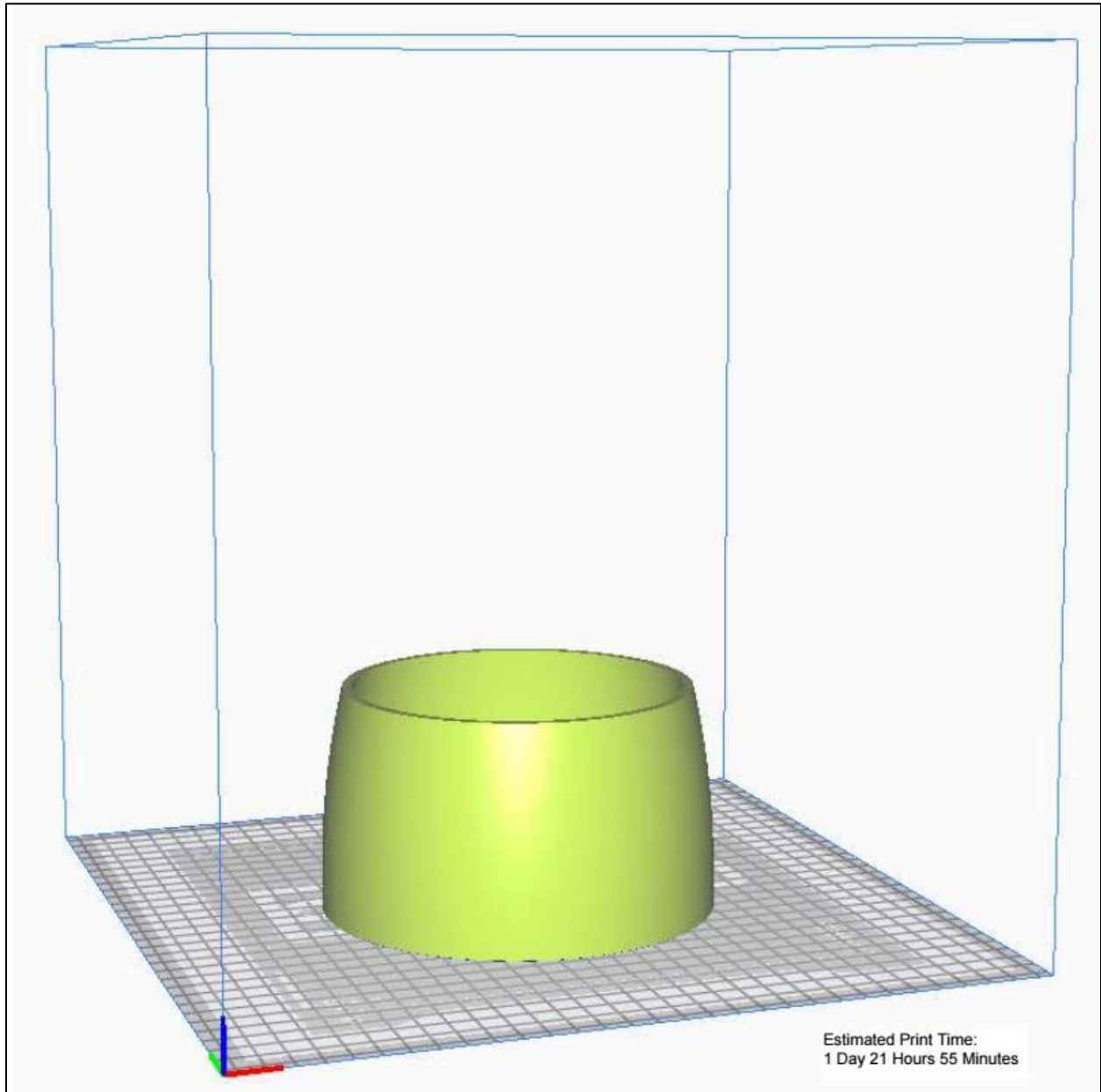


Figure 3-48. Integrated Thrust Plate and Tail Cone

Ultimaker Cura Printing Specifications – FULL-SCALE VEHICLE	
Layer Height	0.15 mm
Infill Density	90%
Infill Pattern	Triangular
Nozzle Temperature	235°C
Build Plate Temperature	110°C
Print Speed	60 mm/s
Support Structure	Tree Structure at 45° Overhang
Support Pattern	Zigzag
Support Density	20%
Build Plate Adhesion Type	10 mm thick Brim

3.1.4.2 Airframe Cutting

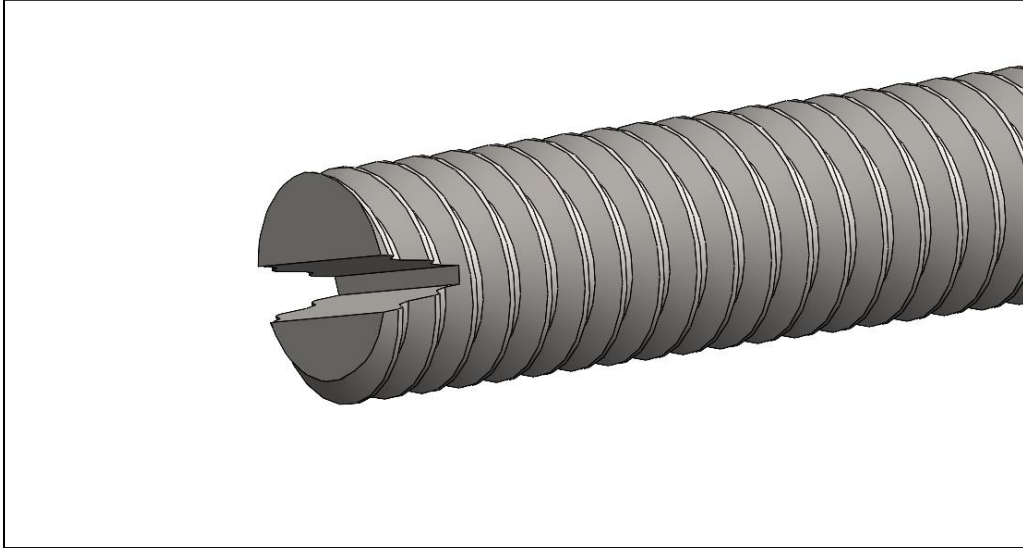
The airframe will be cut to size using a Dremel and Metal Wood cutting wheel attachment. After The airframe sections have been cut to size, the lower payload bay airframe will be sent to the FAMU-FSU COE's in housing manufacturing facility for professional personnel to cut the fin base slots. All other small holes and construction add-ons will be manufactured by the student team under faculty supervision.

3.1.4.3 Bulkhead and Centering Ring Fabrication

The bulkheads and centering rings will be cut using an in-house CNC wood router. After the bulkheads/centering rings have been CNC'd, sandpaper will be used to sand down any rough surfaces or edges.

3.1.4.4 Threaded Rods

The threaded rods for the avionics bay will be delivered in the correct length to accommodate the avionics bay. However, the threaded rods for the thrust structure will be cut to the appropriate size using a Dremel and disk cutting bit. The face at the end of each rod will be cut to replicate a flat head screwdriver. This allows the rods to be taken much quicker using a flat head screwdriver opposed to twisting the rods by hand until free.



3.1.5 Finite Element Analysis

Finite Element Analysis (FEA) simulations were ran on the nose cone bulkhead and the upper payload bay avionics bay bulkhead to ensure that the stress experienced on the bulkhead and U-bolt under recovery system loads will not cause any component failures. The FEA simulations were run in SolidWorks. Shown below are the material properties for each component. The properties found for Baltic Birch plywood were found online and the properties for the U-bolt were already in the SolidWorks database.

AISI 304 Stainless Steel		
Material Property	Value	Unit
Elastic Modulus	27557170.16	psi
Poisson's Ratio	0.29	N/A
Shear Modulus	10877830.32	psi
Mass Density	0.28902	lb/in ³
Tensile Strength	74986.976	psi
Yield Strength	29994.819	psi

Baltic Birch Plywood		
Material Property	Value	Unit
Elastic Modulus	435113.1016	psi
Poisson's Ratio	0.35	N/A
Shear Modulus	101526	psi
Mass Density	0.026	lb/in ³
Tensile Strength	14503.8	psi
Compressive Strength	3727.47	psi

3.1.5.1 Nose Cone Forward Bulkhead U-Bolt

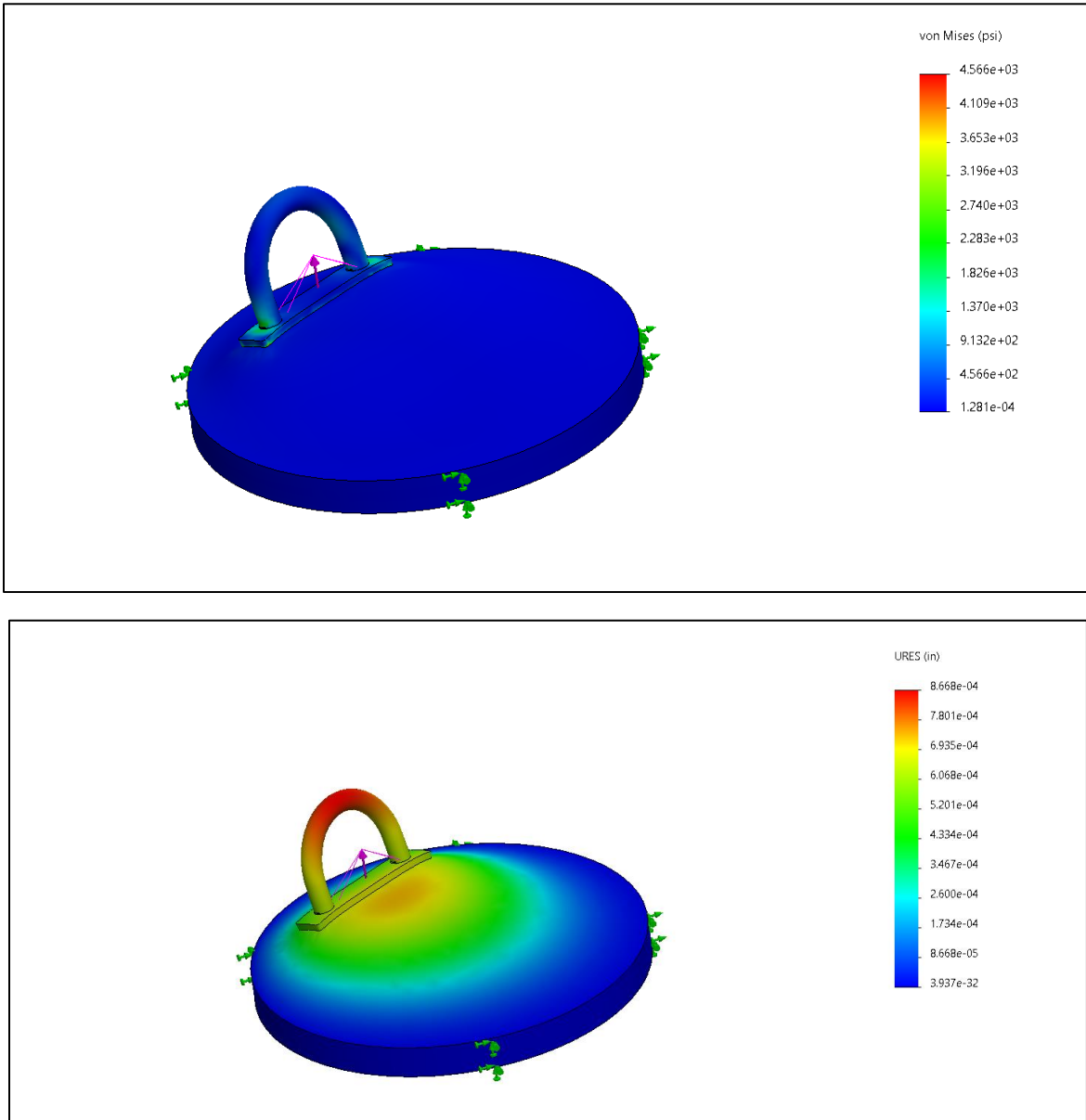


Figure 3-49. Forward Bulkhead FEA

The nose cone bulkhead is 0.5 inch thick Baltic Birch plywood with a 5/16" U-bolt/fastener plate configuration. The FEA was conducted with a force of 71.95 lbf pulling on the U-bolt to simulate the main parachute deploying. The bulkhead is a fixed structure in the simulation to mock the epoxied state of the real-time assembly. Deformations seen in the lower simulation are on the order of thousandths of an inch, therefore we can conclude that this configuration will hold under the load of chute deployment.

3.1.5.2 Avionics Bay Bulkhead U-bolt

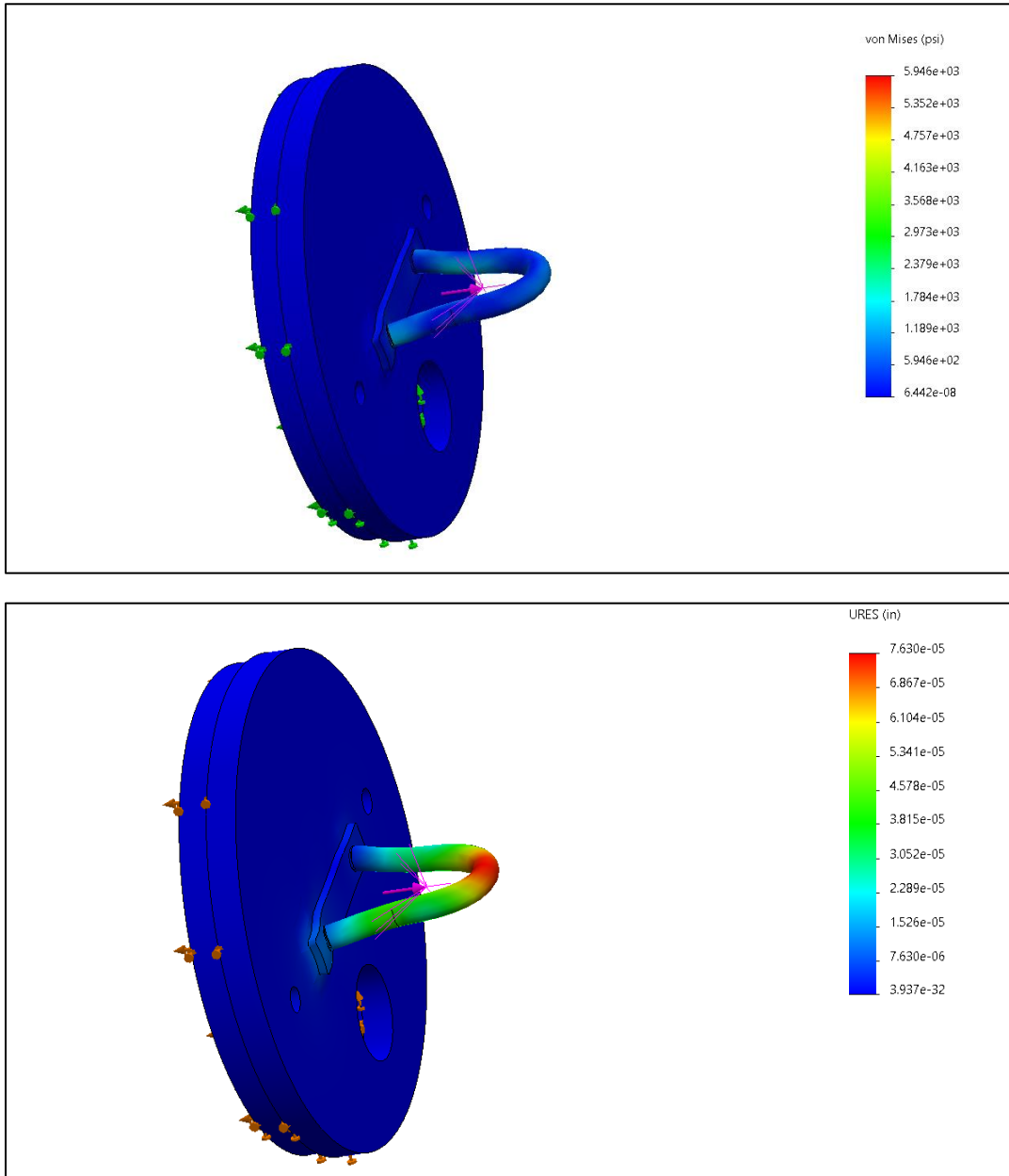


Figure 3-50. Avionics Bulkhead FEA

Similar to the foreword assembly, the avionics bay U-bolt and bulkheads were simulated under the maximum force during parachute deployment of 71.95 lbf. Deformations seen in the lower simulation are on the order of hundreds of thousandths of an inch, even smaller than the forward bulkhead given the U-bolts are centrally located to better distribute the load in this case.

3.1.5.3 Thrust Plate/Tail Cone Configuration

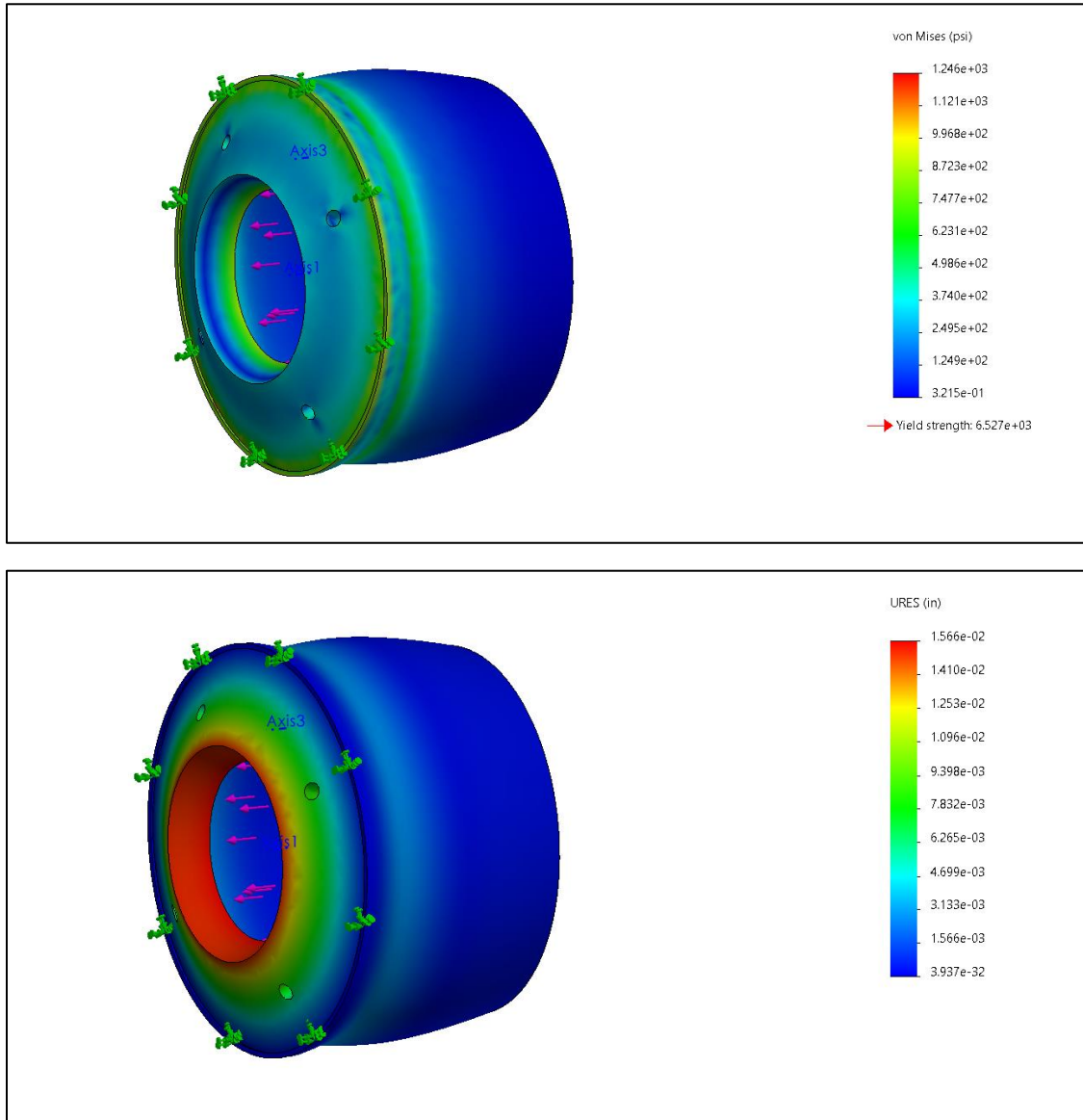


Figure 3-51. Integrated Thrust Plate & Tail Cone FEA

The tail cone and thrust plate were subjected to a simulated force of 420 lbf, the maximum thrust the motor will produce. The force was applied at the point where the retaining ring will contact the thrust plate, pushing up on the plate and transmitting force to the airframe. The largest deformations in this case were on the order of hundredths of an inch, which is acceptable considering that the motor only produces max thrust for ~ 0.8 seconds. The maximum deformation, which is still very small, occurs effectively instantaneously before the load begins to decrease rapidly.

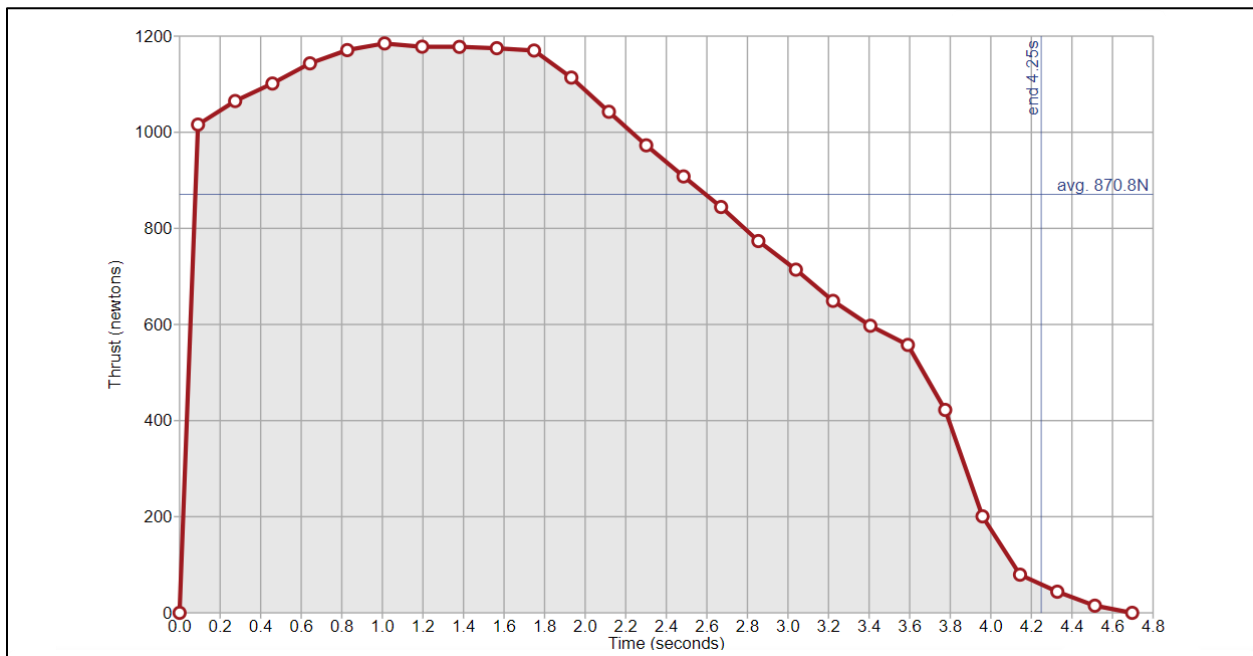
3.1.6 Vehicle Weight Breakdown

Table 3-3. Vehicle Section Weights

Vehicle Section	Mass (lb)
Nosecone	7.28
Upper Payload Bay	3.86
Payload	3.00
Avionics Bay	4.53
Lower Payload Bay + Fin Can	10.40

3.1.7 Final Motor Choice

The final motor selection to power the flight vehicle will be the Aerotech L850W. Originally the leading motor selection mentioned in PDR was the Cesaroni L3200. However, after further analysis of the vehicle’s stability margin, the Aerotech L850W has a longer burn time than the L3200. The longer burn time allows the stability margin to continuously stay well above 2.0 calibers longer and increases apogee by a few hundred feet than if the vehicle was powered by the L3200. The L850W also reaches a lower maximum thrust value and ultimately decreases the amount of thrust forces acting on the thrust structure for better structural integrity. Lastly, in terms of availability in purchasing, the Aerotech L850W was available for early purchase opposed to the L3200. Shown below is an image of the thrust curve of the L850W.



3.2 Subscale Construction Methods



Figure 3-52. Fin Slots

Cuts to the airframe to create the upper and lower payload bay, as well as the fin slots, were made with a bandsaw in the machine shop. Bulkheads and centering rings, after modification and hardware installation, were epoxied inside the airframe or fixed in place by threaded rods running the length of the section.

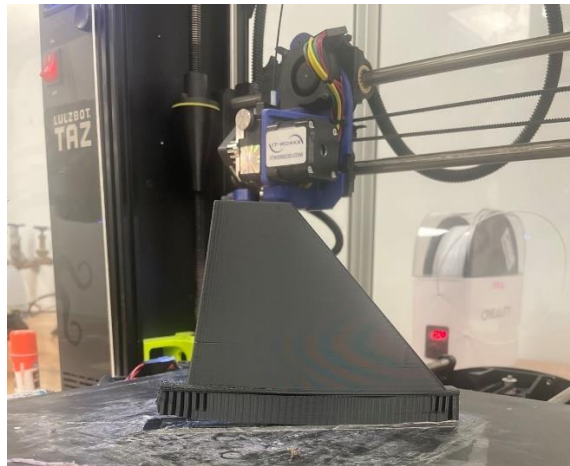


Figure 3-53. Fin on 3D Print Bed

Vehicle fins and nosecone were 3D printed using ABS filament in the Senior Design Lab, as well as on some of the Zenith Program team members' personal printers.

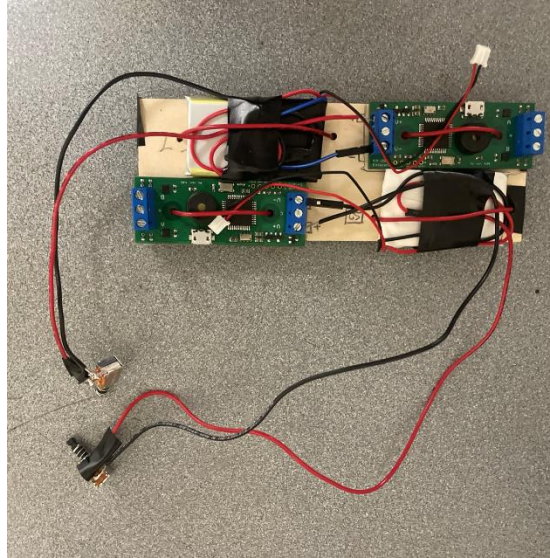


Figure 3-54. Avionics Sled

The avionics sled was constructed from a piece of plywood. Holes were drilled to allow cable to be passed through, holding components down to the sled. Electrical connections were made with standard jumper wires, with some connections, such as the switches, being spliced, soldered, and wrapped in electrical tape to hold firm. Extra length of wire was held down to the battery with electrical tape wraps, and the batteries were oriented with the charging cables pointing away from the sled for ease of access.



Figure 3-55. Avionics Bulkheads, Rods, and Ejection Charges

All holes for hardware such as threaded rods or eyebolts were drilled into bulkheads using a standard power drill. Odd-shaped holes, such as those for the CO₂ ejection charges to pass through, or the + shaped cutouts in the centering rings to slide the fin tabs into, were cut with a combination of chisels and dremel.

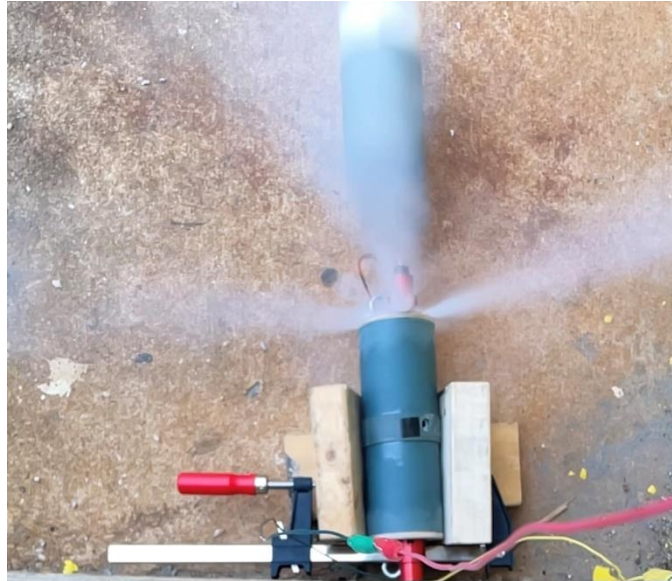


Figure 3-56. Ejection Test

The ejection system was tested in the block and clamp rig shown above, with a small closed-end section of airframe shear pinned to the avionics bay. Ejection was successful validating, that the ejection force was sufficient to snap the shear pins.



Figure 3-57. Vehicle in Paint Process

The vehicle exterior was decorated using matte black and gloss red spray paint, and letter stencils to apply the ZENITH nametape to the upper payload bay. The upper payload bay was first painted all red, then stencils applied, then an overcoat of matte black. Removal of the stencils left a black upper payload bay with the red ZENITH lettering. The nosecone was then sprayed with black paint from a distance to create the black haze over red background effect seen on the final vehicle.



Figure 3-58. The Zenith 0.5

The connection points between nosecone and payload bay, as well as the entirety of the base of each fin, were wrapped or covered in layers of electrical tape to smooth out minor protrusions and cover minor gaps. Battery charge cables were fed through a vent hole in the avionics bay to allow charging prior to flight without any disassembly.



Figure 3-59. Team Prepping Ejection Charges on Sub-scale Launch Day

Final assembly occurred at the launch site, where ejection charges were loaded, the avionics bay sealed, and surface switches tested. The recovery harnesses were then connected to the top and bottom sections of the vehicle and joined at the ends of the avionics bay. Parachutes were quick linked to the recovery harnesses, packed, and stowed in their respective payload bay, before the avionics bay was mated and shear pinned to the upper and lower sections.

3.3 Subscale Flight Results

3.3.1 Flight Simulations and Prediction

OpenRocket Simulation software was used to calculate the subscale vehicle's performance parameters. Each of the component's weights were input into the simulation after completion of manufacturing and assembly, with a small deviation in accuracy before updating.

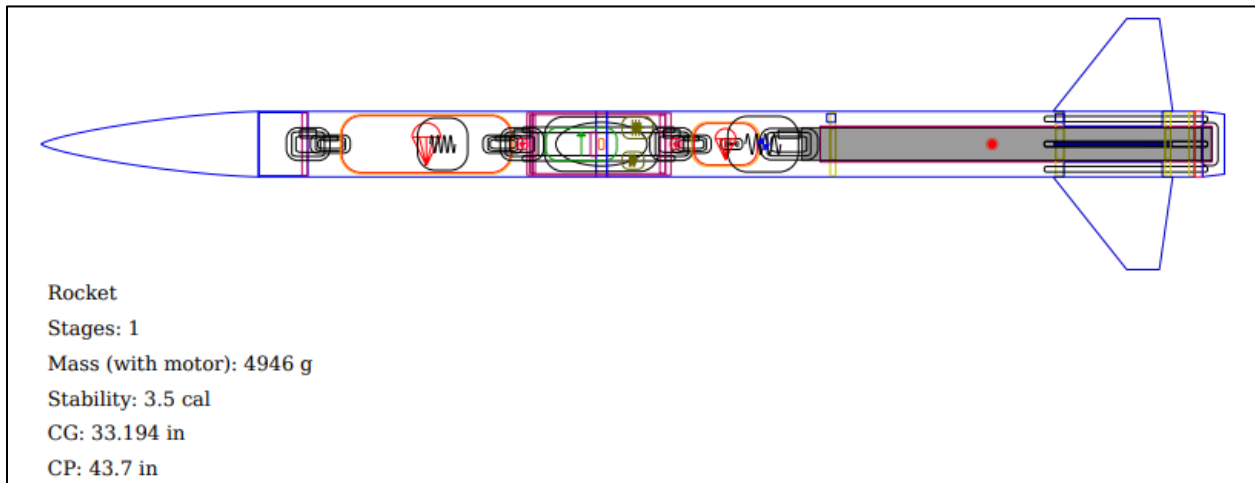


Figure 3-60. Sub-scale OpenRocket Design

Looking at the figure above, the vehicle weighs 4946 grams (11 pounds), which is roughly 1/3 of the full-scale vehicle's weight. The predicted apogee of the subscale vehicle was 3,189 feet at 0 mph winds and a launch angle of 5 degrees using a 96-inch launch rail.

3.3.2 Recovered Configuration



Figure 3-61. Sub-Scale Recovered Configuration

The vehicle was recovered intact on an asphalt road in a community adjacent to the launch site.



Figure 3-62. Detailed Section Views - Recovered Configuration

The only damage sustained during recovery can be seen in the upper left photo, where the paint was stripped from the tip of the upper right fin at the point it impacted the pavement.

3.3.3 Flight Data and Timeline

3.3.3.1 Major Flight Metrics

A MATLAB program was used to process the flight data recovered from both altimeters. Plots were produced using a spline interpolation scheme with a resolution 100x that of the raw data to convert the initial step-plot output to a smooth curve. The program also sought maximums in the data, providing the following outputs for metrics of interest:

Table 3-4. Sub-scale Flight Metrics

	Simulation	Altimeter 1	Altimeter 2
Altitude (ft)	3182	3322	3279
Max Velocity (ft/s)	502	531	543
Max Mach Number	0.45	0.476	0.486

With the data above, a table of deviation and percent error could be generated to evaluate the accuracy of the simulation.

Table 3-5. Sub-scale Flight Error Analysis

	Altimeter 1		Altimeter 2	
	Delta	% Error	Delta	% Error
Altitude (ft)	140	4.40	97	3.04
Max Velocity (ft/s)	29	5.77	41	8.16
Max Mach Number	.026	5.77	.036	8.16

With an error averaged across both altimeters of 3.72% and 6.97% in the altitude and velocity/Mach, respectively, we can conclude that the OpenRocket model very accurately represented the real vehicle in terms of component masses, mass distribution, aerodynamics, and impulse delivered.

The deviation in expected altitude and velocity can be explained by several factors, such as minor errors in component weights and placement in OpenRocket, although the most likely are those pertaining to the motor. Since we exceeded the expected velocity, we can assume that the motor delivered slightly more impulse than expected, either by burning slightly longer than simulated or having denser (more) propellant than advertised. Since the propellant is mixed and cast into grains to solidify, there is some expected deviation in performance between each motor, and the data used for simulation was the average performance as stated by the manufacturer.

3.3.3.2 Flight Timeline

Categorization for each flight event is as follows:

Table 3-6. Event Outcomes

Result	Description
Nominal	As expected
Failure (Class 1)	Deviation from expected performance. Insignificant impact on flight profile and vehicle performance. No vehicle damages.
Failure (Class 2)	Major deviation from expected performance. Significant impact on flight profile and vehicle performance. No vehicle damages.
Failure (Class 3)	Catastrophic failure. Major damages or loss of vehicle.

The sub-scale flight saw a successful launch and recovery of the vehicle with no damage, although two Class 2 and two Class 1 failures were experienced. The order of events for the flight are as follows:

Table 3-7. Sub-scale Flight Timeline

Event	Time (s)	Result	Notes
Ignition/liftoff	0	Nominal	-
Burnout	4	Nominal	-
FC read apogee	15	Nominal	-
Fire ejection charge 1	16	Nominal	-
Separation 1	16	Nominal	-
Drogue deployment	17	Nominal	-
Separation 2	17	Failure (Class 2)	Undersized shear pins broke under load from drogue deployment causing premature separation of the lower half of the vehicle
Main Deployment	18	Failure (Class 2)	Premature main deployment (3175 ft) because of first failure
FC read 550ft AGL	150	Failure (Class 1)	FC was set to read MSL not AGL
Fire ejection charge 2	155.5	Failure (Class 1)	Charge was fired low (500 ft). FC executed default ejection (150m) rather than 550ft programmed by avionics team
Ground Impact	184	Nominal	-

The primary failure on this test flight was the deployment of the main parachute immediately following drogue deployment. Undersized shear pins for the bottom half of the vehicle caused a premature separation due to jerk from the drogue parachute catching the air. The team was able to visually confirm the chute deployment was successive and not simultaneous, and this also shows in the plots discussed later. The team also confirmed that the second ejection charge fired once the avionics bay was recovered and opened, and the flight computer data shows the command to fire was sent at the default altitude of 150m, rather than the programmed 550ft or 168m. The cause of this off-nominal command has yet to be discovered, although the team will continue extensive testing of the new primary flight computer, the TeleMega, as well as the AIM3's used in this flight to ensure that the main parachute deploys above the 550ft hard deck set by NASA requirements.

Post flight discussion with the team mentor regarding the shear pin failure gives us confidence that if the pins were sized correctly, the flight would have been entirely nominal. The first ejection charge fired at apogee as expected and the top half separated without issue. The drogue parachute was able to deploy without entanglement or damage to the vehicle. The second separation, although premature, also occurred without issue, as did the deployment and inflation of the main parachute. This leads us to believe that the design of the recovery system is sound, but there must be extensive drop testing of joined full-scale vehicle sections to ensure the shear pins will not fail under flight loads again. Further separation tests will also be conducted to ensure that pins which do not shear in drop tests will shear as desired when ejection charges are fired.

High altitude winds on launch day caused significant deviation from the expected recovery area. The vehicle was recovered over a mile from the launch pad, where it landed on a paved road. Despite landing on asphalt, the vehicle sustained no damage from the ground impact. The team is confident that correction of the premature main deployment will place the vehicle well within the 2500 ft recovery area as simulations suggest. We also find the lack of damage from impacting pavement at 17 ft/s to be proof that the construction methods, materials, and overall design are sound, and will surely survive impact with soil.

3.3.3.3 Altitude Plots

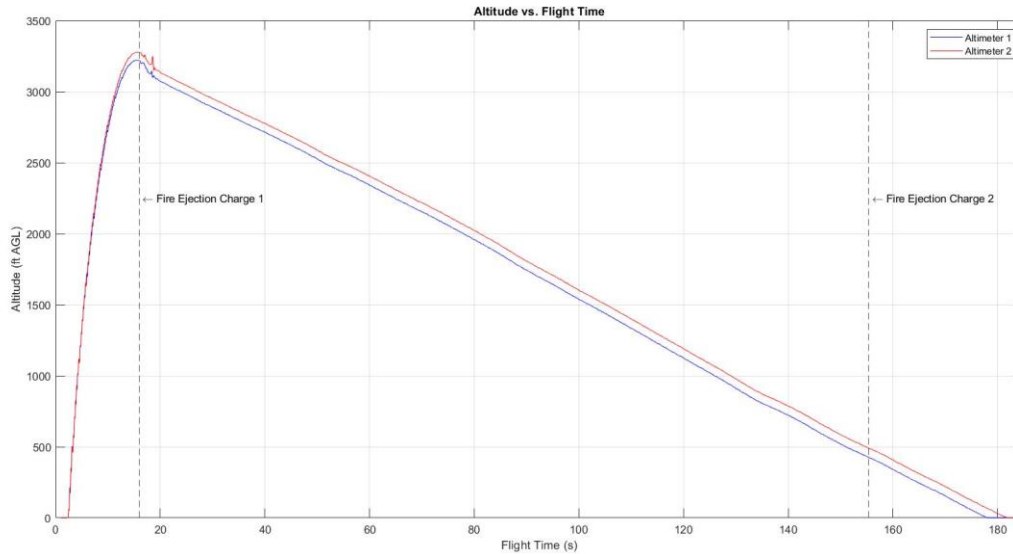


Figure 3-63. Altitude vs. Flight Time Plot

The linear portion of the ascent represents the time during which the motor was burning, followed by a parabolic shaped ascent curve as the vehicle coasted to apogee. The plot shows apogee and the firing of the first ejection charge immediately after. Since this is the flight portion where the two parachutes successively deployed, the plot shows a constant linear descent rate to ground impact. The second ejection charge fired when altimeter 1 read 500ft, as altimeter 2 was in a partial failure mode on launch which prevented it from activating its second pyro channel.

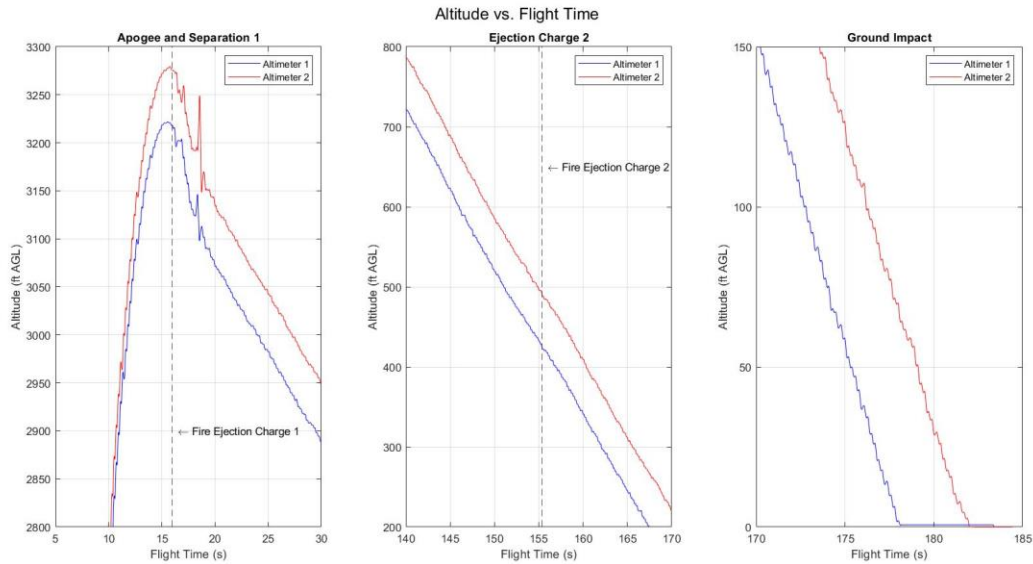


Figure 3-64. Event View, Altitude Plot

From the figure on the left, we can see two peaks after the firing of the ejection charge where the altitude suddenly increases for a short moment. The first peak is far less pronounced than the second, with the first occurring at around 16s and the second at 18s. These peaks represent the successive parachute deployments, as the avionics bay was jerked vertically upwards by the parachute, or swung laterally along a curved path, thereby increasing its altitude. The first jerk/swing is less pronounced because the drogue chute has less area than the main, thereby creating less force on deployment.

The center plot demonstrates that the second ejection charge fired right as the first altimeter read 500ft, or the preset 150m deployment from the manufacturer. The ejection would have occurred sooner, as altimeter 2 detected 500ft prior to altimeter 1, but as previously mentioned altimeter 2 had a known failure of its second pyro channel before launch.

The right plot shows the time at which the altimeters read ground impact. We can surmise from this plot that altimeter 1 (red) is the more accurate of the two, as it did not experience the same partial failure mode in the pyro channels and continued to sense deltas in pressure after altimeter 2 registered no deltas and determined zero altitude. The velocity plots bear out this result as well.

3.3.3.4 Velocity Plots

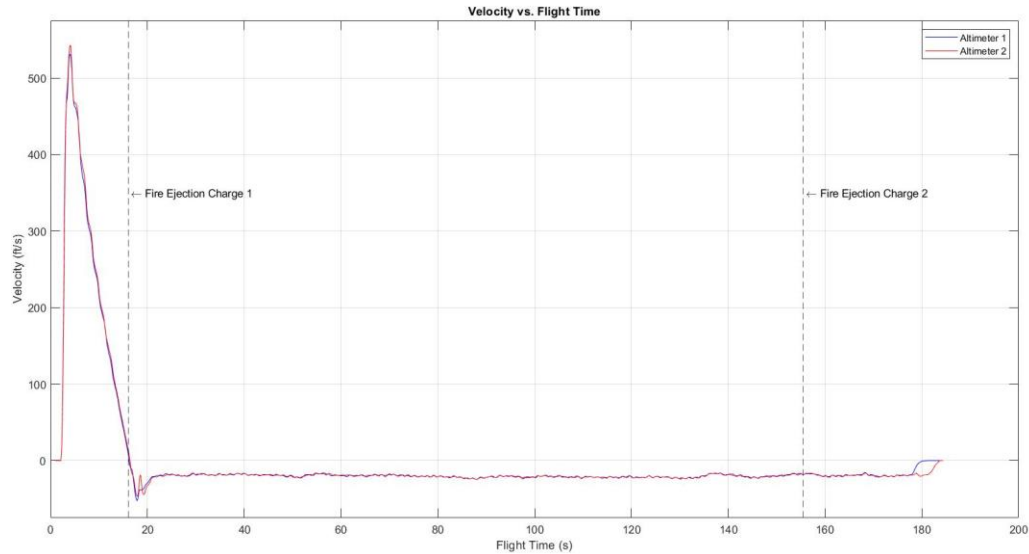


Figure 3-65. Velocity vs. Flight Time

The velocity plot demonstrates a linear increase in airspeed as the motor burned. Small fluctuations are seen as burnout occurred, followed by a constant decrease in velocity until zero is crossed at apogee and the velocity turns negative as the descent begins. Fluctuations are seen as the parachutes successively deploy and the vehicle stabilizes, after which a constant negative velocity is seen until impact.

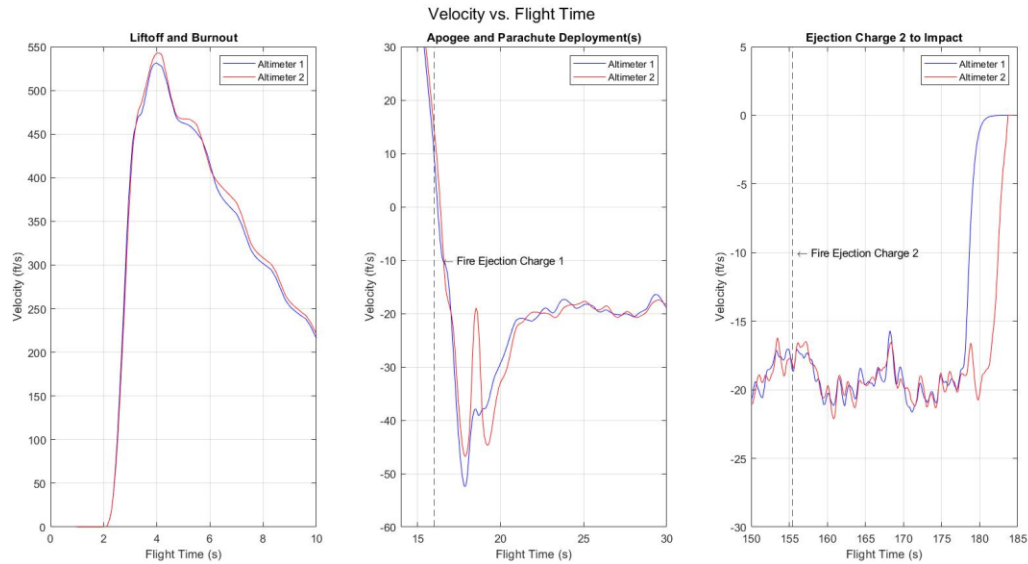


Figure 3-66. Event View, Velocity Plot

The left plot shows liftoff and motor burnout. Around 3 seconds the slope of the velocity decreases slightly, suggesting this is the point where the thrust curve began to fall off. At exactly 4 seconds the direction of the curve reverses as the motor burns out. Burnout is immediately followed by a steep drop in velocity. The slope of the velocity drop becomes shallower as the vehicle's airspeed and stability decrease during the coasting portion of the ascent. Sinusoidal fluctuations can also be seen in the unpowered ascent, which are result from spin stabilization of the vehicle.

The center plot shows the velocity fluctuations following the first ejection charge firing. There are two distinct and rapid drops in the velocity corresponding to the successive deployment of the parachutes. The plot begins with the descent under gravity, with the velocity increasing negative until the drogue deployment where the velocity rapidly decreases. The velocity then rapidly increases due to the phenomena discussed in the altitude section where the avionics bay is jerked or swung upwards rapidly. The main chute then deploys prematurely, causing another rapid velocity decrease which then settles out to a constant approximately -20 ft/s for the duration of the descent. Minor random fluctuations are seen in the velocity across the entire descent which are a result of high-altitude winds and the avionics bay swinging and spinning underneath the main parachute.

The right plot shows a continuation of the random fluctuations about -20 ft/s until ground impact, where the velocity goes to 0 ft/s near instantaneously. The discrepancy between impact time for altimeters 1 and 2 shows again, as altimeter 2 reads zero velocity well before altimeter 1. For reasons previously explained, altimeter 1 will be taken as the more accurate case.

3.3.4 Scaling Factors and Influence on Full-Scale Design

Table 3-8. Sub-scale Vehicle Scaling Factors

Vehicle Parameter	Scaling Factor
Max Thrust	0.45
Impulse	0.22
*Dimensions	0.5
Mass	0.285

NOTE: Airframe diameter, nosecone, and fins scaled down 50%. Hardware and fittings not scaled. Body tube length not exactly 0.5 scale to maintain stability margin.

The intention of the team was for the sub-scale vehicle to be manufactured at 50% size scale and 33% thrust/impulse scale. In reality, motor options available meant that the final scaling was nearer to 20% impulse and 50% thrust. The vehicle was scaled in almost every way possible to 50% size, although the motor being longer and skinnier than the full-scale counterpart forced the scale of the airframe length to be larger than this target. The mass was expected to fall at around 33% of full scale, and the 29% actual value very nearly approaches that goal.

Given that the scaling factors differ radically from one vehicle parameter to another, we cannot estimate full-scale performance by scaling or extrapolating sub-scale data. We can, however, confirm through our post-flight data analysis that the OpenRocket simulation for the vehicle matched reality to within a 5% margin of error, which suggests that the simulation can be relied upon to produce highly accurate performance estimates for the full-scale vehicle as well. The performance of the recovery system in subscale was also validated, and although the forces and loads will be increased for full-scale, the operating concept for the dual-deployment recovery system was successfully demonstrated.

3.4 Recovery System

3.4.1 Recovery System Summary

The entirety of the recovery system will ensure the launch vehicle and all its components safety upon descent. There are two recovery events, drogue parachute deployment and main parachute deployment. The two recovery events will be controlled by an Altus Metrum TeleMega flight computer, the primary altimeter, and an Entacore AIM 4, the secondary altimeter. Each altimeter draws power from separate 3.7 V rechargeable Lithium Polymer batteries and are both armed with simple push-button switches. The ejection charges will both be CO₂ gas charges that are manufactured by Tinder Rocketry. These ejection charges were chosen to limit the amount of pyro events that will occur, which also lowers the many points of failure for the recovery event if black powder was used. The CO₂ charge still requires the use of black powder, but only a small amount of it. Approximately 0.15 grams of 4F black powder is used to propel a piston with a pointed tip that punctures the CO₂ cartridge and releases gas into the payload bays. The black powder is loaded into a charge cup that sits at the end of the charge in the payload bay and is connected to an e-match wire from each altimeter. Both charges are designed to have the CO₂ placed cartridge in the avionics bay attached to the puncture piston mechanism that is threaded through the bulkhead. The figure below shows the interface between the CO₂ charge mechanism (in red) and the AV bay bulkheads. For the full-scale launch vehicle there will be two separate charges for both the drogue and main parachutes, totaling to 4 charges.

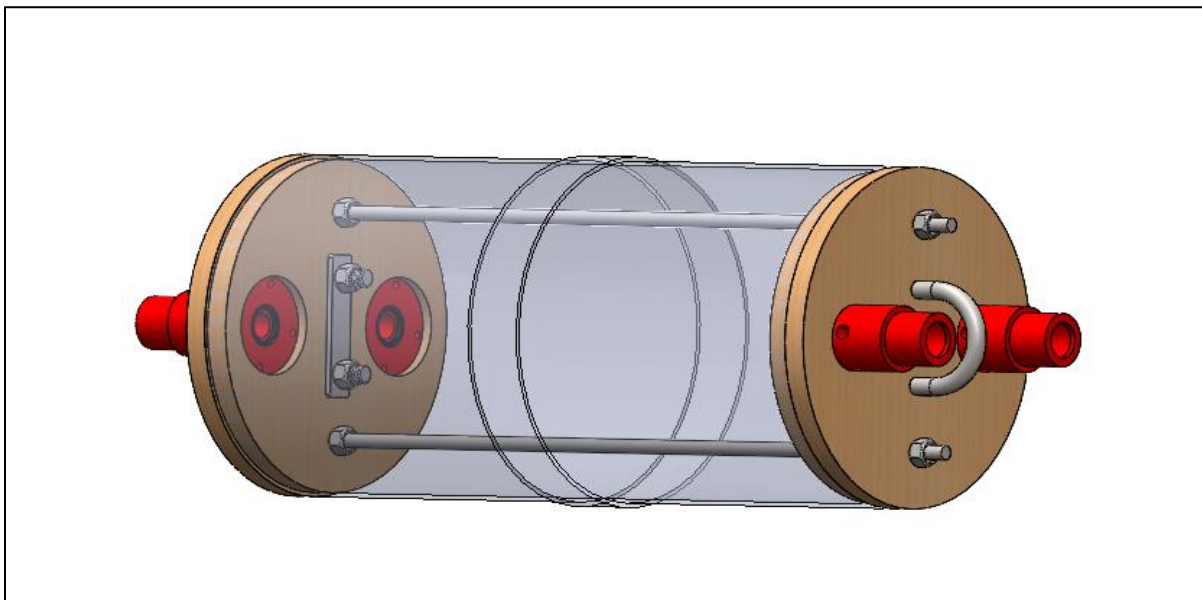


Figure 3-67. CO₂ Ejection Charge (Red) to Bulkhead Interface

At apogee, the TeleMega altimeter will send a current through the e-match that will fire the first ejection charge. The CO₂ gas will rapidly pressurize the lower payload bay and shear the #4-40 nylon pins that connects it to the AV bay, deploying the drogue parachute. A secondary ejection charge on a two-second time delay controlled by the AIM 4 altimeter will fire to ensure proper separation of the vehicle sections. Deployment of the main parachute is similar; the only difference is that the payload will also be tethered to the recovery harness. The primary ejection charge for the main parachute is set to deploy at 550 ft AGL, and the redundant secondary charge will deploy two seconds afterwards. A 24" compact elliptical parachute will be the drogue parachute and an 84" iris ultra-standard will be the main parachute, both of which are manufactured by Fruity Chutes. Both parachutes are tethered to 9/16-inch Nylon webbed shock cord, rated at 3000 lb, with the use of ¼-inch quick links.

3.5 Mission Performance Predictions

3.5.1 Target Altitude

The target altitude for the Zenith 1 is 4600 ft AGL.

3.5.2 Updated Flight Profile

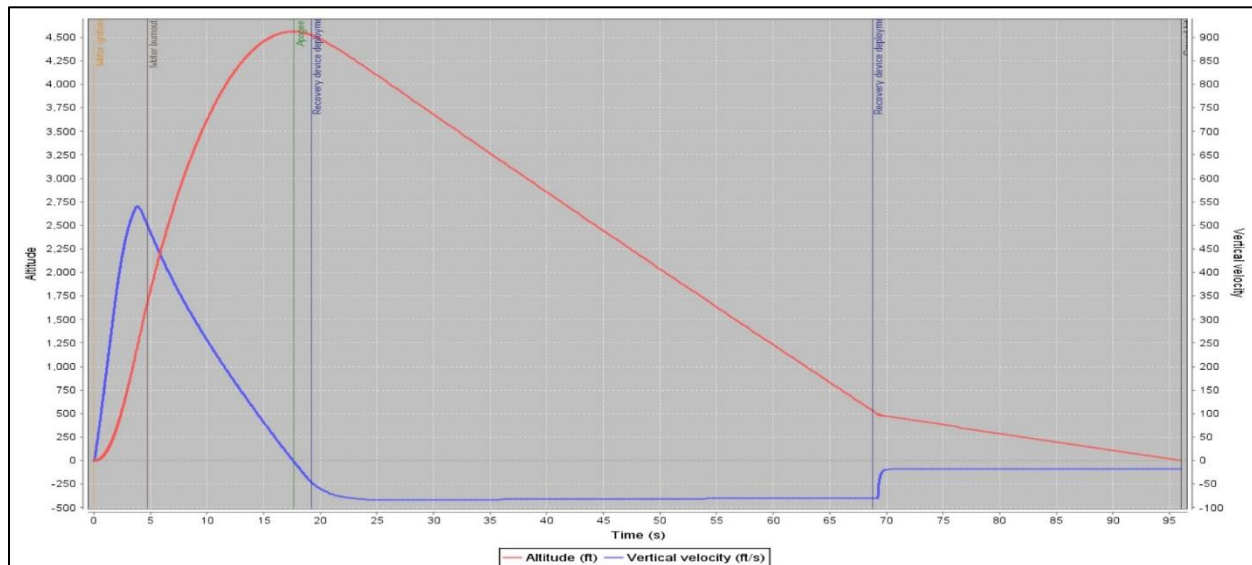


Figure 3-68. Updated Flight Profile – 0 mph Winds

Table 3-9. Nominal Flight Profile (No Wind, 5° Launch Angle)

Event	Flight Time (s)	Notes
Liftoff	0	Rail Exit: 64.5 ft/s
Max Velocity	4	545 ft/s (subsonic)
Motor Burnout	4.5	-
Apogee	17.5	4561 ft AGL
Separation Charge 1 Fire	19	1.5s delay
Separation Charge 2 Fire	68	Deploy Vel: 74.5 ft/s
Ground Impact	96	Impact Vel: 18 ft/s Descent Time: 78.5 s

3.5.3 Apogee Calculations

The theoretical apogee of the rocket can be calculated by first calculating the altitude that the rocket achieves under powered ascent (the solid motor is producing thrust) and then by calculating the altitude that the rocket achieves after powered ascent while in the “coasting phase.” The powered ascent altitude formula can be derived from Newtons 2nd law.

$$F = m * a \quad (1)$$

Where F is Force, m is mass, and a is acceleration. Using definition of acceleration:

$$F = m \frac{dv}{dt} \quad (2)$$

The entire force on the rocket can be written as:

$$F = T - W_{avg} - F_{drag} \quad (3)$$

Where T is the trust force. F_{drag} is the drag force acting on the rocket. W_{avg} is the average weight force during powered ascent, we take the average because as the propellant burns the vehicle will lose weight, decreasing the load. For a more accurate calculation the weight force can be integrated over the duration of the burn, however because the mass of the vehicle (17.368 kg) is large compared to the propellant mass (2.095 kg) and the burn time is relatively low (4.4 s), the method for determining the average mass in equation (4) is sufficient.

$$m_{avg} = m_{takeoff} - 0.5 * m_{propellant} \quad (4)$$

and

$$W_{avg} = g * m_{avg} \quad (5)$$

Where $m_{takeoff}$ is the mass of the vehicle at takeoff, $m_{propellant}$ is the mass of the propellant, and g is the gravitational constant of Earth. Because the rocket's target altitude is not greater than 5,000 ft, we will assume g to be constant. The drag force model we will use is listed in equation (6):

$$F_{drag} = k * v^2 \quad (6)$$

Where v is the velocity of the vehicle and

$$k = 0.5 * \rho * C_d * A \quad (7)$$

Where A is the greatest cross-sectional area of the vehicle. C_d is the coefficient of drag of the vehicle, for this calculation a standard value was chosen for a vehicle of the same size. ρ is the density of the air. Again, because the rocket will only travel 5,000 ft, we will assume this value to be constant. We can now plug equations 2, 5, and 6 into equation 3.

$$m \frac{dv}{dt} = T - g * m_{avg} - k * v^2 \quad (8)$$

Equation 8 can be rearranged, and integrated to eventually obtain:

$$v = \sqrt{\frac{T-g*m_{avg}}{k}} * \frac{1-e^{\frac{-2*t*k*\sqrt{\frac{T-g*m_{avg}}{k}}}{m_{avg}}}}{1+e^{\frac{-2*t*k*\sqrt{\frac{T-g*m_{avg}}{k}}}{m_{avg}}}} \quad (9)$$

Where t is the burn time and v is the velocity of the vehicle after the burn is complete. We can now begin to formulate the equation for the height of the vehicle after the burn and we will use the velocity of the vehicle to determine the height. To find the equation for height of the vehicle, we begin by rewriting equation 2:

$$m * \frac{dv}{dt} = m * \frac{dv}{dh} * \frac{dh}{dt} = m * v * \frac{dv}{dh} \quad (10)$$

By substituting equation 10 into equation 8, then rearranging and integrating, we obtain:

$$h_{burnout} = \frac{m_{avg}}{2*k} * \ln \left(\frac{T - m_{avg}*g}{T - m_{avg}*g - k*v^2} \right) \quad (11)$$

Where $h_{burnout}$ is the height of the vehicle after the powered ascent. Now, we will find the height of the vehicle after its coasting portion of flight. For these calculations we will use the mass of the vehicle without the propellant ($m_{vehicle} = m_{takeoff} - m_{propellant}$) because during this portion of the flight, it is already all burned off. Using similar reasoning as above, with the exception of removing the impulse from the equation of motion, we obtain:

$$h_{coasting} = \frac{m_{vehicle}}{2*k} * \ln \left(\frac{m_{avg}*g + k*v^2}{m_{avg}*g} \right) \quad (12)$$

Now that we have formulated equations for the altitude of both portions of the flight, we can now add them together to find the total altitude of the vehicle that accounts for drag and changing mass.

$$h_{apogee} = h_{burnout} + h_{coasting} \quad (13)$$

Using the above equations, the theoretical apogee of the rocket was found to be 4,431 feet.

The MATLAB program used to execute the above calculations is attached as Appendix D.

3.5.4 Stability Margin Calculations

The vehicle's stability margin is one of the most important parameters that vehicle must be designed around. The stability margin can negatively or positively optimize the vehicle's flight performance and ultimately determines whether the vehicle is successfully designed. Although OpenRocket simulations do not define the real-time launch vehicle's stability margin on launch day, it is a very accurate form of measurement. Shown below is the vehicle's stability margin profile at the maximum allowable launch day wind speed conditions.

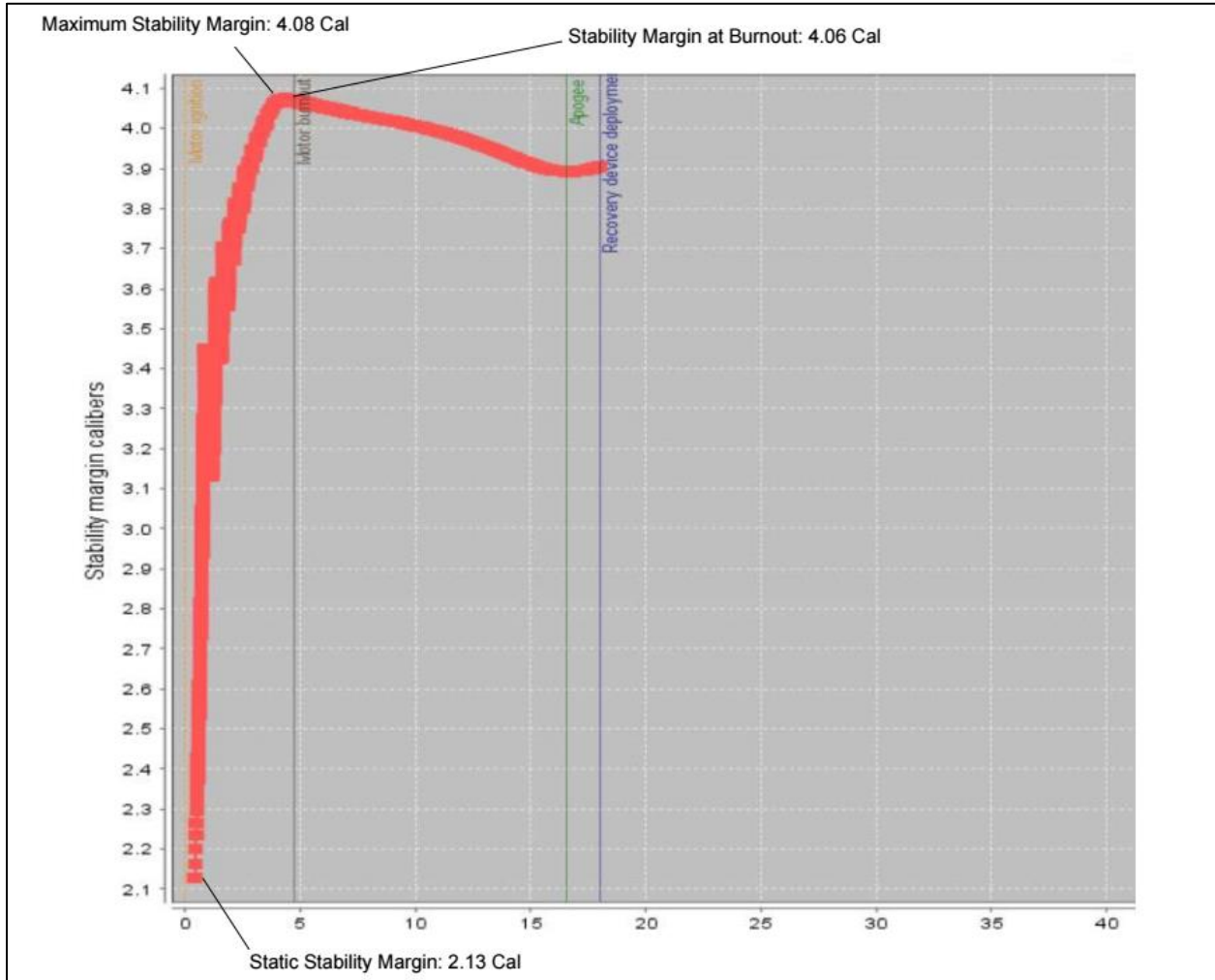


Figure 3-69. Stability vs. Flight Time

Looking at the figure above, the static stability margin of vehicle at rest is 2.13 calibers, the maximum stability margin is 4.08 calibers, and the stability margin at motor burnout is 4.06 calibers. The static stability margin shown above is above NASA’s minimum requirement, ensuring that any other wind speed conditions lower than 20 MPH will also be above NASA’s minimum requirement. For the sake of sanity checking, the table below shows the vehicle’s stability margin at 0, 5, 10, 15, and 20 MPH wind speeds at the launch competition’s geographical location/conditions.

Table 3-10. Wind Speed vs. Stability for 5° Launch Angle

5° Launch Angle	
Wind Speed (mph)	Static Stability Margin
0	3.47
5	2.97
10	2.61
15	2.33
20	2.13

Another method of calculating the static stability margin is the Barrowman's method. The Barrowman's method was written into a MATLAB script and used to calculate the vehicle's static stability margin at 0 MPH wind speeds. The following equation was used to calculate the static stability margin:

$$\text{Stability Margin}_{\text{Static}} = \frac{X_{CP} - X_{CG}}{D}$$

Where X_{CG} is the center of gravity and X_{CP} is the center of pressure, both measured from the tip of the nosecone. The center of gravity is given as 58.578 inches and the center of pressure can be found by

$$X_{CP} = \frac{C_N X_N + C_F X_F}{C_N + C_F}$$

The arm length of the fins, X_F can be found using the following equation

$$X_F = X_B + \frac{X_R C_R + 2C_T}{3(C_R + C_T)} + \frac{1}{6} \left(C_R + C_R - \frac{C_R C_T}{C_R + C_T} \right)$$

Where X_B is the distance from the tip of the nosecone to the fin root chord leading edge, C_R is the length of the fin root chord, and C_T is the length of the fin tip chord.

The fin coefficient shown in equation, C_F , is represented as

$$C_F = \left(1 + \frac{R}{S + R}\right) \left(\frac{4N \left(\frac{S}{2R}\right)^2}{1 + \sqrt{1 + \left(\frac{2L_F}{C_R + C_T}\right)^2}} \right)$$

Where N is the number of fins and L_F is the length of the fin mid-chord line. L_F can be calculated using the fin semispan, S , and the following equation

$$L_F = \sqrt{S^2 + \left(0.5C_T - 0.5C_R + \frac{S}{\tan\theta}\right)^2}$$

The variables in the equations above and their calculated values are shown below in table. The MATLAB script written to calculate the above parameters is attached in Appendix C.

Table 3-11. Stability Parameters

Parameter	Symbol	Value	Unit
Fin Semispan	S	9.00	Inches
Fin Tip Chord	C_T	3.00	Inches
Fin Root Chord	C_R	11.00	Inches
Fin Sweep Angle	θ	37	Degrees
Fin Mid-Chord Line	L_F	8.14	Inches
Radius of Airframe	R	3.00	Inches
Number of Fins	N	4	N/A
Nose Tip to Fin Root Chord Leading Edge	X_B	83.50	Inches
Fin Root Leading Edge to Fin Tip Leading Edge	X_R	6.77	Inches
	X_F	88.18	Inches
Arm Length of Nosecone	X_N	9.32	Inches
Nose Cone Length	L_N	20.00	Inches
Nose Cone Term	C_N	2.00	N/A
Fin term	C_F	16.95	N/A
Center of Pressure	X_{CP}	79.86	Inches
Center of Gravity	X_{CG}	58.58	Inches
Diameter of Airframe	D	6.154	Inches
Static Stability Margin	$Stability\ Margin_{Static}$	3.46	Calibers

Comparing the stability margin values calculated from OpenRocket and the MATLAB Code

Table 3-12. Stability Results

Method	Stability Margin (Calibers)
OpenRocket Simulation Software	3.47
Barrowman's Method	3.46

Any deviation between the two values is more than likely due to rounding the pre-defined MATLAB values in the coded script.

3.5.5 Landing Kinetic Energy Calculations

The kinetic energy of each section of the vehicle during descent is governed by the mass and velocity of each. The equation used to determine the kinetic energy of each section is stated below:

$$KE = \frac{1}{2}mv^2$$

where m is the mass, and v is the velocity of the section. The maximum kinetic energy set by the requirement in the Student Launch Handbook is 75 ft-lb, which can be used to derive the maximum velocity for each descending section. The maximum velocity of each descending section is shown below.

Table 3-13: Maximum Descent Velocity

Section	mass (g)	mass (slug)	Maximum Descent Velocity (ft/s)
Nosecone + UPB	4720	0.3235	21.5329
Payload	1400	0.0960	39.5375
AV bay	2056	0.1409	32.6258
LPB + Fin can	6235	0.4273	18.7351

3.5.6 Descent Time and Drift Calculations

The descent time is determined by the descent velocity of each parachute and the altitudes at which they are deployed. The drift can be calculated, but a few assumptions must be made. The first assumption is that the launch vehicle reaches apogee directly above the launch pad. The second is that at apogee and main deployment altitude, the terminal velocities are reached instantaneously. Lastly, the wind speeds are applied uniformly on the vehicle and it all drifts in one direction. Although these assumptions make the calculations not entirely accurate, it still gives a good understanding of how severe wind conditions can affect the vehicle’s descent. To determine the total descent time of the vehicle the equation below was used:

$$t = \frac{h_a - h_m}{v_d} + \frac{h_m}{v_m}$$

where h_a is the apogee altitude, h_m is the main parachute deployment altitude, v_d is the descent velocity underneath the drogue parachute, and v_m is the descent velocity underneath the main parachute. For the declared altitude of 4600 ft, the calculated descent time is 80.7 seconds.

Table 3-14. Descent Time and Drift

Wind Speed (mph)	Apogee (ft)	Descent Time (s)	Wind Drift (ft)
0	4600	80.7	0
5	4600	80.7	591.8
10	4600	80.7	1183.6
15	4600	80.7	1775.4
20	4600	80.7	2367.2

Once the maximum velocity is known, the descent velocity and subsequent kinetic energy of each section can be determined using the 84-inch Iris Ultra Standard main parachute.

Table 3-15. Maximum Kinetic Energy

Section	mass (g)	mass (lbm)	mass (slug)	Descent Velocity (ft/s)	Kinetic Energy (ft-lb)
Nosecone + UPB	4720	10.4058	0.3234	18.6	55.946
Nosecone + UPB + payload	6120	13.4923	0.4194	18.6	72.540
Payload	1400	3.0865	0.0959	18.6	16.594
AV bay	2056	4.5327	0.1409	18.6	24.370
LPB + Fin can	6235	13.7458	0.4272	18.6	73.903

The table above shows the maximum kinetic energy for each section of the vehicle. The heaviest section of the launch vehicle will be its lower payload bay and fin can section. The maximum kinetic energy calculated for that section is 73.9 ft-lb, which is under the requirement of 75 ft-lb stated in the Student Launch Handbook. The second row of the column highlights a failure mode if the payload does not exit the upper payload bay when the main parachute deploys. In this scenario the second maximum kinetic energy is 72.54 ft-lb, which also satisfies the maximum requirement.

3.5.7 Parachute Opening Shock Calculations

The parachute opening shock calculations is done by finding the rate at which the launch vehicle's sections decelerate once the main parachute is fully open. To get the time it takes for the parachute to unravel the following equation was used from a technical report written by William P. Ludtke:

$$t = \frac{8 \cdot r}{v}$$

where r is the radius of the parachute, and v is the terminal velocity of the launch vehicle before the parachute is deployed. The time calculated for the 84" iris ultra-standard parachute to open was 0.35 seconds. The deceleration rate can then be determined by the following kinematic equation:

$$a = \frac{v_d - v_m}{t}$$

where v_d is the terminal velocity of the launch vehicle under the drogue parachute, v_m is the terminal velocity under the main parachute, and t is the time it takes for the main parachute to open. The deceleration rate calculated was 171.52 ft/s² and used in Newton's 2nd law to get the opening shock force that the recovery harness experiences for each section of the launch vehicle upon main parachute deployment. The shock force values is shown in the table below.

Table 3-16. Main Parachute Opening Shock

Section	Mass (slug)	Opening Shock (lbf)
Nosecone + UPB (slug)	0.3235	55.4881
Payload (slug)	0.0960	16.4583
AV Bay (slug)	0.1409	24.1703
LPB + Fin Can (slug)	0.4286	73.5100

4 Payload Criteria

4.1 Payload Mission Statement

The mission of the Zenith Program Payload Prototype is to employ a sturdy majority 3D printed design to survive ground impact and come to rest camera side up as flat as the terrain allows to execute a RAFCO sequence involving rotation of a camera turret, image capture, and application of filters or effects to the images autonomously through effective Arduino programming.

4.2 Payload Success Criteria

- 1) The payload Deploys with the main parachute.
- 2) The payload body section lands intact.
- 3) The payload electrical connections stay connected during flight and landing.
- 4) The payload receives the entire RAFCO sequence.
- 5) The payload executes the entire RAFCO sequence.
- 6) The payload stores all the images successfully with timestamps and proper filters.

4.3 Payload System Summary

The updated payload design stemmed from a philosophy of including only what is necessary to execute the baseline requirements for the RAFCO mission. The static housing was designed to hold a camera turret and the antenna securely, shield them from ground impact, and come to a stop without tipping or rolling after touchdown.

This section of the report will focus on the redesign and integration of the payload.

Preliminary code to operate the stepper motor, continuously check the antenna for receipt of the RAFCO command string, decode the command string, and execute the requested commands has been attached for review as Appendix E.

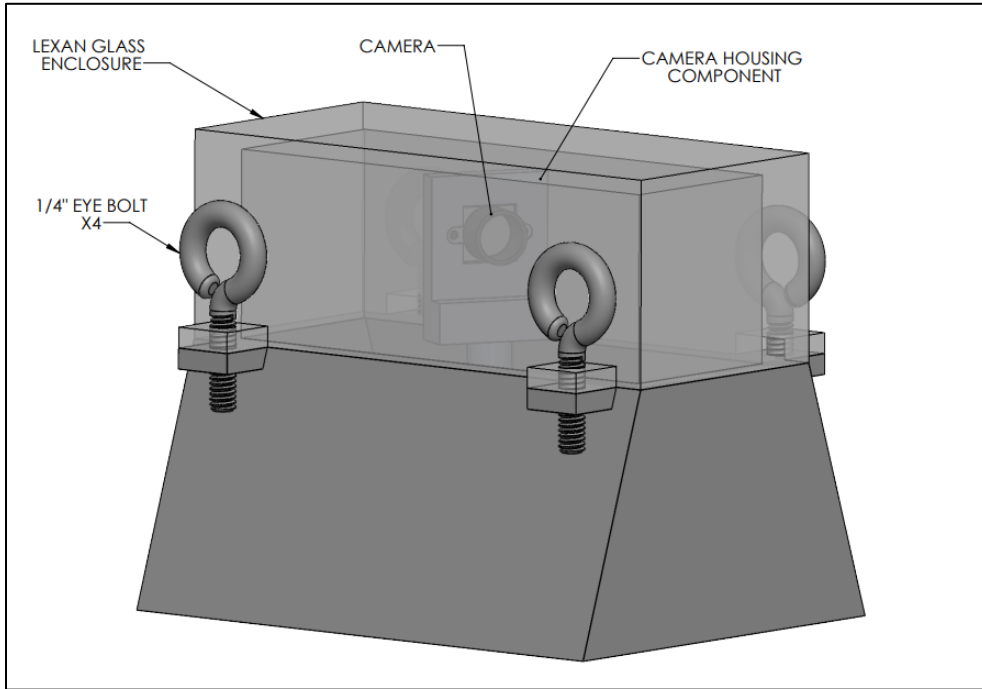


Figure 4-1. Payload design

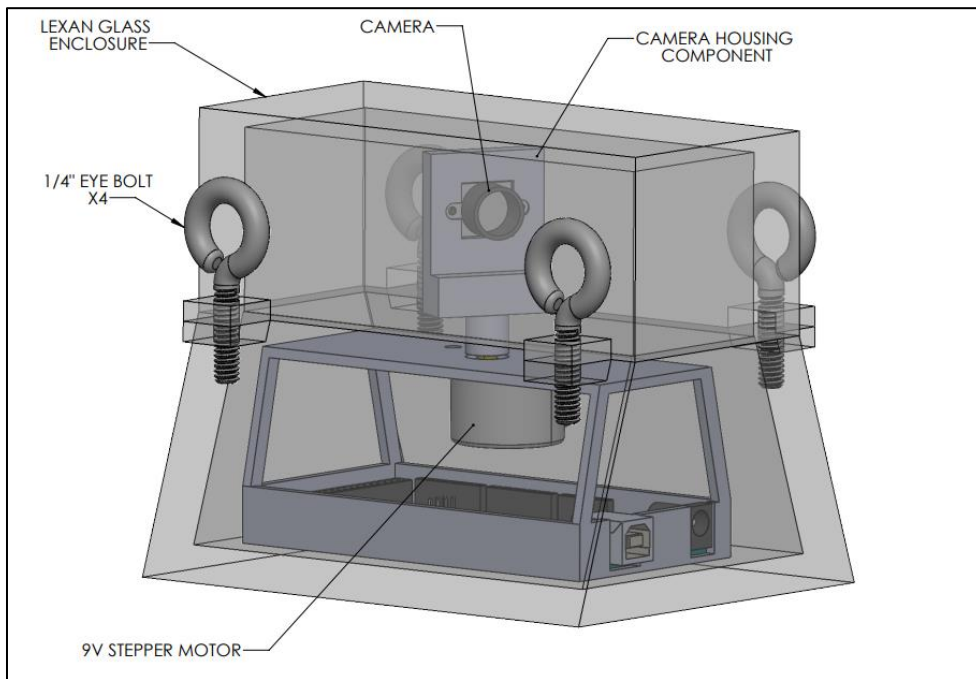


Figure 4-2. Payload Internal View

4.3.1 Component Integration

The long wide base of the payload, which flares out from the lexan enclosure and contains most of the weight of the system in the stepper motor, is intended to give as wide an initial contact surface and drop the center of gravity as low as possible to prevent tipping or rolling on impact. The working idea is that if the payload does not come to an immediate halt on impact, it will most likely slide. If the payload were to impact at an angle, the mass of the stepper motor in the center of the wide base would quickly bring the base down flat to the ground.

Rather than attach at a single connection point, the payload will be suspended on 4 shock cords running to stainless steel eyebolts at the corners. These four cords will connect to a quick link on the recovery harness in between the main parachute and the upper payload bay. Suspending the enclosure by the corners minimizes the potential for swinging under the parachute, as would certainly happen with a single connection point at the top center of the payload.

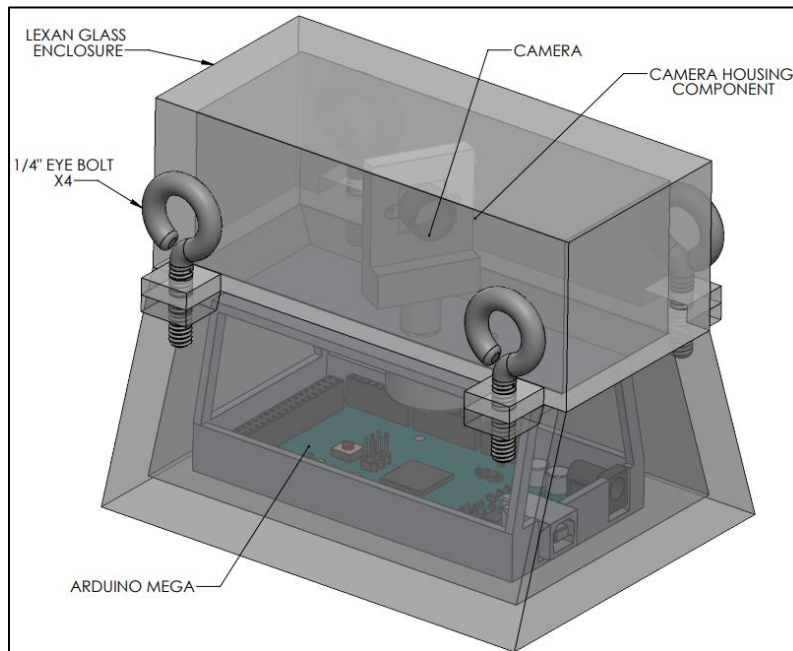


Figure 4-3. Payload Internal Hardware

The ArduCam Mini will be enclosed in a 3D printed housing unit which interfaces with the stepper motor. The motor and Arduino Mega will be retained by a 3D printed internal structure with mounting points for each. Electrical wires will be free to rotate with the camera, as firm connections will be made at each end, and wires passed through the upper deck of the internal structure. Payload batteries will be mounted on top of the microcontroller, with the antenna cord passing through the internal upper deck, and antenna fixed horizontally in the lexan housing.

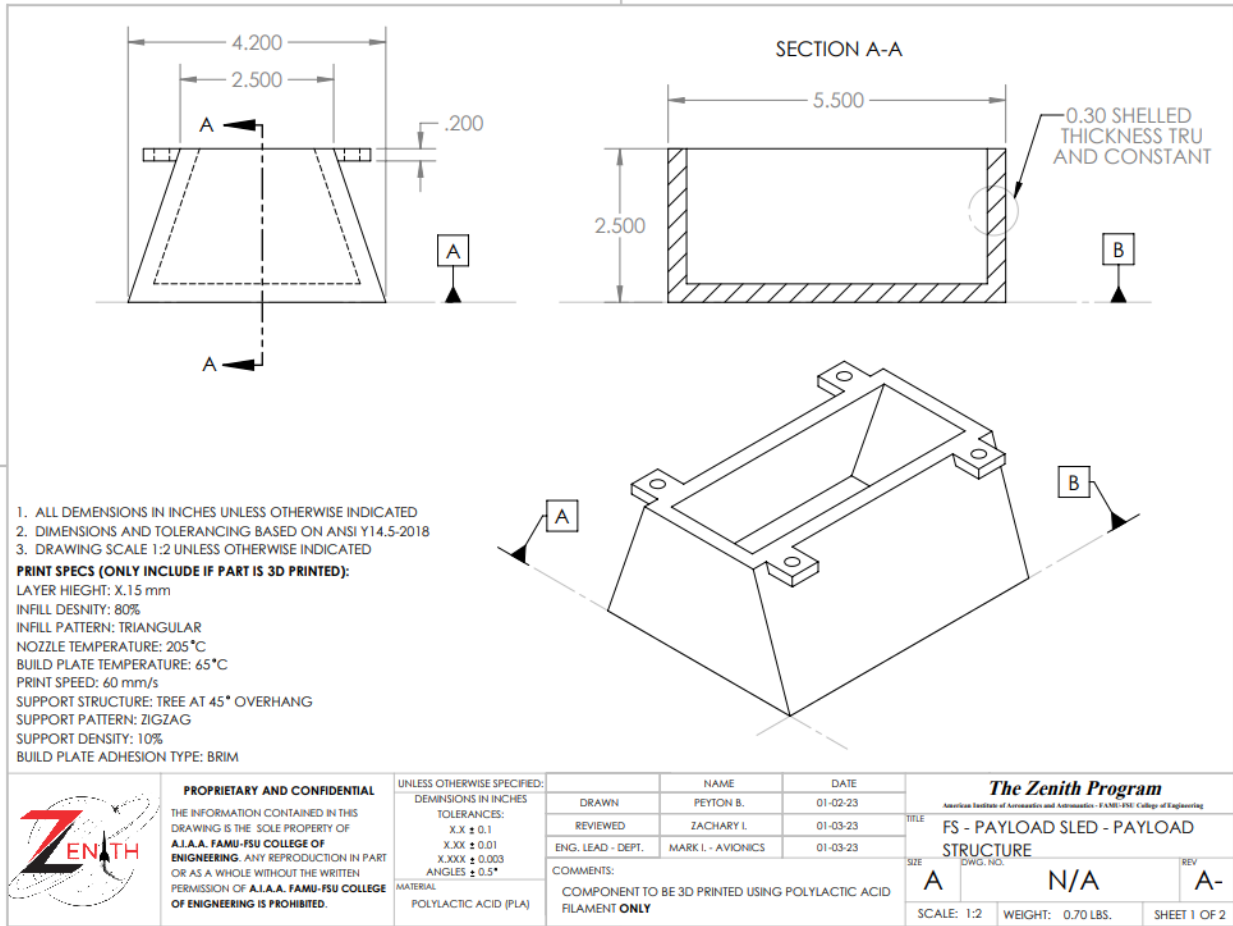


Figure 4-4. Payload Housing Drawing

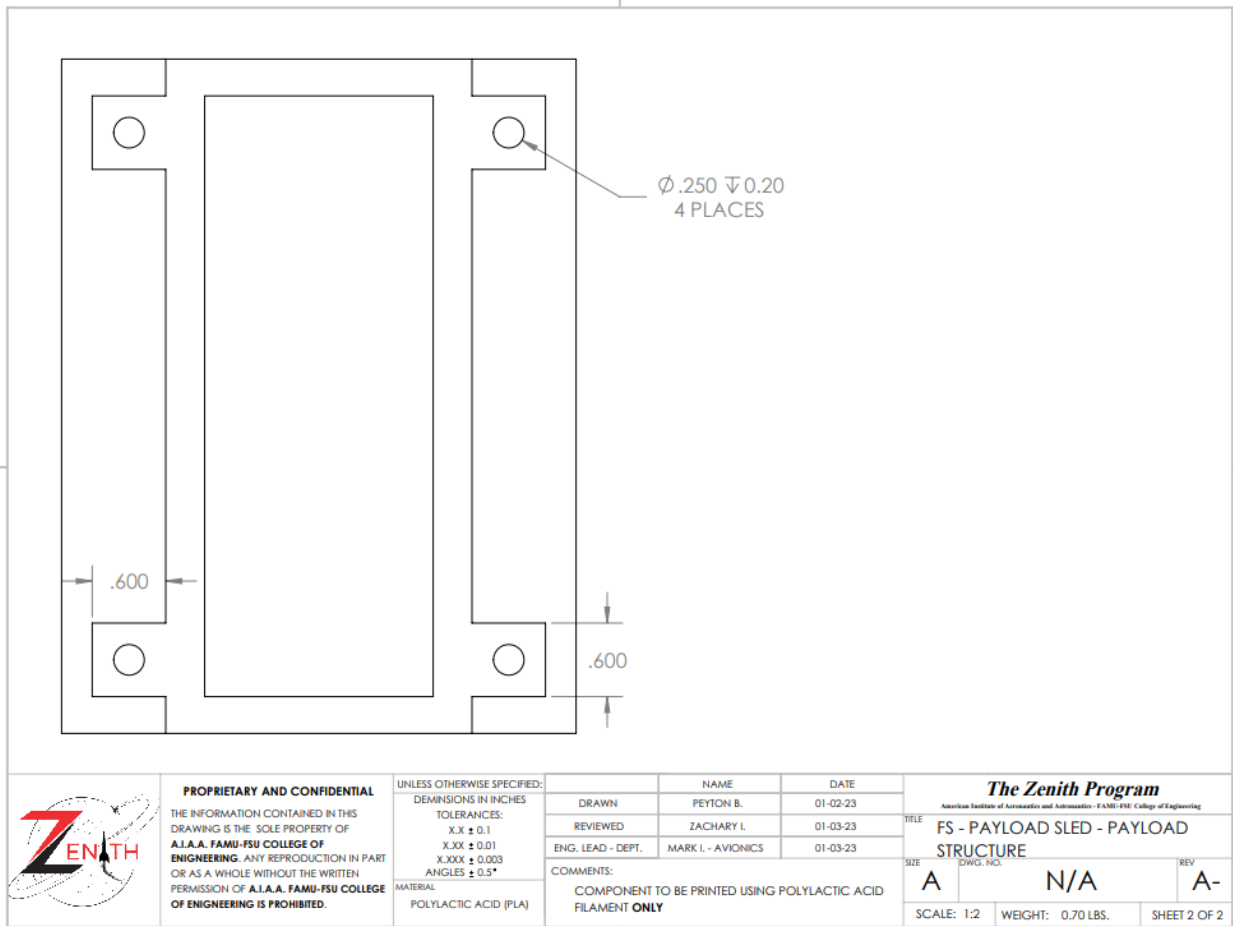


Figure 4-5. Payload Housing Drawing Continued

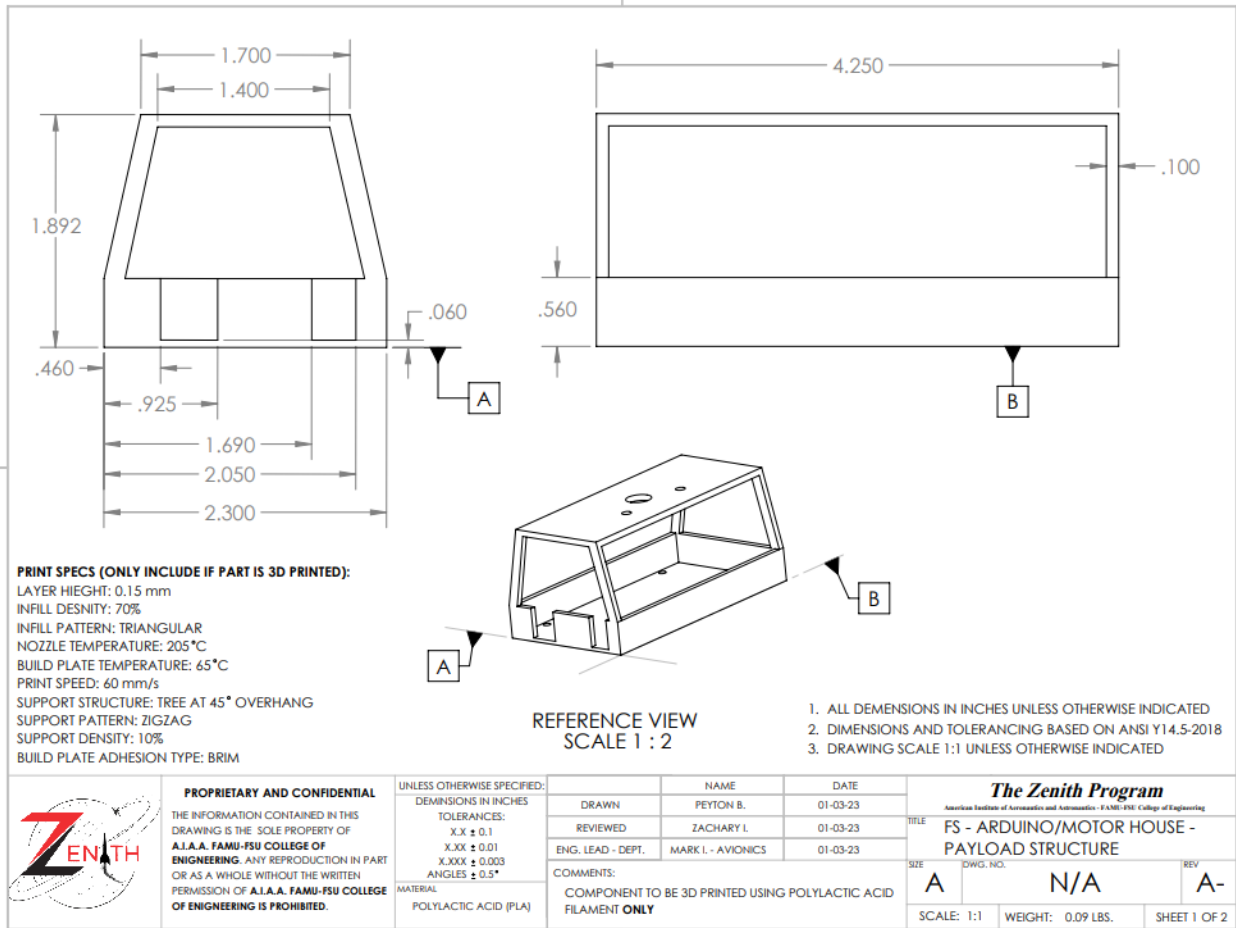


Figure 4-6. Arduino/Motor Housing Drawing

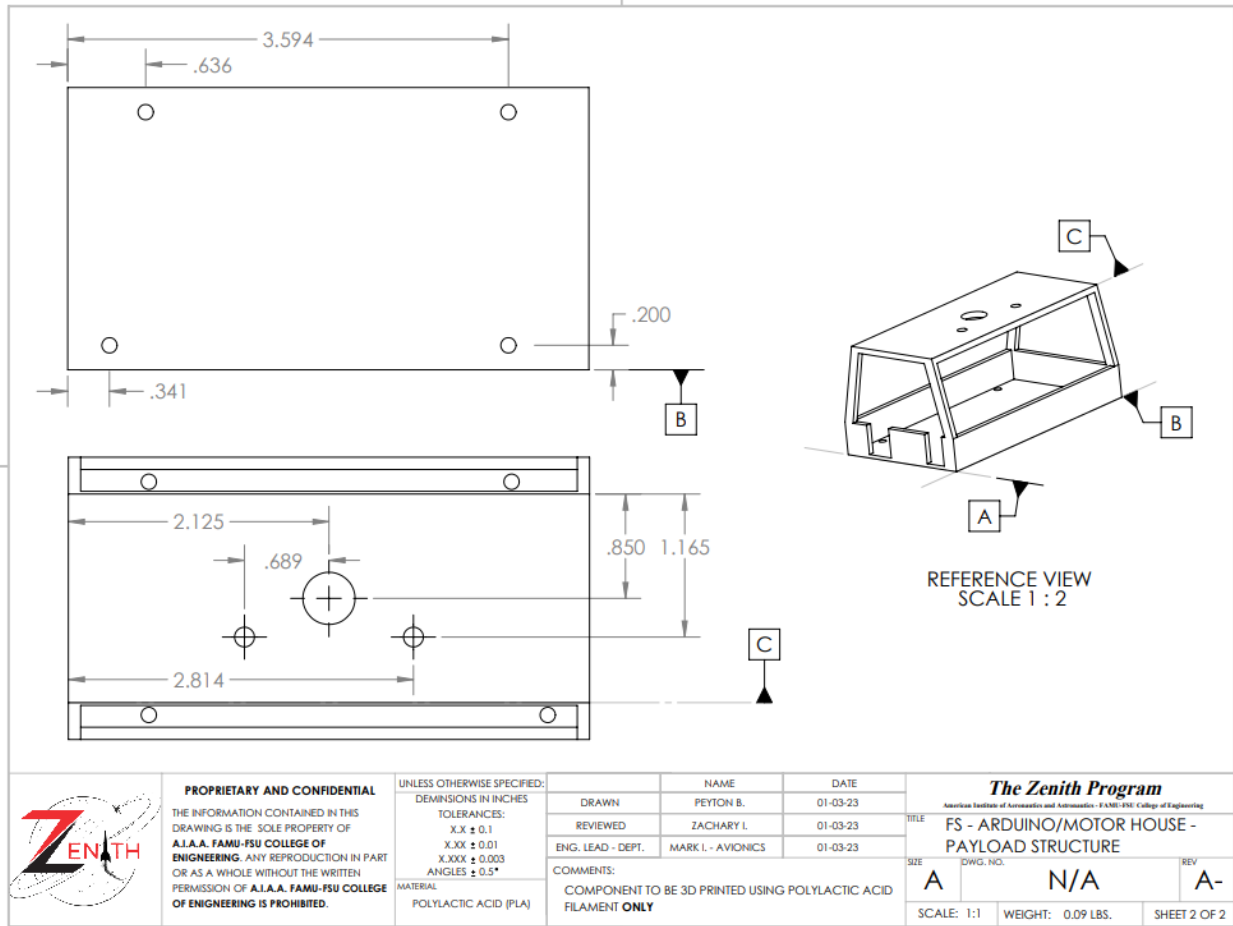


Figure 4-7 Arduino/Motor Housing Drawing (Continued)

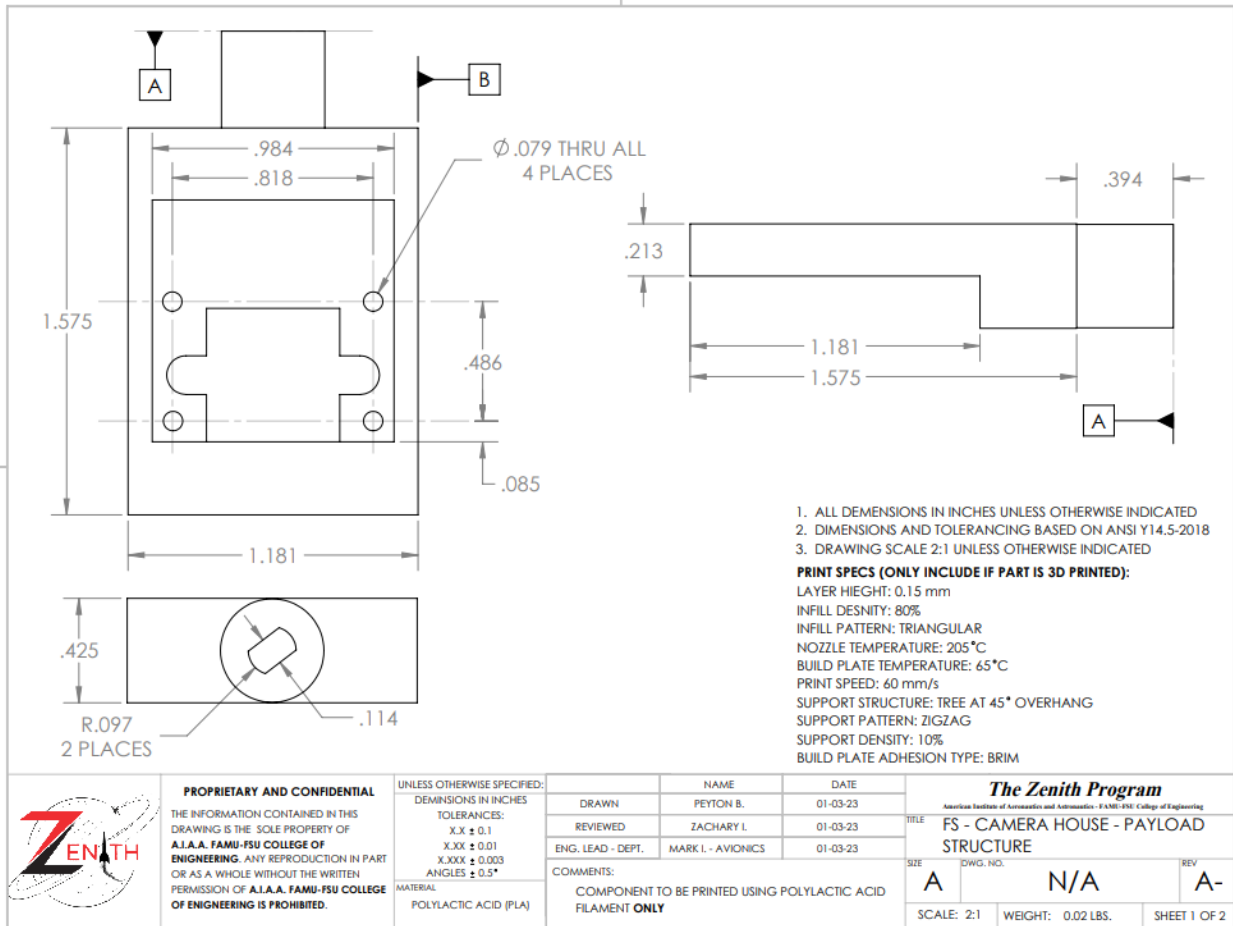


Figure 4-8 Camera Housing Drawing

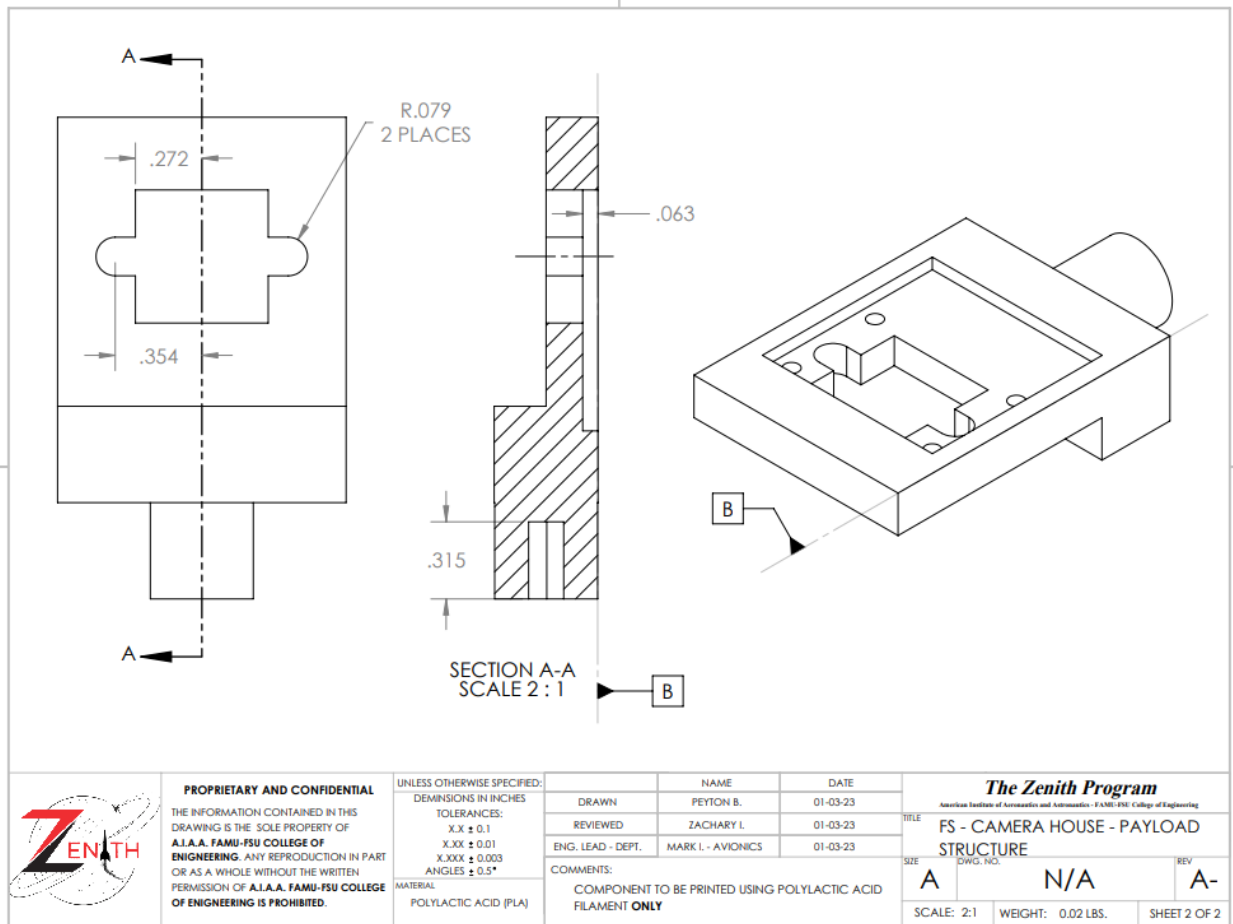


Figure 4-9 Camera Housing Drawing (Continued)

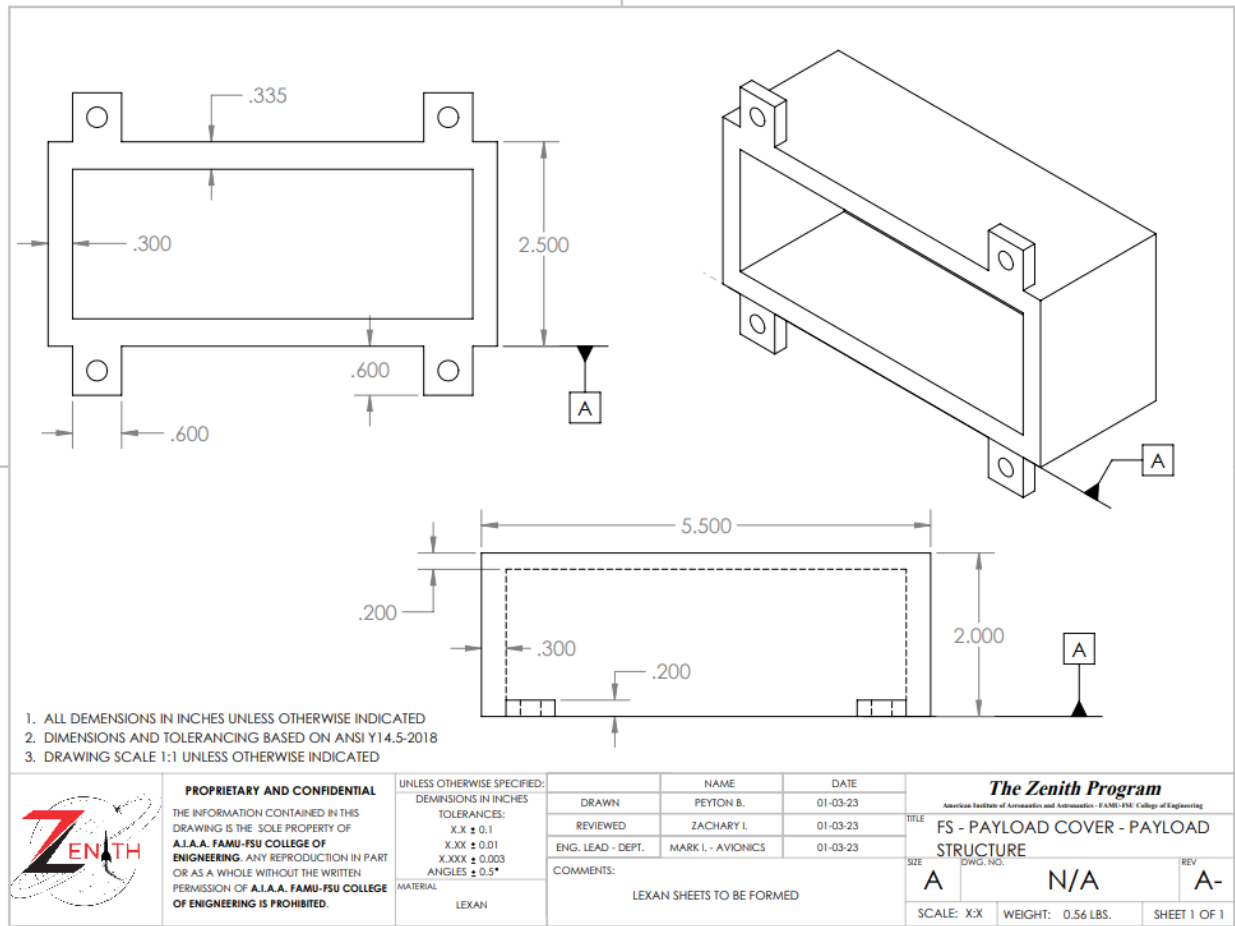


Figure 4-10. Lexan Camera Enclosure

4.3.2 Vehicle integration

The payload will be sandwiched by two 3D printed “bumpers” which follow the surface geometry of the payload housing on their interior, and are rounded externally to the radius of the airframe. The resultant payload package is then effectively a cylinder. The bumpers will be connected to the recovery harness by a short length of shock cord, but not to the payload housing in any way. When seated in the airframe, the bumpers and payload will be effectively immobilized. On main chute deployment, the main parachute will pull the recovery harness from the upper payload bay, pulling out the payload and bumpers. The bumpers will fall away from the payload after exiting the airframe and dangle a ways away from the housing, both exposing the enclosure for ground impact and ensuring the parts do not impede its stable landing.

5 Safety

5.1 Vehicle Assembly and Operation Checklists

The assembly and operation checklists are a chronological order of operations to be executed by the team during launch day assembly, pre-flight, and post-flight. For steps not including the **VERIFY** notice, any member of the team may participate and/or execute the action under the supervision of the associated technical lead (ex: recovery lead supervises connection of wire leads to ejection charge e-matches).

Items that include the **VERIFY** label constitute an all-stop until the Program Director and Safety Officer have both conferred with the associated technical lead, inspected the action described in the **VERIFY** notice, as well as all unverified work up to that point. Both the PD and SO must sign the checklist at each **VERIFY** notice, with approval of the relevant lead, before the team can resume working down the checklist. The purpose of the **VERIFY** notice is to halt progress at mission-critical actions that, if executed incorrectly, could or would result in failure to launch or failures during flight.

A table of justifications for each **VERIFY** notice will follow all checklists.

NOTE:

Checklists announce **Recommended PPE** and **REQUIRED PPE** before an action where PPE would enhance safety or is otherwise required.

While only several checklist steps recommend or require PPE, there are many steps which involve work with low voltage electrical. This is to serve as a blanket notice for all such steps in the interest of brevity on the checklist.

For ANY electrical work, the recommendation of the safety officer is the following:

When making electrical connections – **Recommended PPE: insulating nitrile gloves**

5.1.1 Vehicle Assembly Checklist

Vehicle Assembly Checklist					
Step	Verification	Action	Complete	Program Director	Safety Officer
Avionics Bay					
1	VERIFY	Batteries are charged prior to assembly. Altimeters turn on when switches pressed			
2		Fasten avionics sled inside bay			
3		Route A channel wires and corresponding grounds to one side			
4		Route B channel wires and corresponding grounds to opposite side			
5		Screw CO2 cartridges into all charge bases on inside of bulkheads			
6		Replace avionics bulkhead and fasten			
7	VERIFY	Altimeters turn on when switches are pressed			
For Today's Launch					
	Channel	Color			
	A				
	B				
	G				
Ejection Charges					
8		Place O-ring around base of e-match			
9		PPE Recommended: respirator Place small amount of 5-minute epoxy on O-ring. Pass through charge cup until O-ring contacts bottom			
10		Wait 10 minutes for e-matches to become secured in place			
11		While waiting: prepare 4 pre-measured black powder loads			
12		Once cured: load black powder into charge cups and cover with red sticker			
13	VERIFY	E-matches secure. Charge cups loaded. Stickers firmly attached.			
14		Unscrew red housings from external AV bay. Place charge cups in red housing			

15		Place spring vertical on table. Place steel pointed plug point side down on top of screw		
16		Invert red housing w/ charge cup. Push down against plug until cup is seated at bottom of red housing and plug is directly above		
17	VERIFY	Charge cups properly seated and plugs flush with cup tops		
18		Keeping spring pressed against plug, screw red housing into base on outside of AV bay		
19		Connect A-channel and ground leads to e-match 1 & 2 leads		
20		Connect B-channel and ground leads to e-match 3 & 4 leads		
21	VERIFY	Each e-match is connected to an A/B channel AND a ground wire. Reference wire color table above		
22		Tape external wires to red charge housings, clear of recovery harness attachment bolts		
Upper PL Bay, Payload, and Main Chute				
23		Connect recovery harness end to foreword nosecone bulkhead		
24		Connect main parachute to midpoint quick link of recovery harness		
25	VERIFY	Payload battery is charged. Payload activates when switch is in "on" position		
26		Switch payload electronics to "on"		
27	VERIFY	Payload is on before installation		
28		Place payload in housing. Connect to PL quick link between foreword bulkhead and main chute		
29		Connect recovery harness end to avionics B side bulkhead		
30	VERIFY	Main parachute harness is connected to avionics B side		

31		Lay out horizontal: Nose section, payload, main chute, av bay		
32	VERIFY	All quick links are attached to the correct location and fully closed		
33		Insert payload into housing. Insert payload housing into upper payload bay.		
34		Pack main parachute		
35	VERIFY	Main parachute is correctly packed		
36		Insert packed main chute into upper payload bay. Reeve remaining shock cord		
37		Join upper payload bay and B-side of avionics bay		
38	VERIFY	B-channel ejection charges are inserted into upper payload bay		
39		Screw shear pins into pre-drilled holes to join UPLB and AV bay		
Motor Installation				
52		Unscrew motor retainer ring. Remove motor casing and motor tube from vehicle		
53		<u>PPE Recommended: nitrile gloves</u> Lightly grease aft, forward, and foreword seal disk O-rings		
54		Install forward seal disk O-ring onto foreword seal disk. Install foreword seal disk in motor case.		
55		Install foreword closure with threaded adapter to receive eye bolt		
56	VERIFY	Eye bolt adapter installed to motor case. Install eye bolt		
57		<u>PPE REQUIRED: nitrile gloves, safety goggles, long sleeves, pants, closed-toed shoes</u> Insert liner containing propellant grains into motor tube. Insert tube into motor casing		
58	VERIFY	No motor delay or ejection charge installed.		

59		Screw on aft closure. Replace motor retainer			
60	VERIFY	Motor retainer reinstalled. Nozzle cap fixed over nozzle.			
Lower PL Bay, Fin Can, and Drogue Chute					
40		Connect recovery harness end to eye bolt at top of motor case			
41		Connect drogue parachute to midpoint quick link of recovery harness			
42		Connect recovery harness end to avionics A side bulkhead			
43	VERIFY	Drogue parachute harness is connected to avionics A side			
44		Lay out horizontal: av bay, drogue chute, LPLB/fin can			
45	VERIFY	All quick links are attached to the correct location and fully closed			
46		Pack drogue parachute			
47	VERIFY	Drogue parachute is correctly packed			
48		Insert packed drogue chute into lower payload bay. Reeve remaining shock cord			
49		Join lower payload bay and A-side of avionics bay			
50	VERIFY	A-channel ejection charges are inserted into upper payload bay			
51		Screw shear pins into pre-drilled holes to join LPLB and AV bay			
Final Sign-Off					
61	VERIFY	All checklist steps completed. Vehicle prepared for pre-flight.			

5.1.2 Pre-flight Checklist

Pre-Flight Checklist					
Step	Verification	Action	Complete	Program Director	Safety Officer
1		Confirm launch group/time with NASA RSO			
2		Confirm launch pad with NASA RSO			
3	VERIFY	Cleared by RSO to approach pad			
4		Inspect launch rail cant. Note and refer to simulations			
5		Install vehicle on 1515 launch rail			
6		Switch on flight computers			
7	VERIFY	Flight computers both active			
8		Connect 12V lanch leads to igniter leads on vehicle			
9		Continuity check			
10	VERIFY	Good continuity			
Final Sign-Off					
11	VERIFY	All checklist steps completed. Vehicle prepared for flight.			

5.1.3 Terminal Count and In-Flight Checklist

Terminal Count and In-Flight Checklist					
Step	Verification	Action	Complete	Program Director	Safety Officer
1		Ensure active communication with TeleMega flight computer			
2		Ensure avionics batteries sufficiently charged (live telemetry from TeleMega)			
3	VERIFY	Cleared for launch by RSO			
4		Begin terminal count			
Launch					
5		Avionics lead, using live telemetry, confirms apogee charges fire. Callout: "Sep 1"			
6		Team visually confirms drogue deployment. Callout: "Good drogue"			
7		Avionics lead confirms reduction in descent velocity from telemetry. Callout: "Av Concurs"			
8		Team maintains visual on vehicle during descent			
9		Avionics lead, using live telemetry, confirms 550ft charges fire. Callout: "Sep 2"			
10		Team visually confirms main deployment. Callout: "Good main"			
11		Avionics lead confirms reduction in descent velocity from telemetry. Callout: "Av Concurs"			
12		Team maintains visual on vehicle during descent			

13		Team visually confirms landing. Callout: "Impact"			
14		Avionics lead confirms zero descent velocity from telemetry. Callout: "Av Concurs"			
Final Sign-Off					
15	VERIFY	All checklist steps completed. Vehicle successfully recovered.			

5.1.4 Post-Flight Checklist

Post-Flight Checklist					
Step	Verification	Action	Complete	Program Director	Safety Officer
1	VERIFY	Cleared by RSO to approach pad			
2		Measure distance from pad to point of vehicle impact			
3		Disconnect recovery harnesses from both sides of avionics bay			
4	VERIFY	Avionics bay turned over to avionics lead			
5		Vehicle components returned to staging area. Lay upper and lower sections on table and inspect for damage			
6	VERIFY	Visual confirmation that all ejection charges fired before work on av bay begins			
7		Detach removable av bay bulkhead and remove sled			
8		Avionics team connects to flight computers and downloads data			
9	VERIFY	Data has been downloaded and saved before computer shutdown			
10		Flight computers shutdown			
Final Sign-Off					
11	VERIFY	All checklist steps completed			

5.1.5 Verify Notice Justifications

Table 5-1. Safety Verification(s) Rationale

Checklist	Step #	Step to Verify	Reason for Verification
Assembly	1	Batteries are charged prior to assembly. Altimeters turn on when switches pressed	Uncharged batteries could cause failure to launch or loss of power in flight
Assembly	7	Altimeters turn on when switches are pressed	Ensures connections were not disturbed after av bay is sealed
Assembly	13	E-matches secure. Charge cups loaded. Stickers firmly attached.	Ensures e-matches will not slip from cups and cups cannot spill out black powder. Either case can cause failed separation.
Assembly	17	Charge cups properly seated and plugs flush with cup tops	Improper cup and plug seating can fail to puncture CO2 cartridge, causing failed separation
Assembly	21	Each e-match is connected to an A/B channel AND a ground wire. Reference wire color table above	Ensures a complete circuit is connected to each e-match. Failure to connect ground would mean a dud charge and no separation
Assembly	25	Payload battery is charged. Payload activates when switch is in "on" position	Ensures payload will not experience power loss during mission and switch is functional
Assembly	27	Payload is on before installation	Ensures payload is powered up to execute RAFCO mission
Assembly	30	Main parachute harness is connected to avionics B side	B side is 550ft deployment. If connected to A side, main would deploy at apogee
Assembly	32	All quick links are attached to the correct location and fully closed	Ensures chute is in proper position and connected to sections to avoid entanglement
Assembly	35	Main parachute is correctly packed	Poor packing can cause entanglement
Assembly	38	B-channel ejection charges are inserted into upper payload bay	B side is 550ft deployment. If A side was inserted, upper payload bay would separate at apogee and deploy main chute
Assembly	44	Eye bolt adapter installed to motor case. Install eye bolt	Ensures non-stock foreword closure is used and connection point to fin can is present

Checklist	Step #	Step to Verify	Reason for Verification
Assembly	46	No motor delay or ejection charge installed.	Installation of ejection charge could cause motor jettison, or explosion in airframe if motor was retained after blast
Assembly	48	Motor retainer reinstalled. Nozzle cap fixed over nozzle.	Ensures motor cannot be jettisoned and nozzle will remain debris free
Assembly	52	Drogue parachute harness is connected to avionics A side	A side is apogee deployment. If connected to B, drogue would deploy at 550ft
Assembly	54	All quick links are attached to the correct location and fully closed	Ensures chute is in proper position and connected to sections to avoid entanglement
Assembly	56	Drogue parachute is correctly packed	Poor packing can cause entanglement
Assembly	59	A-channel ejection charges are inserted into upper payload bay	A side is apogee deployment. If B side was inserted, lower payload would separate at 550ft and deploy drogue chute
Pre-Flight	3	Cleared by RSO to approach pad	Ensures range is safe for team members to exit the viewing and staging areas
Pre-Flight	7	Flight computers both active	Failure to activate computers would result in failure to launch
Pre-Flight	10	Good continuity	Bad continuity in 12V igniter system would result in failure to launch
Terminal Count	3	Cleared for launch by RSO	Ensures pad and range are clear for flight
Post-Flight	1	Cleared by RSO to approach pad	Ensures pad and range are safe to approach
Post-Flight	4	Avionics bay turned over to avionics lead	Ensures hand-off of flight data to the team responsible for download and storage
Post-Flight	6	Visual confirmation that all ejection charges fired before work on av bay begins	Prevents possibility of team accidentally triggering charges that failed to fire
Post-Flight	9	Data has been downloaded and saved before computer shutdown	Data may be deleted if power to computer is cut

5.2 Hazard Analysis

**for the convenience of the review board: the payload section and vehicle structures regarding payload retention have been updated to reflect the changes to risk as a result of the radical design change, as has recovery with the removal of electronic chute releases. The team felt all other FMEA's were sufficiently detailed and have presented them as they appeared in PDR. A section discussing verification for mitigation strategies has been added after the FMEA's.*

5.2.1 Risk Matrix and Definitions

To conduct a Failure Mode and Effects Analysis for each vehicle system, environmental risk assessment, and personnel risk assessment, the risk classification matrix in Table 5-1 was used. Tables 5-1 and 5-2 on the following page define each severity and likelihood class.

Table 5-2. Risk Classification Matrix

Risk Classification Matrix			Event Likelihood			
			Possible	Plausible	Probable	Highly Probably
			A	B	C	D
Event Severity	Marginal	1	1A	1B	1C	1D
	Significant	2	2A	2B	2C	2D
	Major	3	3A	3B	3C	3D
	Catastrophic	4	4A	4B	4C	4D

Table 5-3. Severity Classification Definitions

Severity	Vehicle Outcomes	Personnel Outcomes
Marginal	Little to no impact to vehicle integrity. Flight profile consistent with expectation. Safe recovery. Payload intact and deployed. Vehicle can be reused.	No potential for injury created.
Significant	Vehicle integrity compromised. Minor repair required. Deviation from expected flight profile. Safe recovery. Payload intact and deployable. Vehicle can be reused.	Minor risk of injury created. No injuries.
Major	Vehicle integrity compromised. Substantial repair required. Large deviation from expected flight profile. Recovery may endanger personnel. Payload and deployment mechanism damaged. Vehicle can be reused.	Great risk of injury created. Injuries reported. Injuries are manageable with basic first-aid.
Catastrophic	Vehicle breakup in flight. Irreparable damage. Unarrested descent. Recovery not possible. Payload destroyed. Complete loss of vehicle and payload.	Great risk of injury created. Injuries reported. Injuries require professional medical attention.

Table 5-4. Likelihood Classification Definitions

Likelihood	Definition
Possible	Within the set of all conceivable outcomes. Not likely to occur.
Plausible	Reasonable chance of occurrence due to uncertainty bounds.
Probable	Likely to occur. Uncertainty is now in whether the event will not occur.
Highly Probable	Near certainty. Statistical chance of occurrence far outweighs the chance of no occurrence.

5.2.2 Vehicle Systems Failure Mode and Effects Analysis

Table 5-5. Avionics and Power Systems FMEA

Failure Mode	Cause(s)	Hazard Category
(PS.1) Power loss on pad	<ul style="list-style-type: none"> • Dead battery • Disconnection of leads 	1A
Primary Effect(s)	Secondary Effect(s)	Mitigations
<ul style="list-style-type: none"> • Loss of power to flight computer 	<ul style="list-style-type: none"> • Vehicle launch cannot be commanded • Battery replacement required • Personnel must approach cold vehicle – minimal risk 	<ul style="list-style-type: none"> • Ensure battery is charged pre-flight • Have flight computer transmit battery condition • Firm lead attachment • Redundant power/avionics
Failure Mode	Cause(s)	Hazard Category
(PS.2) Power loss in flight	<ul style="list-style-type: none"> • Dead battery • Disconnection of leads 	4A
Primary Effect(s)	Secondary Effect(s)	Mitigations
<ul style="list-style-type: none"> • Loss of power to flight computer 	<ul style="list-style-type: none"> • Loss of vehicle control • No control authority over recovery system • Unable to measure altitude • Unable to command deployment events • Unarrested descent • Risk to personnel 	<ul style="list-style-type: none"> • Ensure battery is charged pre-flight • Have flight computer transmit battery condition • Firm lead attachment • Redundant power/avionics
Failure Mode	Cause(s)	Hazard Category
(PS.3) Power loss after recovery	<ul style="list-style-type: none"> • Dead battery • Disconnection of leads 	1A
Primary Effect(s)	Secondary Effect(s)	Mitigations
<ul style="list-style-type: none"> • Loss of power to flight computer 	<ul style="list-style-type: none"> • Loss of control authority over payload deployment mechanism • Unable to deploy payload 	<ul style="list-style-type: none"> • Ensure battery is charged pre-flight • Have flight computer transmit battery condition • Firm lead attachment • Redundant power/avionics

Failure Mode	Cause(s)	Hazard Category
(AV.1) In-flight barometer failure	<ul style="list-style-type: none"> • Bad component • Poor component calibration • Power loss 	2A
Primary Effect(s)	Secondary Effect(s)	Mitigations
<ul style="list-style-type: none"> • Altitude cannot be determined from atmospheric pressure 	<ul style="list-style-type: none"> • Vehicle relies on double integration of accelerometer data for altitude • Large compounding errors in integration may cause off-nominal main deployment • Nominal drogue deployment using accelerometer 	<ul style="list-style-type: none"> • Purchase components from reputable dealer • Test components extensively before flight • Firm electrical lead attachments • Redundant power/avionics
Failure Mode	Cause(s)	Hazard Category
(AV.2) In-flight accelerometer failure	<ul style="list-style-type: none"> • Bad component • Poor component calibration • Power loss 	2A
Primary Effect(s)	Secondary Effect(s)	Mitigations
<ul style="list-style-type: none"> • Altitude and velocity cannot be determined by integration of acceleration data 	<ul style="list-style-type: none"> • Vehicle relies on inflection of barometric data to determine apogee (pressure begins increasing) • Potential off-nominal drogue deploy • Nominal main chute deployment using barometer 	<ul style="list-style-type: none"> • Purchase components from reputable dealer • Test components extensively before flight • Firm electrical lead attachments • Redundant power/avionics
Failure Mode	Cause(s)	Hazard Category
(AV.3) Simultaneous in-flight accelerometer/barometer failure	<ul style="list-style-type: none"> • Power loss 	2A
Primary Effect(s)	Secondary Effect(s)	Mitigations
<ul style="list-style-type: none"> • Altitude and velocity cannot be determined 	<ul style="list-style-type: none"> • Recovery events reliant on time-commanded backup charges • Off-nominal drogue deploy • Off-nominal main deploy 	<ul style="list-style-type: none"> • Purchase components from reputable dealer • Test components extensively before flight • Firm electrical lead attachments • Redundant power/avionics

Failure Mode	Cause(s)	Hazard Category
(AV.4) In-flight/post-flight GPS unit failure	<ul style="list-style-type: none"> • Bad component • Poor component calibration • Power loss 	2A
Primary Effect(s)	Secondary Effect(s)	Mitigations
<ul style="list-style-type: none"> • Vehicle landing site cannot be precisely determined 	<ul style="list-style-type: none"> • Sonic beacon becomes primary locator • Visual tracking to ground aids in recovery 	<ul style="list-style-type: none"> • Purchase components from reputable dealer • Test components extensively before flight • Firm electrical lead attachments • Redundant power/avionics
Failure Mode	Cause(s)	Hazard Category
(AV.5) Flight computer failure (pre-flight)	<ul style="list-style-type: none"> • Bad component • Power loss 	2A
Primary Effect(s)	Secondary Effect(s)	Mitigations
<ul style="list-style-type: none"> • Loss of control authority over vehicle 	<ul style="list-style-type: none"> • Vehicle launch cannot be commanded • Personnel must approach cold vehicle – minimal risk 	<ul style="list-style-type: none"> • Same as previous
Failure Mode	Cause(s)	Hazard Category
(AV.6) Flight computer failure (in-flight)	<ul style="list-style-type: none"> • Bad component • Power loss 	4A
Primary Effect(s)	Secondary Effect(s)	Mitigations
<ul style="list-style-type: none"> • Loss of control authority over vehicle 	<ul style="list-style-type: none"> • No control authority over recovery system • Unable to measure altitude • Unable to command deployment events • Unarrested descent • Risk to personnel 	<ul style="list-style-type: none"> • Same as previous
Failure Mode	Cause(s)	Hazard Category
(AV.7) Flight computer failure (post-flight)	<ul style="list-style-type: none"> • Bad component • Power loss 	1A
Primary Effect(s)	Secondary Effect(s)	Mitigations
<ul style="list-style-type: none"> • Loss of control authority over vehicle 	<ul style="list-style-type: none"> • Loss of control authority over payload deployment mechanism • Unable to deploy payload 	<ul style="list-style-type: none"> • Same as previous

Failure Mode	Cause(s)	Hazard Category
(AV.8) Wire leads disconnect	<ul style="list-style-type: none"> Excessive vehicle vibration Poor terminal connections 	4D
Primary Effect(s)	Secondary Effect(s)	Mitigations
<ul style="list-style-type: none"> Any combination of AV.1 – AV.4, AV.6, and AV.7 failure modes 	<ul style="list-style-type: none"> Loss of control authority over vehicle No control authority over recovery system Unable to measure altitude Unable to command deployment events Unarrested descent Risk to personnel Loss of control authority over payload deployment mechanism Unable to deploy payload 	<ul style="list-style-type: none"> Ensure proper soldering of terminal leads Extensively test robustness of connections to tension and vibration Implement vibration damping measures for electrical components Redundant power/avionics

Table 5-6. Avionics and Power Systems Risk Matrix

Risk Classification Matrix			Event Likelihood			
			Possible	Plausible	Probable	Highly Probably
			A	B	C	D
Event Severity	Marginal	1	PS.1 1A AV.7 PS.3	1B	1C	1D
	Significant	2	AV.1 AV.4 AV.2 2A AV.3 AV.5	2B	2C	2D
	Major	3	3A	3B	3C	3D
	Catastrophic	4	PS.2 4A AV.6	4B	4C	AV.8 4D

Table 5-7. Energetics and Pyrotechnics FMEA

Failure Mode	Cause(s)	Hazard Category
(PRO.1) Failed motor igniter	<ul style="list-style-type: none"> E-match fails to ignite Black powder pellet fails to ignite after E-match 	3B
Primary Effect(s)	Secondary Effect(s)	Mitigations
<ul style="list-style-type: none"> Vehicle remains on launchpad in unknown state 	<ul style="list-style-type: none"> E-match/igniter replacement required Personnel must approach warm vehicle – significant risk Dud ignition converts vehicle cold Random ignition in time following dud – significant risk to personnel approaching 	<ul style="list-style-type: none"> Redundant e-matches E-match close proximity to black powder pellet
Failure Mode	Cause(s)	Hazard Category
(PRO.2) Ejection charge initiation failure	<ul style="list-style-type: none"> E-match fails to ignite 	2B
Primary Effect(s)	Secondary Effect(s)	Mitigations
<ul style="list-style-type: none"> Body sections do not separate 	<ul style="list-style-type: none"> Separation dependent on backup charge (time initiated) Off-nominal parachute deployment 	<ul style="list-style-type: none"> Redundant e-matches
Failure Mode	Cause(s)	Hazard Category
(PRO.3) Ejection charge fails to separate sections	<ul style="list-style-type: none"> Insufficient black powder load Excessive friction in coupler Shock cord entanglement 	2B
Primary Effect(s)	Secondary Effect(s)	Mitigations
<ul style="list-style-type: none"> Body sections do not fully separate 	<ul style="list-style-type: none"> Structural damage between colliding body sections Separation dependent on backup charge (time initiated) Off-nominal parachute deployment 	<ul style="list-style-type: none"> Redundant ejection charges: Time-commanded backup charge

Failure Mode	Cause(s)	Hazard Category
(EN.1) Unintentional motor ignition	<ul style="list-style-type: none"> • Static Discharge • Human Error 	4B
Primary Effect(s)	Secondary Effect(s)	Mitigations
<ul style="list-style-type: none"> • Launch vehicle departs launch rails unexpectedly 	<ul style="list-style-type: none"> • Flight computer not prepared to execute profile • Unable to command recovery sequence • Burns and hearing damage to personnel in immediate vicinity of vehicle 	<ul style="list-style-type: none"> • Ensure vehicle is grounded in prep area and on pad • Ensure proper communication during count sequence
Failure Mode	Cause(s)	Hazard Category
(EN.2) Unintentional ejection charge initiation (pre-flight)	<ul style="list-style-type: none"> • Static Discharge • Human Error 	4B
Primary Effect(s)	Secondary Effect(s)	Mitigations
<ul style="list-style-type: none"> • Unexpected black powder detonation 	<ul style="list-style-type: none"> • Creation of large audible signature and expulsion of hot exhaust gasses • Great injury to personnel standing in line with and near charge. Medical emergency • Burns and hearing damage to personnel in immediate vicinity of vehicle • Body section(s) are ejected • Body sections impact nearby personnel. Minor to significant injuries 	<ul style="list-style-type: none"> • Ensure vehicle is grounded in prep area and on pad • Ensure proper communication during count sequence • Implement CO2 ejection system

Failure Mode	Cause(s)	Hazard Category
(EN.3) Uneven combustion in solid fuel	<ul style="list-style-type: none"> Poor mixing of fuel and oxidizer Poor distribution of propellant in case 	4C
Primary Effect(s)	Secondary Effect(s)	Mitigations
<ul style="list-style-type: none"> Asymmetric thrust about vehicle z-axis 	<ul style="list-style-type: none"> Deviation from expected flight path Loss of vehicle stability In-flight break up of vehicle. Loss of vehicle Unarrested descent. Risk to personnel 	<ul style="list-style-type: none"> Purchase motor from reputable dealer (Cesaroni is the current selection)
Failure Mode	Cause(s)	Hazard Category
(EN.4) Motor exhaust in body tube	<ul style="list-style-type: none"> Motor case rupture Nozzle foreword of thrust plate 	4B
Primary Effect(s)	Secondary Effect(s)	Mitigations
<ul style="list-style-type: none"> Damage to body tube Loss of vehicle integrity 	<ul style="list-style-type: none"> Mid-flight fin detachment Catastrophic body rupture Vehicle in-flight breakup Loss of vehicle 	<ul style="list-style-type: none"> Aluminum motor case, thrust plate, and motor retainer Extensive sealing in motor compartment
Failure Mode	Cause(s)	Hazard Category
(EN.5) Motor jettison	<ul style="list-style-type: none"> Thrust plate or motor retainer failure 	3A
Primary Effect(s)	Secondary Effect(s)	Mitigations
<ul style="list-style-type: none"> Motor and casing separate from launch vehicle after burnout 	<ul style="list-style-type: none"> Changes to stability margin as Cg shifts towards nose Deviation from projected flight profile Risk to personnel from uncontrolled, unarrested descent of metal motor casing 	<ul style="list-style-type: none"> Aluminum thrust plate and motor retainer to ensure dynamic loading margins are not exceeded

Failure Mode	Cause(s)	Hazard Category
(EN.6) Avionics damage	<ul style="list-style-type: none"> Hot/corrosive ejection charge exhaust gasses 	4B
Primary Effect(s)	Secondary Effect(s)	Mitigations
<ul style="list-style-type: none"> Development of any AV.1 – AV.4 and AV.6 Failure Modes 	<ul style="list-style-type: none"> No control authority over recovery system Unable to measure altitude Unable to command deployment events Unarrested descent Risk to personnel 	<ul style="list-style-type: none"> Insulate void space in body Implement CO2 ejection system
Failure Mode	Cause(s)	Hazard Category
(EN.7) Burned parachute(s)	<ul style="list-style-type: none"> Hot/corrosive ejection charge exhaust gasses 	4D
Primary Effect(s)	Secondary Effect(s)	Mitigations
<ul style="list-style-type: none"> Drogue and/or main parachute unable to provide sufficient drag to slow descent 	<ul style="list-style-type: none"> Partially or fully unarrested descent Fire inside body tube Fire in canopy on descent 	<ul style="list-style-type: none"> Kevlar blankets to retain chutes Insulate void space Implement CO2 ejection system
Failure Mode	Cause(s)	Hazard Category
(EN.8) Chain detonation of ejection charges	<ul style="list-style-type: none"> Hot/corrosive ejection charge exhaust gasses 	3B
Primary Effect(s)	Secondary Effect(s)	Mitigations
<ul style="list-style-type: none"> Multiple separation event at apogee Simultaneous deployment of drogue and main chute 	<ul style="list-style-type: none"> Deviation from intended flight profile Risk to personnel from (4) and (5) structural damage to colliding body sections Parachute entanglement. Increased descent rate Uncontrolled descent. Decreased descent rate. Increased wind drift. Vehicle exits recovery zone 	<ul style="list-style-type: none"> Insulate void space in body Implement CO2 cooling system to black powder ejection charges

Table 5-8. Energetics and Pyrotechnics Risk Matrix

Risk Classification Matrix			Event Likelihood			
			Possible	Plausible	Probable	Highly Probably
			A	B	C	D
Event Severity	Marginal	1	1A	1B	1C	1D
	Significant	2	2A	PRO.2 2B PRO.3	2C	2D
	Major	3	EN.5 3A	PRO.1 3B EN.8	3C	3D
	Catastrophic	4	4A	EN.1 EN.4 4B EN.2 EN.6	EN.3 4C	EN.7 4D

Table 5-9. Recovery System FMEA

Failure Mode	Cause(s)	Hazard Category
(RS.1) Drogue parachute entanglement	<ul style="list-style-type: none"> Poor shock cord stowage in body Snag hazards in deployment path 	4B
Primary Effect(s)	Secondary Effect(s)	Mitigations
<ul style="list-style-type: none"> High descent rate after apogee Main parachute deployment at higher speed 	<ul style="list-style-type: none"> Main parachute canopy damaged in high-speed deployment Main parachute cords tear or rupture Partially or fully unarrested vehicle descent Over tensioning of vehicle shock cord. Cord tearing or rupture Unarrested descent of body sections Risk to personnel Major repair needed 	<ul style="list-style-type: none"> Design for no snag hazards in deployment path of parachute Reeve loose shock cord Implement cord routing solutions
Failure Mode	Cause(s)	Hazard Category
(RS.2) Main parachute entanglement	<ul style="list-style-type: none"> Poor shock cord stowage in body Snag hazards in deployment path 	3B
Primary Effect(s)	Secondary Effect(s)	Mitigations
<ul style="list-style-type: none"> High descent rate after main deployment High ground impact velocity 	<ul style="list-style-type: none"> Partially arrested descent Damage to vehicle structures Damage to internal components Major repair required 	<ul style="list-style-type: none"> Design for no snag hazards in deployment path of parachute Reeve loose shock cord Implement cord routing solutions
Failure Mode	Cause(s)	Hazard Category
(RS.3) Shock cord rupture	<ul style="list-style-type: none"> Excessive tension on cord 	3A
Primary Effect(s)	Secondary Effect(s)	Mitigations
<ul style="list-style-type: none"> Tether between body sections compromised 	<ul style="list-style-type: none"> Unarrested descent of body section(s) 	<ul style="list-style-type: none"> Extensive simulation pre-flight Select shock cord with large factor of safety

Failure Mode	Cause(s)	Hazard Category
(RS.4) Shock cord entanglement	<ul style="list-style-type: none"> Poor shock cord stowage in body Snag hazards in deployment path 	1B
Primary Effect(s)	Secondary Effect(s)	Mitigations
<ul style="list-style-type: none"> Shock cord unable to extend to full length 	<ul style="list-style-type: none"> Collision of body sections on descent Very minor damage to structure 	<ul style="list-style-type: none"> Reeve loose shock cord Implement cord routing solutions

Table 5-10. Recovery System Risk Matrix

Risk Classification Matrix			Event Likelihood			
			Possible	Plausible	Probable	Highly Probably
			A	B	C	D
Event Severity	Marginal	1	1A	RS.4 1B	1C	1D
	Significant	2	2A	2B	2C	2D
	Major	3	RS.3 3A	RS.2 3B	3C	3D
	Catastrophic	4	4A	RS.1 4B	4C	4D

Table 5-11. Vehicle Structures FMEA

Failure Mode	Cause(s)	Hazard Category
(STR.1) Melting of fin assembly during motor burn	<ul style="list-style-type: none"> Heat transfer from motor case Lack of heat resistance in fin material 	4B
Primary Effect(s)	Secondary Effect(s)	Mitigations
<ul style="list-style-type: none"> Loss of flight stability 	<ul style="list-style-type: none"> Vehicle breakup in-flight Loss of vehicle Unarrested descent of body sections Risk to personnel 	<ul style="list-style-type: none"> Use heat resistant print material Treat for heat resistance Minimize heat transfer
Failure Mode	Cause(s)	Hazard Category
(STR.2) Fins shear off	<ul style="list-style-type: none"> Fin flutter Aerodynamic loading 	4B
Primary Effect(s)	Secondary Effect(s)	Mitigations
<ul style="list-style-type: none"> Loss of flight stability 	<ul style="list-style-type: none"> Vehicle breakup in-flight Loss of vehicle Unarrested descent of body sections Risk to personnel 	<ul style="list-style-type: none"> Extensive simulation pre-flight Ensure flutter speed >> max vehicle velocity
Failure Mode	Cause(s)	Hazard Category
(STR.3) Body tube zippering	<ul style="list-style-type: none"> Shock cord contact with body on deployment 	3B
Primary Effect(s)	Secondary Effect(s)	Mitigations
<ul style="list-style-type: none"> Loss of vehicle integrity 	<ul style="list-style-type: none"> Vehicle damage on descent Major repair needed 	<ul style="list-style-type: none"> Implement “bumpers” to avoid cord contact Implement cord routing
Failure Mode	Cause(s)	Hazard Category
(STR.4) Damaged motor retainer	<ul style="list-style-type: none"> Defect in part Excessive dynamic loading 	3A
Primary Effect(s)	Secondary Effect(s)	Mitigations
<ul style="list-style-type: none"> Potential motor jettison after burnout 	<ul style="list-style-type: none"> Unarrested descent of motor casing Risk to personnel Minor repair required 	<ul style="list-style-type: none"> Aluminum motor retainer to absorb far larger loads than necessary

Failure Mode	Cause(s)	Hazard Category
(STR.5) Bulkhead or U-bolt torn loose	<ul style="list-style-type: none"> Excessive loading during chute deployment Late chute deployment 	4B
Primary Effect(s)	Secondary Effect(s)	Mitigations
<ul style="list-style-type: none"> Body section(s) disconnected from parachute 	<ul style="list-style-type: none"> Unarrested descent of body section(s) Risk to personnel Major repairs required 	<ul style="list-style-type: none"> Extensive pre-flight simulation Extra thick bolts and wide bracing on bulkheads
Failure Mode	Cause(s)	Hazard Category
(STR.6) Dislodged centering ring(s)	<ul style="list-style-type: none"> Defect in part(s) Excessive dynamic loading Poor connection to threaded rods 	3A
Primary Effect(s)	Secondary Effect(s)	Mitigations
<ul style="list-style-type: none"> Motor long axis no longer colinear with vehicle z-axis 	<ul style="list-style-type: none"> Deviation from flight profile Minor loss of stability Risk to personnel 	<ul style="list-style-type: none"> Fix centering rings to threaded rods with hex nuts Use thread lock to fix nuts
Failure Mode	Cause(s)	Hazard Category
(STR.7) Damaged payload retainer	<ul style="list-style-type: none"> Defect in part(s) Poor 3D print Excessive dynamic loading Excessive ground impact velocity 	1B
Primary Effect(s)	Secondary Effect(s)	Mitigations
<ul style="list-style-type: none"> Payload sits loose in bay 	<ul style="list-style-type: none"> Minor decrease in vehicle stability Minor camera housing damage Improper or impossible rover deployment 	<ul style="list-style-type: none"> Extensive pre-flight testing Minimize ground impact velocity Cushion landing
Failure Mode	Cause(s)	Hazard Category
(STR.8) Damaged avionics sled retainer(s)	<ul style="list-style-type: none"> Defect in part(s) Poor 3D print Excessive dynamic loading Excessive ground impact velocity 	3B
Primary Effect(s)	Secondary Effect(s)	Mitigations
<ul style="list-style-type: none"> Avionics sleds sit loose in av bay 	<ul style="list-style-type: none"> Potential for AV.8 failure mode Loss of control authority over vehicle 	<ul style="list-style-type: none"> Extensive pre-flight testing Minimize ground impact velocity Cushion landing

Table 5-12. Vehicle Structures Risk Matrix

Risk Classification Matrix			Event Likelihood			
			Possible	Plausible	Probable	Highly Probably
			A	B	C	D
Event Severity	Marginal	1	STR.7 1A	1B	1C	1D
	Significant	2	2A	STR.4 2B	2C	2D
	Major	3	STR.6 3A	STR.3 3B STR.8	3C	3D
	Catastrophic	4	4A	STR.1 4B STR.5 STR.2	4C	4D

Table 5-13. Payload FMEA

Failure Mode	Cause(s)	Hazard Category
(PLD.1) 3-D printed housing damaged	<ul style="list-style-type: none"> High ground impact velocity Defects in 3D print 	1C
Primary Effect(s)	Secondary Effect(s)	Mitigations
<ul style="list-style-type: none"> Structure of camera housing compromised 	<ul style="list-style-type: none"> Internal wiring shifted. Leads torn from Arduino 	<ul style="list-style-type: none"> Extensive pre-flight testing Minimize ground impact velocity Cushion landing
Failure Mode	Cause(s)	Hazard Category
(PLD.2) Payload lands in a manner where camera is not right side up	<ul style="list-style-type: none"> Improper connection to shock cord High lateral landing velocity 	1B
Primary Effect(s)	Secondary Effect(s)	Mitigations
<ul style="list-style-type: none"> Payload may be in a configuration which occludes camera view 	<ul style="list-style-type: none"> Images gathered during RAFCO sequence are poor 	<ul style="list-style-type: none"> Design connection points to maximize possibility of landing z-axis up Implement anti-roll measures in the design
Failure Mode	Cause(s)	Hazard Category
(PLD.3) Power loss	<ul style="list-style-type: none"> Dead battery Electrical lead disconnection 	1B
Primary Effect(s)	Secondary Effect(s)	Mitigations
<ul style="list-style-type: none"> Loss of control authority over camera 	<ul style="list-style-type: none"> RAFCO Mission failure 	<ul style="list-style-type: none"> Charge battery pre-flight Firm electrical connections
Failure Mode	Cause(s)	Hazard Category
(PLD.4) Antenna disconnection from microcontroller	<ul style="list-style-type: none"> Excessive vibration in flight Excessive ground impact velocity 	1D
Primary Effect(s)	Secondary Effect(s)	Mitigations
<ul style="list-style-type: none"> Loss of control authority over camera and antenna 	<ul style="list-style-type: none"> RAFCO Mission failure 	<ul style="list-style-type: none"> Firm electrical connections Pad landing, reduce velocity

Failure Mode	Cause(s)	Hazard Category
(PLD.5) Microcontroller unit failure	<ul style="list-style-type: none"> • Bad component • Power loss 	1A
Primary Effect(s)	Secondary Effect(s)	Mitigations
<ul style="list-style-type: none"> • Loss of control authority over camera and antenna 	<ul style="list-style-type: none"> • RAFCO Mission failure 	<ul style="list-style-type: none"> • Firm electrical connections • Reputable supplier
Failure Mode	Cause(s)	Hazard Category
(PLD.6) Camera failure	<ul style="list-style-type: none"> • Broken lens during ground impact • Power loss 	1A
Primary Effect(s)	Secondary Effect(s)	Mitigations
<ul style="list-style-type: none"> • Loss of image capturing ability 	<ul style="list-style-type: none"> • RAFCO Mission failure 	<ul style="list-style-type: none"> • Padding or protection around camera assembly • Firm electrical connections
Failure Mode	Cause(s)	Hazard Category
(PLD.7) Camera actuation system failure	<ul style="list-style-type: none"> • Motor failure • Obstructed gears • Power loss 	1B
Primary Effect(s)	Secondary Effect(s)	Mitigations
<ul style="list-style-type: none"> • Camera cannot swivel camera 	<ul style="list-style-type: none"> • RAFCO Mission failure 	<ul style="list-style-type: none"> • Firm electrical connections • Clean gear mechanism • Use self-contained stepper motor

Table 5-14. Payload Risk Matrix

Risk Classification Matrix			Event Likelihood			
			Possible	Plausible	Probable	Highly Probably
			A	B	C	D
Event Severity	Marginal	1	PLD.5 1A PLD.6	PLD.2 1B PLD.3 PLD.7	PLD.1 1C	PLD.4 1D
	Significant	2	2A	2B	2C	2D
	Major	3	3A	3B	3C	3D
	Catastrophic	4	4A	4B	4C	4D

Table 5-15. Environment FMEA

Vehicle Risks to Environment		
Failure Mode	Cause(s)	Hazard Category
(ENV.1.1) Launch pad/recovery area fire (energetic initiated)	<ul style="list-style-type: none"> • Dry vegetation in vicinity of motor ignition 	3B
Primary Effect(s)	Secondary Effect(s)	Mitigations
<ul style="list-style-type: none"> • Danger to wildlife • Danger to habitat • Danger to personnel 	<ul style="list-style-type: none"> • Potential for fire growth if left unmitigated 	<ul style="list-style-type: none"> • Clear launch area of vegetation
Failure Mode	Cause(s)	Hazard Category
(ENV.1.2) Launch pad/recovery area fire (LiPo battery initiated)	<ul style="list-style-type: none"> • Battery overcharge, over discharge, overtemp 	4B
Primary Effect(s)	Secondary Effect(s)	Mitigations
<ul style="list-style-type: none"> • Danger to wildlife • Danger to habitat • Danger to personnel • HazMat release 	<ul style="list-style-type: none"> • Pollution of crops with HazMat • Pollution of groundwater with HazMat 	<ul style="list-style-type: none"> • Clear launch area of vegetation • Do not use battery improperly
Failure Mode	Cause(s)	Hazard Category
(ENV.1.3) Interstage insulation littered in launch/recovery area	<ul style="list-style-type: none"> • Insulation used in body tube to minimize void space and insulate parachutes from ejection charge gasses 	1C
Primary Effect(s)	Secondary Effect(s)	Mitigations
<ul style="list-style-type: none"> • Ingestion of insulation by wildlife 	<ul style="list-style-type: none"> • Disrespectful to property owners to eject litter on their land 	<ul style="list-style-type: none"> • Biodegradable insulation (popcorn)
Failure Mode	Cause(s)	Hazard Category
(ENV.1.4) Litter spread over launch site by personnel	<ul style="list-style-type: none"> • Lack of trashcans • Poor team leadership 	1D
Primary Effect(s)	Secondary Effect(s)	Mitigations
<ul style="list-style-type: none"> • Ingestion of litter by wildlife 	<ul style="list-style-type: none"> • Disrespectful to property owners to litter on their land 	<ul style="list-style-type: none"> • Bring trash bags • Firm leadership. Zero tolerance for littering

Environmental Risks to Vehicle		
Failure Mode	Cause(s)	Hazard Category
(ENV.2.1) Vehicle touches down in nearby trees	<ul style="list-style-type: none"> Excessive wind drift 	4B
Primary Effect(s)	Secondary Effect(s)	Mitigations
<ul style="list-style-type: none"> Difficulty in or inability to recover launch vehicle Minor damage to vehicle components 	<ul style="list-style-type: none"> Loss of vehicle Repairs required 	<ul style="list-style-type: none"> Extra-long shock cord to bring components closer to ground
Failure Mode	Cause(s)	Hazard Category
(ENV.2.2) Vehicle touches down in nearby body of water	<ul style="list-style-type: none"> Excessive wind drift 	3B
Primary Effect(s)	Secondary Effect(s)	Mitigations
<ul style="list-style-type: none"> Damage to body tube structure Damage to avionics or payload electronics 	<ul style="list-style-type: none"> Major repairs required 	<ul style="list-style-type: none"> Extensive sealing of avionics bay and rover GNC unit
Failure Mode	Cause(s)	Hazard Category
(ENV.2.3) In-flight Collision	<ul style="list-style-type: none"> Tall infrastructure (power lines) Bird strike 	4A
Primary Effect(s)	Secondary Effect(s)	Mitigations
<ul style="list-style-type: none"> Loss of stability Damage to animal or object impacted 	<ul style="list-style-type: none"> Loss of vehicle Repair to damaged infrastructure required 	<ul style="list-style-type: none"> Ensure vehicle is launched away from all infrastructure Await clear skies
Failure Mode	Cause(s)	Hazard Category
(ENV.2.4) Vehicle or components dropped	<ul style="list-style-type: none"> Uneven launch site terrain causes personnel tripping 	3B
Primary Effect(s)	Secondary Effect(s)	Mitigations
<ul style="list-style-type: none"> Damage to vehicle structures Damage to payload structures Damage to avionics Damage to payload electronics 	<ul style="list-style-type: none"> Inability to launch Repairs required 	<ul style="list-style-type: none"> Practice extreme caution while handling vehicle components

Table 5-16. Environmental Risk Matrix

Risk Classification Matrix			Event Likelihood			
			Possible	Plausible	Probable	Highly Probably
			A	B	C	D
Event Severity	Marginal	1	1A	1B	ENV.1.3 1C	ENV.1.4 1D
	Significant	2	2A	2B	2C	2D
	Major	3	3A	ENV.1.1 3B ENV.2.2 ENV.2.4	3C	3D
	Catastrophic	4	ENV.2.3 4A	ENV.1.2 4B ENV.2.1	4C	4D

5.2.3 Personnel Risk Assessment

Personnel risk assessment was conducted using the same FMEA format as was used for vehicle systems and environmental risk assessment.

Table 5-17. Personnel FMEA

Failure Mode	Cause(s)	Hazard Category
(PPL.1) Skin contact with APCP solid propellant	<ul style="list-style-type: none"> Improper material handling Lack of PPE 	3D
Primary Effect(s)	Secondary Effect(s)	Mitigations
<ul style="list-style-type: none"> Chemical burns Eye irritation 	<ul style="list-style-type: none"> None 	<ul style="list-style-type: none"> Provide safety training Provide PPE
Failure Mode	Cause(s)	Hazard Category
(PPL.2) Electrocutation	<ul style="list-style-type: none"> Improper safety procedures followed Live electrical while wiring 	2D
Primary Effect(s)	Secondary Effect(s)	Mitigations
<ul style="list-style-type: none"> Discomfort/pain Burns 	<ul style="list-style-type: none"> Greater or grave injury with prolonged exposure 	<ul style="list-style-type: none"> Provide safety training
Failure Mode	Cause(s)	Hazard Category
(PPL.3) Proximity to high-pressure burst event (CO2 charge)	<ul style="list-style-type: none"> Overpressure in pressure vessel Pressure vessel tipping Human error 	3B
Primary Effect(s)	Secondary Effect(s)	Mitigations
<ul style="list-style-type: none"> Hearing damage Struck/Impaled by flying object(s) 	<ul style="list-style-type: none"> None 	<ul style="list-style-type: none"> Provide safety training Do not overfill pressure vessels Pressure vessels chained to walls Declare all testing and clear area prior to initiation

Failure Mode	Cause(s)	Hazard Category
(PPL.4) Proximity to explosive event (Black powder charge)	<ul style="list-style-type: none"> Accidental initiation (human error, static discharge) 	4B
Primary Effect(s)	Secondary Effect(s)	Mitigations
<ul style="list-style-type: none"> Hearing damage Burns from expanding hot gasses 	<ul style="list-style-type: none"> Severity increased with proximity Severity increased with decreased angle-off-bore of charge 	<ul style="list-style-type: none"> Ground vehicle components Minimize personnel handling charges Isolate firing mechanism until range clear
Failure Mode	Cause(s)	Hazard Category
(PPL.5) Proximity to combustion event	<ul style="list-style-type: none"> Motor ignition (intentional) Motor ignition (unintentional) Loose black powder burn 	4B
Primary Effect(s)	Secondary Effect(s)	Mitigations
<ul style="list-style-type: none"> Hearing damage Burns from expanding hot gasses 	<ul style="list-style-type: none"> Severity increased with proximity Severity increased with decreased angle-off-bore of charge 	<ul style="list-style-type: none"> Ground vehicle components Minimize personnel handling motor Isolate ignition mechanism until range clear
Failure Mode	Cause(s)	Hazard Category
(PPL.6) Injury: slip and fall, minor cuts, accidental collisions	<ul style="list-style-type: none"> Uneven terrain Tripping hazards on flat ground Improperly stored sharp objects 	3B
Primary Effect(s)	Secondary Effect(s)	Mitigations
<ul style="list-style-type: none"> Pain/discomfort Bruises Small lacerations 	<ul style="list-style-type: none"> Infection of lacerations not immediately treated 	<ul style="list-style-type: none"> Situational awareness Clean lab spaces Proper safety procedures
Failure Mode	Cause(s)	Hazard Category
(PPL.7) Dehydration, heat exhaustion, heat stroke	<ul style="list-style-type: none"> Lack of water Lack of adequate sun protection or shade 	4B
Primary Effect(s)	Secondary Effect(s)	Mitigations
<ul style="list-style-type: none"> Thirst Disorientation Loss of consciousness 	<ul style="list-style-type: none"> None 	<ul style="list-style-type: none"> Provide ample water Bring portable awning/tent Bring sunscreen, hats, etc.

Failure Mode	Cause(s)	Hazard Category
(PPL.8) Soldering iron burns	<ul style="list-style-type: none"> Improper use or stowage of soldering iron 	3D
Primary Effect(s)	Secondary Effect(s)	Mitigations
<ul style="list-style-type: none"> Minor burns 	<ul style="list-style-type: none"> Increased severity with prolonged contact 	<ul style="list-style-type: none"> Proper training in use of soldering iron Minimize personnel involved

Table 5-18. Personnel Risk Matrix

Risk Classification Matrix			Event Likelihood			
			Possible	Plausible	Probable	Highly Probably
			A	B	C	D
Event Severity	Marginal	1	1A	1B	1C	1D
	Significant	2	2A	2B	2C	PPL.2 2D
	Major	3	3A	PPL.3 3B	3C	PPL.1 3D PPL.8
	Catastrophic	4	4A	PPL.4 4B PPL.5 PPL.7	4C	4D

5.3 Verification Strategies for proposed mitigations

Table 5-19. Risks, Mitigations, and Verifications

Avionics and Power Systems			
Failure Mode	Cause(s)	Mitigations	Verification Strategy
(PS.1) Power loss on pad	<ul style="list-style-type: none"> • Dead battery • Disconnection of leads 	<ul style="list-style-type: none"> • Ensure battery is charged pre-flight • Have flight computer transmit battery condition • Firm lead attachment • Redundant power/avionics 	<ul style="list-style-type: none"> • Assembly/Operations Checklist • Pre-flight hardware testing (vibration test)
(PS.2) Power loss in flight	<ul style="list-style-type: none"> • Dead battery • Disconnection of leads 	<ul style="list-style-type: none"> • Ensure battery is charged pre-flight • Have flight computer transmit battery condition • Firm lead attachment • Redundant power/avionics 	<ul style="list-style-type: none"> • Assembly/Operations Checklist • Pre-flight hardware testing (vibration test)
(PS.3) Power loss after recovery	<ul style="list-style-type: none"> • Dead battery • Disconnection of leads 	<ul style="list-style-type: none"> • Ensure battery is charged pre-flight • Have flight computer transmit battery condition • Firm lead attachment • Redundant power/avionics 	<ul style="list-style-type: none"> • Assembly/Operations Checklist • Pre-flight hardware testing (vibration test)
(AV.1) In-flight barometer failure	<ul style="list-style-type: none"> • Bad component • Poor component calibration • Power loss 	<ul style="list-style-type: none"> • Purchase components from reputable dealer • Test components extensively before flight • Firm electrical lead attachments • Redundant power 	<ul style="list-style-type: none"> • Mentor input • Pre-flight hardware testing (vibration test)
(AV.2) In-flight accelerometer failure	<ul style="list-style-type: none"> • Bad component • Poor component calibration • Power loss 	<ul style="list-style-type: none"> • Purchase components from reputable dealer • Test components extensively before flight 	<ul style="list-style-type: none"> • Mentor input • Pre-flight hardware testing (vibration test)

		<ul style="list-style-type: none"> • Firm electrical lead attachments • Redundant power/avionics 	
<p>(AV.3) Simultaneous in-flight accelerometer/ barometer failure</p>	<ul style="list-style-type: none"> • Power loss 	<ul style="list-style-type: none"> • Purchase components from reputable dealer • Test components extensively before flight • Firm electrical lead attachments • Redundant power/avionics 	<ul style="list-style-type: none"> • Mentor input • Pre-flight hardware testing (vibration test)
<p>(AV.4) In-flight/post-flight GPS unit failure</p>	<ul style="list-style-type: none"> • Bad component • Poor component calibration • Power loss 	<ul style="list-style-type: none"> • Purchase components from reputable dealer • Test components extensively before flight • Firm electrical lead attachments <p>Redundant power/avionics</p>	<ul style="list-style-type: none"> • Mentor input • Pre-flight hardware testing (vibration test)
<p>(AV.5) Flight computer failure (pre-flight)</p>	<ul style="list-style-type: none"> • Bad component • Power loss 	<ul style="list-style-type: none"> • Same as previous 	<ul style="list-style-type: none"> • Mentor input • Pre-flight hardware testing (vibration test)
<p>(AV.6) Flight computer failure (in-flight)</p>	<ul style="list-style-type: none"> • Bad component • Power loss 	<ul style="list-style-type: none"> • Same as previous 	<ul style="list-style-type: none"> • Mentor input • Pre-flight hardware testing (vibration test)
<p>(AV.7) Flight computer failure (post-flight)</p>	<ul style="list-style-type: none"> • Bad component • Power loss 	<ul style="list-style-type: none"> • Same as previous 	<ul style="list-style-type: none"> • Mentor input • Pre-flight hardware testing (vibration test)
<p>(AV.8) Wire leads disconnect</p>	<ul style="list-style-type: none"> • Excessive vehicle vibration • Poor terminal connections 	<ul style="list-style-type: none"> • Ensure proper soldering of terminal leads • Extensively test robustness of connections to tension and vibration • Implement vibration damping measures for electrical components <p>Redundant power</p>	<ul style="list-style-type: none"> • Pre-flight hardware testing (vibration test)

Energetics and Pyrotechnics			
Failure Mode	Cause(s)	Mitigations	Verification Strategy
(PRO.1) Failed motor igniter	<ul style="list-style-type: none"> E-match fails to ignite Black powder pellet fails to ignite after E-match 	<ul style="list-style-type: none"> Redundant e-matches E-match close proximity to black powder pellet 	<ul style="list-style-type: none"> Assembly/Operations Checklist
(PRO.2) Ejection charge initiation failure	<ul style="list-style-type: none"> E-match fails to ignite 	<ul style="list-style-type: none"> Redundant e-matches 	<ul style="list-style-type: none"> Assembly/Operations Checklist
(PRO.3) Ejection charge fails to separate sections	<ul style="list-style-type: none"> Insufficient black powder load Excessive friction in coupler Shock cord entanglement 	<ul style="list-style-type: none"> Redundant ejection charges Time-commanded backup charge 	<ul style="list-style-type: none"> Assembly/Operations Checklist Pre-flight hardware testing (separation test) Pre-flight simulations (Shear pin FEA)
(EN.1) Unintentional motor ignition	<ul style="list-style-type: none"> Static Discharge Human Error 	<ul style="list-style-type: none"> Ensure vehicle is grounded in prep area and on pad Ensure proper communication during count sequence 	<ul style="list-style-type: none"> Assembly/Operations Checklist
(EN.2) Unintentional ejection charge initiation (pre-flight)	<ul style="list-style-type: none"> Static Discharge Human Error 	<ul style="list-style-type: none"> Ensure vehicle is grounded in prep area and on pad Ensure proper communication during count sequence CO2 ejection system 	<ul style="list-style-type: none"> Assembly/Operations Checklist
(EN.3) Uneven combustion in solid fuel	<ul style="list-style-type: none"> Poor mixing of fuel and oxidizer Poor distribution of propellant in case 	<ul style="list-style-type: none"> Purchase motor from reputable dealer 	<ul style="list-style-type: none"> Mentor input
(EN.4) Motor exhaust in body tube	<ul style="list-style-type: none"> Motor case rupture Nozzle foreword of thrust plate 	<ul style="list-style-type: none"> Aluminum motor case, thrust plate, and motor retainer Extensive sealing in motor compartment 	<ul style="list-style-type: none"> Assembly/Operations Checklist Mentor input

(EN.5) Motor jettison	<ul style="list-style-type: none"> Thrust plate or motor retainer failure 	<ul style="list-style-type: none"> Aluminum thrust plate and motor retainer to ensure dynamic loading margins are not exceeded 	<ul style="list-style-type: none"> Pre-flight hardware testing (load test) Pre-flight simulations (FEA)
(EN.6) Avionics damage	<ul style="list-style-type: none"> Hot/corrosive ejection charge exhaust gasses 	<ul style="list-style-type: none"> Insulate void space in body Implement CO2 ejection system 	<ul style="list-style-type: none"> Pre-flight hardware testing (separation test) Pre-flight simulations (CFD heat transfer)
(EN.7) Burned parachute(s)	<ul style="list-style-type: none"> Hot/corrosive ejection charge exhaust gasses 	<ul style="list-style-type: none"> Kevlar blankets to retain chutes Insulate void space Implement CO2 ejection system 	<ul style="list-style-type: none"> Pre-flight hardware testing (separation test) Pre-flight simulations (CFD heat transfer)
(EN.8) Chain detonation of ejection charges	<ul style="list-style-type: none"> Hot/corrosive ejection charge exhaust gasses 	<ul style="list-style-type: none"> Insulate void space in body Implement CO2 cooling system to black powder ejection charges 	<ul style="list-style-type: none"> Pre-flight hardware testing (separation test) Pre-flight simulations (CFD heat transfer)
Recovery System			
Failure Mode	Cause(s)	Mitigations	Verification Strategy
(RS.1) Drogue parachute entanglement	<ul style="list-style-type: none"> Poor shock cord stowage in body Snag hazards in deployment path 	<ul style="list-style-type: none"> Design for no snag hazards in deployment path of parachute Reeve loose shock cord Implement cord routing solutions 	<ul style="list-style-type: none"> Assembly/Operations Checklist Mentor input
(RS.2) Main parachute entanglement	<ul style="list-style-type: none"> Poor shock cord stowage in body Snag hazards in deployment path 	<ul style="list-style-type: none"> Design for no snag hazards in deployment path of parachute Reeve loose shock cord Implement cord routing solutions 	<ul style="list-style-type: none"> Assembly/Operations Checklist Mentor input
(RS.3) Shock cord rupture	<ul style="list-style-type: none"> Excessive tension on cord 	<ul style="list-style-type: none"> Extensive simulation pre-flight Select shock cord with large factor of safety 	<ul style="list-style-type: none"> Pre-flight hardware testing (weighted drop test) Pre-flight simulations
(RS.4) Shock cord entanglement	<ul style="list-style-type: none"> Poor shock cord stowage in body Snag hazards in deployment path 	<ul style="list-style-type: none"> Reeve loose shock cord Implement cord routing solutions 	<ul style="list-style-type: none"> Assembly/Operations Checklist Mentor input

Vehicle Structures			
Failure Mode	Cause(s)	Mitigations	Verification Strategy
(STR.1) Melting of fin assembly during motor burn	<ul style="list-style-type: none"> Heat transfer from motor case Lack of heat resistance in fin material 	<ul style="list-style-type: none"> Use heat resistant print material Treat for heat resistance Minimize heat transfer 	<ul style="list-style-type: none"> Material testing with High Performance Materials Institute
(STR.2) Fins shear off	<ul style="list-style-type: none"> Fin flutter Aerodynamic loading 	<ul style="list-style-type: none"> Extensive simulation pre-flight Ensure flutter speed >> max vehicle velocity 	<ul style="list-style-type: none"> Aerodynamic testing with Florida Center for Advanced Aero Propulsion
(STR.3) Body tube zippering	<ul style="list-style-type: none"> Shock cord contact with body on deployment 	<ul style="list-style-type: none"> Implement “bumpers” to avoid cord contact Implement cord routing 	<ul style="list-style-type: none"> Assembly/Operations Checklist Mentor input
(STR.4) Damaged motor retainer	<ul style="list-style-type: none"> Defect in part Excessive dynamic loading 	<ul style="list-style-type: none"> Aluminum motor retainer to absorb far larger loads than necessary 	<ul style="list-style-type: none"> Pre-flight simulations (FEA)
(STR.5) Bulkhead or U-bolt torn loose	<ul style="list-style-type: none"> Excessive loading during chute deployment Late chute deployment 	<ul style="list-style-type: none"> Extensive pre-flight simulation Extra thick bolts and wide bracing on bulkheads 	<ul style="list-style-type: none"> Pre-flight hardware testing (jerk) Pre-flight simulations (FEA)
(STR.6) Dislodged centering ring(s)	<ul style="list-style-type: none"> Defect in part(s) Excessive dynamic loading Poor connection to threaded rods 	<ul style="list-style-type: none"> Fix centering rings to threaded rods with hex nuts Use thread lock to fix nuts 	<ul style="list-style-type: none"> Pre-flight hardware testing (jerk) Pre-flight simulations (FEA)
(STR.7) Damaged payload retainer	<ul style="list-style-type: none"> Defect in part(s) Poor 3D print Excessive dynamic loading Excessive ground impact velocity 	<ul style="list-style-type: none"> Extensive pre-flight testing Minimize ground impact velocity Cushion landing 	<ul style="list-style-type: none"> Material testing with High Performance Materials Institute Pre-flight hardware testing (vibration and drop test)
(STR.8) Damaged avionics sled retainer(s)	<ul style="list-style-type: none"> Defect in part(s) Poor 3D print Excessive dynamic loading Excessive ground impact velocity 	<ul style="list-style-type: none"> Extensive pre-flight testing Minimize ground impact velocity Cushion landing 	<ul style="list-style-type: none"> Material testing with High Performance Materials Institute Pre-flight hardware testing (vibration and drop test)

Payload			
Failure Mode	Cause(s)	Mitigations	Verification Strategy
(PLD.1) 3-D printed housing damaged	<ul style="list-style-type: none"> High ground impact velocity Defects in 3D print 	<ul style="list-style-type: none"> Extensive pre-flight testing Minimize ground impact velocity Cushion landing 	<ul style="list-style-type: none"> Pre-flight hardware testing (drop test)
(PLD.2) Payload lands in a manner where camera is not right side up	<ul style="list-style-type: none"> Improper connection to shock cord High lateral landing velocity 	<ul style="list-style-type: none"> Design connection points to maximize possibility of landing z-axis up Implement anti-roll measures in the design 	<ul style="list-style-type: none"> Pre-flight hardware testing (drop test)
(PLD.3) Power loss	<ul style="list-style-type: none"> Dead battery Electrical lead disconnection 	<ul style="list-style-type: none"> Charge battery pre-flight Firm electrical connections 	<ul style="list-style-type: none"> Assembly/Operations Checklist Pre-flight hardware testing (vibration test)
(PLD.4) Antenna disconnection from microcontroller	<ul style="list-style-type: none"> Excessive vibration in flight Excessive ground impact velocity 	<ul style="list-style-type: none"> Firm electrical connections Pad landing, reduce velocity 	<ul style="list-style-type: none"> Pre-flight hardware testing (vibration test)
(PLD.5) Microcontroller failure	<ul style="list-style-type: none"> Bad component Power loss 	<ul style="list-style-type: none"> Firm electrical connections Reputable supplier 	<ul style="list-style-type: none"> Pre-flight hardware testing (vibration test)
(PLD.6) Camera failure	<ul style="list-style-type: none"> Broken lens during ground impact Power loss 	<ul style="list-style-type: none"> Padding or protection around camera assembly Firm electrical connections 	<ul style="list-style-type: none"> Pre-flight hardware testing (drop test) Pre-flight hardware testing (vibration test)
(PLD.7) Camera actuation system failure	<ul style="list-style-type: none"> Motor failure Obstructed gears Power loss 	<ul style="list-style-type: none"> Firm electrical connections Clean gear mechanism Use self-contained stepper motor 	<ul style="list-style-type: none"> Pre-flight hardware testing (drop test) Pre-flight hardware testing (vibration test)
Vehicle Risks to Environment			
Failure Mode	Cause(s)	Hazard Category	Verification Strategy
(ENV.1.1) Launch pad/recovery area fire (energetic initiated)	<ul style="list-style-type: none"> Dry vegetation in vicinity of motor ignition 	<ul style="list-style-type: none"> Clear launch area of vegetation 	<ul style="list-style-type: none"> Team has no control over this. NASA has stated pad will be in plowed field (only topsoil)

(ENV.1.2) Launch pad/recovery area fire (LiPo battery initiated)	<ul style="list-style-type: none"> Battery overcharge, over discharge, overtemp 	<ul style="list-style-type: none"> Clear launch area of vegetation Do not use battery improperly 	<ul style="list-style-type: none"> Team has no control over this. NASA has stated pad will be in plowed field (only topsoil) Assembly/Operations Checklist Battery storage/charging rules implemented in fabrication shop
(ENV.1.3) Interstage insulation littered in launch/recovery area	<ul style="list-style-type: none"> Insulation used in body tube to minimize void space and insulate parachutes from ejection charge gasses 	<ul style="list-style-type: none"> Biodegradable insulation (popcorn) 	<ul style="list-style-type: none"> Assembly/Operations Checklist May not need to insulate interstage...subscale did fine without any
(ENV.1.4) Litter spread over launch site by personnel	<ul style="list-style-type: none"> Lack of trashcans Poor team leadership 	<ul style="list-style-type: none"> Bring trash bags Firm leadership. Zero tolerance for littering 	<ul style="list-style-type: none"> Pre-launch week departure purchase and packing list
Environmental Risks to Vehicle			
Failure Mode	Cause(s)	Mitigations	Verification Strategy
(ENV.2.1) Vehicle touches down in nearby trees	<ul style="list-style-type: none"> Excessive wind drift 	<ul style="list-style-type: none"> Extra-long shock cord to bring components closer to ground 	<ul style="list-style-type: none"> Assembly/Operations Checklist
(ENV.2.2) Vehicle touches down in nearby body of water	<ul style="list-style-type: none"> Excessive wind drift 	<ul style="list-style-type: none"> Extensive sealing of avionics bay and camera system 	<ul style="list-style-type: none"> Assembly/Operations Checklist
(ENV.2.3) In-flight Collision	<ul style="list-style-type: none"> Tall infrastructure (power lines) Bird strike 	<ul style="list-style-type: none"> Ensure vehicle is launched away from all infrastructure Await clear skies 	<ul style="list-style-type: none"> Assembly/Operations Checklist
(ENV.2.4) Vehicle or components dropped	<ul style="list-style-type: none"> Uneven launch site terrain causes personnel tripping 	<ul style="list-style-type: none"> Practice extreme caution while handling vehicle components 	<ul style="list-style-type: none"> Assembly/Operations Checklist

Personnel			
Failure Mode	Cause(s)	Mitigations	Verification Strategy
(PPL.1) Skin contact with APCP solid propellant	<ul style="list-style-type: none"> Improper material handling Lack of PPE 	<ul style="list-style-type: none"> Provide safety training Provide PPE 	<ul style="list-style-type: none"> Posted laboratory safety rules Safety Officer supervision PPE freely available in fabrication shop PPE included in launch week packing list
(PPL.2) Electrocution	<ul style="list-style-type: none"> Improper safety procedures followed Live electrical while wiring 	<ul style="list-style-type: none"> Provide safety training 	<ul style="list-style-type: none"> Posted laboratory safety rules Safety Officer supervision PPE freely available in fabrication shop
(PPL.3) Proximity to high-pressure burst event (CO2 charge)	<ul style="list-style-type: none"> Overpressure in pressure vessel Pressure vessel tipping Human error 	<ul style="list-style-type: none"> Provide safety training Do not overfill pressure vessels Pressure vessels chained to walls Declare all testing and clear area prior to initiation 	<ul style="list-style-type: none"> Posted laboratory safety rules Safety Officer supervision
(PPL.4) Proximity to explosive event (Black powder charge)	<ul style="list-style-type: none"> Accidental initiation (human error, static discharge) 	<ul style="list-style-type: none"> Ground vehicle components Minimize personnel handling charges Isolate firing mechanism until range clear 	<ul style="list-style-type: none"> Posted laboratory safety rules Safety Officer supervision
(PPL.5) Proximity to combustion event	<ul style="list-style-type: none"> Motor ignition (intentional) Motor ignition (unintentional) Loose black powder burn 	<ul style="list-style-type: none"> Ground vehicle components Minimize personnel handling motor Isolate ignition mechanism until range clear 	<ul style="list-style-type: none"> Posted laboratory safety rules Safety Officer supervision
(PPL.6) Injury: slip and fall, minor cuts, accidental collisions	<ul style="list-style-type: none"> Uneven terrain Tripping hazards on flat ground Improperly stored sharp objects 	<ul style="list-style-type: none"> Situational awareness Clean lab spaces Proper safety procedures 	<ul style="list-style-type: none"> Posted laboratory safety rules Safety Officer supervision Fabrication shop manager appointed to

			ensure clean/safe environment
(PPL.7) Dehydration, heat exhaustion, heat stroke	<ul style="list-style-type: none"> • Lack of water • Lack of adequate sun protection or shade 	<ul style="list-style-type: none"> • Provide ample water • Bring portable awning/tent • Bring sunscreen, hats, etc. 	<ul style="list-style-type: none"> • Safety Officer supervision • Water, sunscreen, portable tents included in launch week packing list
(PPL.8) Soldering iron burns	<ul style="list-style-type: none"> • Improper use or stowage of soldering iron 	<ul style="list-style-type: none"> • Proper training in use of soldering iron • Minimize personnel involved 	<ul style="list-style-type: none"> • Safety Officer supervision • PPE (thick gloves) provided freely in fab shop • Training offered before use

6 Project Plan

6.1 Testing

Table 6-1. Vehicle Component and Assembly Tests

Test	Objective	Items of Interest	Success Criteria	Methodology
Drop	Determine impact resistance of vehicle sections	Breaks or cracks in vehicle or payload structures Electrical leads disconnecting	Fins do not crack Airframe does not crack or rupture Payload housing and clear camera shroud do not crack or break	Simple Newtonian physics calculation using known mass and desired impact velocity to determine drop height. Drop vehicle sections and/or payload. Inspect
Jerk	Verify connection points do not fail under large instantaneous load	Bending, warping, or cracking of bulkheads, hardware, or epoxied connections	U-bolts and eyebolts remain intact No deformation of bulkheads No dislodging of epoxied bulkhead to airframe connections No unintended breakage of shear pins	Connect recovery harness to U-bolt or eyebolt. Affix end of harness to test rig on second story of college. Drop individual vehicle sections, multiple tethered sections, or avionics pinned to upper or lower payload bay. Inspect airframe structures. Inspect shear pins.

Continued on following page

<p>Vibration</p>	<p>Ensure electrical and hardware connections are robust enough to withstand powered ascent phase</p>	<p>Severity of vibration or RPM of spin before connections begin to loosen</p>	<p>No electrical leads disconnect No nuts, bolts, etc begin to come undone</p>	<p>Affix vehicle section to LabView controlled electric motor. Spin section about z-axis to max RPM from simulations. Inspect hardware connections and av bay. Physically shake vehicle section (by hand) progressively harder and faster so as to well exceed the minor vibrations experienced on launch. Inspect hardware connections and av bay.</p>
<p>Separation</p>	<p>Validate that shear pins will break and sections will forcefully separate when ejection charges are fired</p>	<p>Grams in CO2 cartridge Shear pin size Distance vehicle section is ejected from avionics bay</p>	<p>Shear pins break Vehicle section is ejected from test rig Vehicle section travels far enough to deploy parachute from payload bay</p>	<p>Load ejection charges in av bay with long alligator leads to be manually attached to a battery. Join av bay to vehicle section with shear pins. Place joined sections onto “test sled” rig, ensuring the rear of the av bay is firm against the rear brace. Connect alligator clips to battery terminal to light charge. Inspect result.</p>

6.2 Requirements Verification

6.2.1 Team Derived Requirements

Table 6-2: Safety Team Derived Verification Matrix

Safety Team Derived Requirements				
Number	Description	Justification	Success Criteria	Verification Method
1	Proper safety equipment shall be provided to all personnel	The use of PPE helps to reduce the likelihood of injury while working	Entrances to all team shops are stocked with all necessary PPE	Fabrication Shop Manager
2	Launch day attendees shall keep a reasonable pace during all aspects of activities	Maintaining a steady pace reduces the likelihood of falling or tripping	Team members are to walk, meaning having one foot on the ground at a time	Safety Officer Supervision Operations Checklists
3	All major hazards identified in the risk assessment matrix shall be decreased to yellow or green by CDR through mitigations	Mitigating potentially dangerous/frequent hazards creates a more robust system	All hazards identified in the CDR document fall in the yellow or green zones after the mitigation.	Operations Checklists

Table 6-3: Launch Vehicle Team Derived Verification Matrix

Launch Vehicle Team Derived Requirements				
Number	Description	Justification	Success Criteria	Verification Method
1	The launch vehicle shall not exceed 16Gs of acceleration during ascent	Acceleration higher than 16Gs could cause problems for the payload or vehicle structure	Simulations are done in OpenRocket	Pre-flight Simulation
2	The launch vehicle shall have symmetrical fins	This ensures that the launch vehicle is aerodynamic and ensures the CG is on center by causing equal aerodynamics on both sides and equal weight distribution	The launch vehicle has four fins equally spaced from each other around the airframe along with one camera positioned at the center of the nosecone	Visual Inspection
3	The lower payload bay shall have at least 6 inches of interior length	This is to give the payload team enough space for any lower payload electronics	The lower payload bay is designed to have 6 inches of interior length	Physical Measurement Assembly checklist
4	The airframe shall be capable of launching in temperatures between 20- and 100-degrees Fahrenheit	The launch vehicle is planned to operate in a variety of launch fields and seasons	The airframe material is rated to not be damaged or deformed under these temperatures	Pre-flight Testing
5	The launch vehicle shall not go above Mach 0.7	Higher speeds and accelerations are not necessary they endanger the payload and other structural components	Simulations are done in OpenRocket to confirm the launch vehicles maximum velocity	Pre-flight Simulation
6	The launch vehicle shall use at least 2 centering rings to support the motor tube	This ensures that the motor tube has the adequate support to experience the high force caused by the motor	Two centering rings along with the engine block will be used to support the motor tube	Pre-flight Simulation Pre-flight testing Assembly checklist

7	The launch vehicle shall have a stability margin between 2.5 and 3.5 calibers	Stability margins lower than 2 are prohibited by NASA. Margins of stability greater than 2.2 are more stable	The aerodynamics lead designs the launch vehicle such that minimum stability margin of 2.5 calibers.	Pre-flight simulation Sub-scale result verification
---	---	--	--	--

Table 6-4. Recovery Team Derived Requirements

Recovery Team Derived Requirements				
Number	Description	Justification	Success Criteria	Verification Method
1	Fully charged batteries shall be used for the altimeters before every flight	Insufficient voltage supply can lead to the altimeter powering off	New batteries will be chosen and verified to be full before being placed on the AV sled	Operations checklist
2	U-bolts shall be used for all shock cord connections	U-bolts provide two points where shock can go through the bulkhead to increase stability	U-bolts are installed on the bulkheads as anchor points for the recovery harness	Assembly Checklist
3	All electronic components in the launch vehicle shall be removable.	Removable electronics allow for easier changes and adjustments to design	None of the electronic components in the launch vehicle are permanently fixed in place	Pre-flight testing Assembly checklist
4	There shall be no more than 4 sections of the vehicle recovered	NASA gives a requirement that there can be no more than 4 of the vehicle	The vehicle will be designed to have only 4 sections	Pre-flight simulation Pre-flight testing Assembly checklist
5	The secondary ejection charges shall be based off a configured time set on the redundant altimeter	This will guarantee proper parachute deployments if the primary altimeter fails	Both altimeters are completely independent of each other	Pre-flight testing Sub-scale flight result verification

Table 6-5. Payload Team-Derived Requirments

Payload Team Derived Requirements				
Number	Description	Justification	Success Criteria	Verification Method
1	The payload vehicle SHALL have a diameter of less than 4.5 inches.	The Inner diameter of the launch vehicle is already limited to 6 inches. The extra space is needed for the rover housing	The Payload fits inside of its housing.	Physical measurement Assembly checklist
2	The payload shall be supported within the launch vehicle	The payload is subjected to the different forces during the launch. To limit the movement during the launch it must be supported from all sides.	The payload integration system supports the payload so that it is not dislodged before deployment	Pre-flight testing
3	The payload integration system shall be a maximum of 7 inches long	Limiting the length of the integration system also limits the payload length. This all lends to a more favorable static stability margin	The payload integration system is less than 7 inches	Pre-flight simulation Pre-flight testing Assembly checklist

6.3 Budgeting and Timeline

6.3.1 Budget

The following table summarizes the remaining project expenses for full-scale and payload component acquisition and shipping, propellant for test flights, and travel to test launches and launch week.

Table 6-6. Project Budget Summary

Project Component	Expected Cost
Full-scale airframe and propellant	\$1900.00
Avionics system improvements	\$650.00
Payload Materials	\$50.00
Shipping and Handling	\$125.00
Transportation and logistics	\$1,900.00
Remaining Project Cost:	\$4,625.00

6.3.2 Funding and Material Acquisition

6.3.2.1 Funding Sources

Funding for this year's project team is being graciously provided through two sources: the Aero-Propulsion, Mechatronics, and Energy (AME) center has diverted \$2,000 of their NASA MUREP Grant funding to Zenith Program to facilitate Florida A&M student involvement with a complex aerospace project, and to facilitate FAMU student relations with NASA at large, in hopes of creating a firm feeder pipeline of underrepresented minority students to NASA. This MUREP funding has been expended to cover a portion of the subscale vehicle. The FAMU-FSU COE Mechanical Engineering Department has generously agreed to cover the difference in project costs for parts and material, transportation to the test launch facility, and transportation and lodging for Launch Week. At this point in the project the ME Department has taken on material acquisition after the AME funding was expended.

6.3.2.2 Funding Allocation

Using the budget sheet, now excluding all purchased components, a determination of project cost vs. time (or milestones) was made. These expenditures to achieve each milestone will be used to coordinate with the project sponsors for funding disbursement and to monitor the whether the project is on-budget when reaching each milestone.

Remaining Expenditure by Milestone		
Full-scale	\$1,884.83	
Propellant	\$289.99	
Logistics	\$103.60	
Add:	\$2,278.42	Test Flight 2
		\$2,278.42
Payload	\$43.85	
Propellant	\$289.99	
Logistics	\$103.60	
Add:	\$437.44	Test Flight 3
		\$2,715.86
Propellant	\$289.99	
Logistics	\$1,678.40	
Add:	\$1,968.39	Competition Flight
		\$4,684.25

Figure 6-1. Expenditure by Flight Milestone

6.3.2.3 Material Acquisition Plan

Material acquisition has been streamlined with the initial investment by the AME Center expended and the full and sole support of the Mechanical Engineering department. The Program Director was given a point of contact in the office of the ME Department Chair to relay all material requests. The department then either places online orders with expedited shipping using Florida State P-Cards (university issued credit cards), or coordinates with local hardware vendors who have existing accounts with the University.

6.3.3 Project Timeline

The updated project Gantt chart has been attached as Appendix B.

From the Gantt chart, major project milestones and their corresponding completion dates and expected durations are summarized in the table below, which lists activities through the payload demonstration flight, submission of FRR, and completion of project phase 3.

The team has assessed adherence to the Gantt chart from Proposal to CDR and has determined that engineering milestones are being met appropriately. STEM engagement, however, has been chronically delayed. The updated timeline submitted in PDR pushed back establishing points of contact and event planning into mid-November and December of 2022. Points of contact were established in mid-December 2022 and event planning will not begin until roughly a week after the public school system begins their spring semester. The team plans to aggressively pursue firm dates for STEM engagement events to not allow any further delay.

Table 6-7. Project Timeline Summary Sub-Scale through FRR

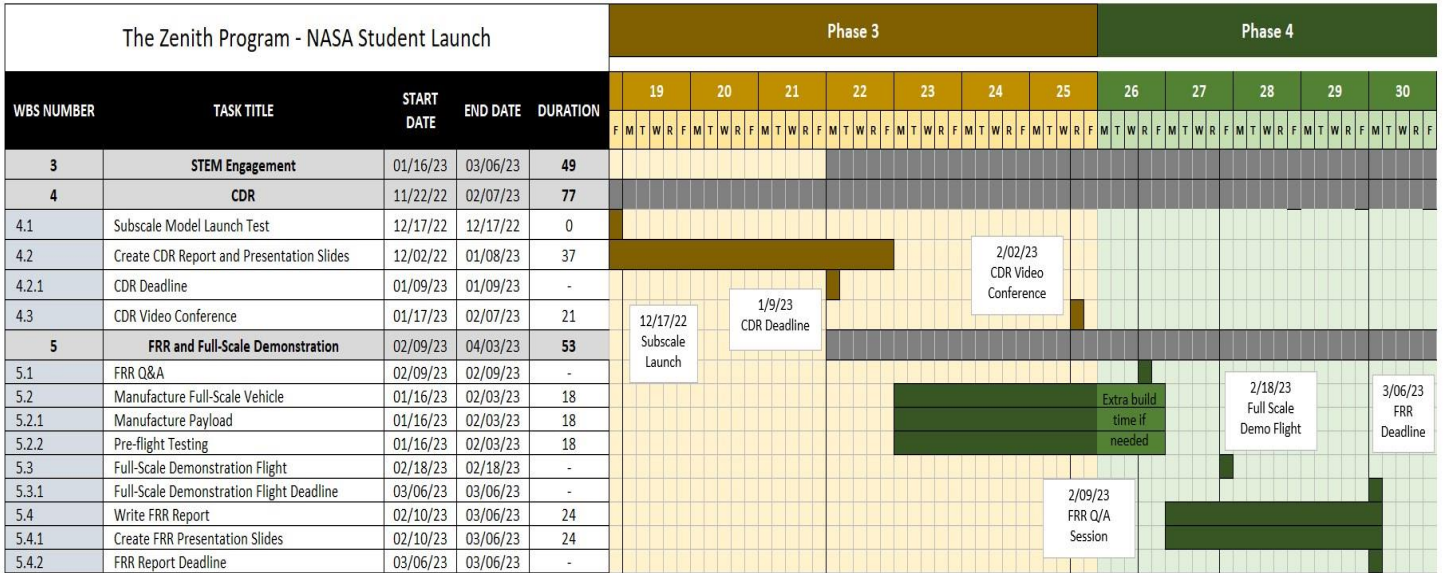
Goal Owner	Milestone or Deliverable	Expected (*Required) Completion Date	Estimated Activity Duration
Zenith	Subscale test flight	12/17/2022	1 day
Zenith	Begin CDR Report and sub-scale data analysis	*1/9/2023	30 days

NASA SLI	Submit CDR Report and slides	*1/9/2023	30 days
Zenith	Submit full-scale parts order to ME department	1/13/2023	5 days
Zenith	Schedule STEM Engagement events with points of contact	1/16/2023	7 days
Zenith	Full-scale assembly and testing	2/3/2023	30 days
Zenith	Payload assembly and testing	2/3/2023	30 days
NASA SLI	FRR Q/A Session	2/9/2023	1 day
Zenith	STEM Engagement Events	3/1/2023	30 days
Zenith	Begin FRR Report	*3/6/2023	25 days
Zenith	Full-Scale demonstration flight	NET: 2/11/2023 2/18/2023	1 day
Zenith	Full-Scale data analysis	NET: 2/15/2023	2 days
NASA SLI	Submit FRR Report and slides	*3/6/2023	25 days

Appendix A. Revised Budget

Zenith Program Budget (Rev: 12/2022)			
Part Name	Quantity	Cost	Quantity Cost
Avionics System			
TeleMega	1	\$400.00	\$400.00
TeleBT Ground Module	1	\$165.00	\$165.00
Arrow Antenna 3E Yagi	1	\$74.99	\$74.99
Subtotal:			\$639.99
Full-Scale Vehicle			
ID = 6.0", L = 48" Airframe - Blue Tube 2.0	2	\$77.42	\$154.84
6" to 75mm Centering Ring - Baltic Birch	3	\$9.50	\$28.50
6" Airframe Bulkhead	6	\$8.95	\$53.70
OD = 6", L = 12" Avionics Bay w/ Hardware	1	\$72.00	\$72.00
AeroPack 75mm retainer (flanged)	1	\$75.83	\$75.83
AeroTech 75mm Hardware Kit	1	\$629.99	\$629.99
Aerotech L1150-R	3	\$289.99	\$869.97
Subtotal:			\$1,884.83
Payload			
12V DC brushed motor	1	\$17.86	\$17.86
Arducam Mini 8MP	1	\$25.99	\$25.99
Subtotal:			\$43.85
General/Uncategorized Components			
Shipping and handling - all budget bulk estimate	1	\$125.00	\$125.00
Subtotal:			\$125.00
Transportation and Logistics			
Gas reimbursement - SRA test launches (Orlando)	2	\$103.60	\$207.20
Gas reimbursement - NASA MSFC (Huntsville)	1	\$118.40	\$118.40
Student IHG Hotel Rooms (4 days, \$90/day)	2	\$360.00	\$720.00
Food Stipend (4 comp. days, \$35/day/student)	6	\$140.00	\$840.00
Subtotal:			\$1,885.60

Appendix B. Gantt Chart



Appendix C. Stability and Flutter Speed MATLAB Code

Flutter Speed (Material --> ABS Fialment)

```
% Defining Initial parameters

E = 416258.3; % Young's Modulus (psi) v = 0.37; %
Poisson's Ratio (unitless) Cr = 11; % Root Chord in
inches Ct = 3; % Tip Chord in inches t = 0.47; %
Thickness in inches b = 9; % Fin Height relative to the
root chord in inches

% The following equations will calculate the fin flutter speed for the
% leading design's fin configuration using ABS filament as the
material of % choice

G = E/(2*(1+v));
h = 4600; % Max height the rocket will reach in feet S = (1/2)*(Cr +
Ct)*b; % Wing Area (inches squared) AR = (b.^2)/S; % Aspect Ratio
(unitless) lambda = Ct/Cr; % Taper Ratio (unitless) T = 59 -
0.00356*h; % Temp (Fahrenheit) P = (2116/144)*((T +
459.7)/518.6).^5.256; % Pressure (also converts to lb/in^2)
a = sqrt(1.4*1716.59*(T + 459.7)); %Speed of sound (ft/s)
Vf = a*sqrt((G/(1.337*(AR.^3)*P*(lambda+1)))*(2*(AR+2)*(t/
Cr).^3)); % Fin Flutter Speed

% The follwing code is written simply to output the answers on the
script % publication

fprintf('The flutter speed of the fin is %.4f ft/s. \n\n', Vf)

The flutter speed of the fin is 1446.2738 ft/s.
```

Stability Margin Calculations

```

L_N = 20;
S = 9;
X_R = 6.773;
C_T = 3;
C_R = 11;
R = 3.077;
N = 4;
X_B = 83.5;
X_CG = 58.575;
C_N = 2; d =
6.154;

X_N = 0.466*L_N;

theta = 37; L_F = sqrt(S^2 + ((1/2)*C_T - (1/2)*C_R +
(S/tan(theta)))));

% C_F = (1 + (R/(S+R))) * ((4*N*(2/(2*R))^2) / (1 + sqrt(1+((2*L_F)/C_R
+C_T)^2)));

a = 1 + ((R)/(S+R)); b =
4*N*((S/d)^2); c =
((2*L_F)/(C_R + C_T))^2; g =
1+sqrt(1+c); C_F = a*(b/g);

X_F = X_B + (X_R/3)*((C_R + 2*C_T)/(C_R + C_T)) + (1/6)*(C_R + C_T -
(C_R*C_T/(C_R + C_T))); X_CP =
(C_N*X_N + C_F*X_F)/(C_N + C_F);

S_M = (X_CP - X_CG)/d;

```

Published with MATLAB® R2021a

Appendix D. Apogee Calculation MATLAB Code

```
clc
clear all
```

Finding Apogee of Zenith Rocket with air resistance and changing mass

```
burntime = 4.4; %burntime in seconds
totimp = 3646.2; %Total impulse in Newton seconds
m_takeoff = 17.368; %Mass of rocket at takeoff in kg
m_prop = 2.095; %Mass of propellant in kg

M = m_takeoff - 0.5*m_prop; %average weight of the rocket in kg
M2 = m_takeoff - m_prop; %weight of the vehicle after powered ascentg in kg

g = 9.81; %acceleration of gravity m/s^2
rho = 1.2; %density of the atmosphere kg/m^3
Cd = 0.5; %coefficient of drag
A = 0.0182; %cross sectional area of the rocket m^2

k = 0.5*rho*Cd*A;
T = totimp/burntime; %thrust forc

v_burnout = (sqrt((T - M*g) / k))*(1-exp(-(2*k*(sqrt((T - M*g) / k)) / M)*burntime)) / (1+exp(-(2*k*(sqrt((T - M*g) / k)) / M)*burntime)));
alt_burnout = (-M / (2*k))*log((T - M*g - k*v_burnout^2) / (T - M*g));

alt_coast = (+M2 / (2*k))*log((M2*g + k*v_burnout^2) / (M2*g));

totalalt = alt_burnout + alt_coast;

fprintf('The apogee of the rocket is %.2f ft \n', 3.28*totalalt)
```

The apogee of the rocket is 4431.75 ft

Published with MATLAB® R2022b

Appendix E. RAFCO Mission Preliminary Arduino Code

```
1. // This code is a rough draft for camera operation and control for the FAMU-FSU College of
   Engineering Student Launch "Zenith" Team.
2. // Image filtering is still in development.
3.
4. //=====
   =====
5. //==          ArduCam Camera Initialization          ==
6. //=====
   =====
7. #include "Arducam_Mega.h"
8. // #include "Platform.h"
9. #include <SD.h>
10. #include <ArduCAM.h> 11. #include "image_provider.h"
11.
12.
13. #define BUFFER_SIZE 0xff
14.
15. #if defined(ARDUINO) && !defined(ARDUINO_ARDUINO_NANO33BLE)
16. #define ARDUINO_EXCLUDE_CODE
17. #endif // defined(ARDUINO) && !defined(ARDUINO_ARDUINO_NANO33BLE) 18.
19. #ifndef ARDUINO_EXCLUDE_CODE
20.
21. // Required by Arducam library
22. #include <SPI.h>
23. #include <Wire.h>
24. #include <memorysaver.h>
25. // Arducam library
26. #include <ArduCAM.h>
27. // JPEGDecoder library 28. #include <JPEGDecoder.h>
28.
```

```
29.
30. // The size of our temporary buffer for holding
31. // JPEG data received from the Arducam module
32. #define MAX_JPEG_BYTES 4096
33. // The pin connected to the Arducam Chip Select
34. #define CS 7

35.

36. int8_t* image_send;
37. int index_test;

38.

39. // Camera library instance
40. ArduCAM myCAM(OV2640, CS);
41. // Temporary buffer for holding JPEG data from camera
42. uint8_t jpeg_buffer[MAX_JPEG_BYTES] = {0};
43. // Length of the JPEG data currently in the buffer 44. uint32_t jpeg_length = 0;
44.
46.

47. const int CS = 7;
48. const int SD_CS = 9;
49. uint8_t count = 0;
50. char name[10] = {0}; 51. uint8_t rtLength = 0;
51.
52.
53. File outFile;
54. uint8_t imageData = 0;
55. uint8_t imageDataNext = 0;
56. uint8_t headFlag = 0;
57. unsigned int i = 0;
58. uint8_t imageBuff[BUFFER_SIZE] = {0};
59.
60. Arducam_Mega myCAM( CS );

61.
```

```
62. uint8_t keyState = 0;
63. uint8_t isCaptureFlag = 0;
64.
65.
66. //=====
=====
67. //==          ArduCam Camera Initialization          ==
68. //=====
=====
69.
70.
71.
72.

73. //=====
=====
74. //==          Reciever Initialization          ==
75. //=====
=====

76. // Receives and displays data message formats for RF sensors
77.
78. // Input port for RF receiver data
    79. #define Pulse_In 2 // INTO 80.

81. // All times in microseconds
82. #define Min_Gap_Time 3000
83. #define Max_Gap_Time 16000
84. #define Min_Bit_Time 100
85. #define Max_Bit_Time 1500
86. #define Uncertainty 200 // Data bit pulse width uncertainty
87.
88. byte RF_Bit_Count = 0;
```

```
89. byte RF_Byte_Count = 0;
90. byte RF_Byte = 0;
91. char ASCII[] = "0123456789ABCDEF";
92. byte RF_Message[] = {0, 0, 0, 0, 0, 0, 0};
93. unsigned long Start_Time = 0;
94. int Pulse_Width;
95. byte Started = false;
96. int Gap_Time;
97. int Bit_Time1; // elapsed time of first bit
98. int Bit_Time2; // elapsed time of bit that mismatches first bit
99. byte Invert_Flg; // invert message byte if first bit was actually "0" instead of "1"
100. byte Msg_Complete;
101. char command[];
102. //=====
=====

103. //==          Reciever Initialization          ==
104. //=====
=====

105.
106.
107.
108.
109. //=====
=====

110. //==          Motor Initialization          ==
111. //=====
=====

112. //Array of half steps for motor, 0.9 degrees per half step
113. int halfSteps[8] = {0b0001, 0b1001, 0b1000, 0b1010, 0b0010, 0b0110, 0b0100, 0b0101
};
114.
115. //global variables
116. int desPos = 0; //desired position
```

```

117. int curPos = 0; //current position
118. //=====
=====

119. //==          Motor Initialization          ==
120. //=====
=====

121.
122.
123.
124.

125. void setup() {
126. start_capture = 0;
127. char str[8];
128. File outFile;
129. char VH,VL;
130. int i,j = 0;
131. int h=3;
132.
133. //=====
=====

134. //==          Motor Setup          ==
135. //=====
=====

136. DDRA = 0xFF; //motor port on arduino
137. Serial.begin(9600);
138. //=====
=====

139. //==          Motor Setup          ==
140. //=====
===== 141.

142.
143.
144.
145.

```



```
146.
147. //=====
=====
148. //==          ArduCam Camera Setup          ==
149. //=====
=====

150. pinMode(SD_CS, OUTPUT);
151. myCAM.begin();
152. myCAM.takePicture(CAM_IMAGE_MODE_QVGA,CAM_IMAGE_PIX_FMT_JPG);
153.
154. while(!SD.begin(SD_CS))
155. {
156. Serial.println(F("SD Card Error!"));
157. arducamDelayMs(1000);
158.
159.   }
160.
161. Serial.println(F("SD Card detected."));
162. //=====
=====

163. //==          ArduCam Camera Setup          ==
164. //=====
=====

165.
166.
167.
168.
169.
170.
171. //=====
=====
```

```

172. //==                               Reciever Setup                               ==
173. //=====
=====

174. digitalWrite(Pulse_In, INPUT_PULLUP); //turn on pullup
175. Msg_Complete = false;
176.
177. // Enable INT0 external interrupt, trigger on both edges
178. bitSet(EICRA, ISCR0);
179. bitSet(EIMSK, INT0);
180. //=====
=====

181. //==                               Reciever Setup                               ==
182. //=====
=====

183.
184. }
185.
186.
187.
188.
189.
190. void loop() {
191.
192. //=====
=====

193. //==                               Reciever Loop                               ==
194. //=====
=====

195. byte i;
196.     byte temp;
197.

```

```
198.  if ((Msg_Complete == true) && (RF_Byte_Count > 2) && (RF_Byte_Count < 8)) {
199.  noInterrupts();
200.  Msg_Complete = false;
201.  Serial.write("Gap_Time: ");
202.  Serial.print(Gap_Time);
203.  Serial.write(" Bit_Time1: ");
204.  Serial.print(Bit_Time1);
205.  Serial.write(" Bit_Time2 ");
206.  Serial.print(Bit_Time2); 207. Serial.write(" Raw Bytes: ");
207.
208.
209.  i = 0;
210.  while (i < RF_Byte_Count) {
211.  if (Invert_Flg == true)
212.  RF_Message[i] = ~RF_Message[i]; 213.
214.  Serial.write(ASCII[RF_Message[i] >> 4]); // display upper nibble first
215.  Serial.write(ASCII[RF_Message[i] & 0x0F]);
216.  i++;
217.  }
218.
219.  Serial.println();
220.  RF_Byte_Count = 0;
221.  Started = false;
222.  PCIFR = 0; // clear all pin change interrupt flags
223.  interrupts();
224.  }
225.
226.
227.  // INT0 interrupt handler
228.  ISR (INT0_vect)
229.  {
230.  //when the pin goes LOW record the pulse start time
231.  if (digitalRead(Pulse_In) == LOW) {
232.  Start_Time = micros();
```

```
233. }
234. else // pin went high
235. if (Start_Time != 0) {
236. //calculate the pulse width
237. Pulse_Width = ((volatile int)micros() - Start_Time);
238. //clear the timer
239. Start_Time = 0;
240.
241. // Now check for valid message
242. if (Pulse_Width < Max_Gap_Time) { 243. if (Started == true) {
244.
245. if ((Pulse_Width > Min_Bit_Time) && (Pulse_Width <
    Max_Bit_Time)) {
246. // bit value in range
247.
248. if (Bit_Time1 == 0) {
249. // first bit
250. Bit_Time1 = Pulse_Width;
251. }
252.
253. if ((Pulse_Width > (Bit_Time1 - Uncertainty)) && (Pulse_Width < (Bit_Time1 +
    Uncertainty))) {
254. // bit = 1
255. RF_Bit_Count--; // bits received MSB first
256. bitSet(RF_Message[RF_Byte_Count], RF_Bit_Count);
257. if (RF_Bit_Count == 0) {
258. RF_Byte_Count++;
259. RF_Bit_Count = 8;
260. }
261. }
262. else {
263. // bit = 0
264. RF_Bit_Count--; // bits received MSB first
265. bitClear(RF_Message[RF_Byte_Count], RF_Bit_Count);
```

```
266.  if (RF_Bit_Count == 0) {
267.  RF_Byte_Count++;
268.  RF_Bit_Count = 8;
269.  }
270.  if (Bit_Time2 == 0) {
271.  // Mismatch of first bit
272.  Bit_Time2 = Pulse_Width;
273.      if (Bit_Time1 > Bit_Time2)
274.  Invert_Flg = true;
275.  else
276.  Invert_Flg = false;
277.  }
278.  }
279.  }
280.
281.  else { // bad bit or end of message
282.  if (Pulse_Width > Min_Gap_Time) {
283.  Msg_Complete = true;
284.  }
285.  Started = false;
286.  }
287.  } // Started
288.
289.  else if (Pulse_Width > Min_Gap_Time) {
290.  // start of the message
291.  Started = true;
292.  RF_Byte_Count = 0;
293.  RF_Bit_Count = 8;
294.  Gap_Time = Pulse_Width; // save for display
295.  Bit_Time1 = 0;
296.  Bit_Time2 = 0;
297.  }
298.  }
299.  else { // invalid message
```

```
300. Started = false;
301. }
302. }
303. //=====
=====

304. //==          Reciever Loop          ==
305. //=====
=====

306.
307.

308. //=====
=====

309. //==          Decoder Loop          ==
310. //=====
=====

311. //1 A1-Turn camera 60° to the right
312. //2 B2-Turn camera 60° to the left
313. //3 C3-Take picture
314. //4 D4-Change camera mode from color to grayscale
315. //5 E5-Change camera mode back from grayscale to color
316. //6 F6-Rotate image 180° (upside down).
317. //7 G7-Special effects filter (Apply any filter or image distortion you want and state
      what filter or distortion was used).
```

```
318. //8 H8-Remove all filters.
319.
320. // Parse the JPEG headers. The image will be decoded as a sequence of Minimum
321. // Coded Units (MCUs), which are 16x8 blocks of pixels.
322. JpegDec.decodeArray(jpeg_buffer, jpeg_length);
323.
324. // Crop the image by keeping a certain number of MCUs in each dimension
325. const int keep_x_mcus = image_width / JpegDec.MCUWidth;
326.     const int keep_y_mcus = image_height / JpegDec.MCUHeight;
327.
328. // Calculate how many MCUs we will throw away on the x axis
329. const int skip_x_mcus = JpegDec.MCUSPerRow - keep_x_mcus;
330. // Roughly center the crop by skipping half the throwaway MCUs at the
331. // beginning of each row
332. const int skip_start_x_mcus = skip_x_mcus / 2;
333. // Index where we will start throwing away MCUs after the data
334. const int skip_end_x_mcu_index = skip_start_x_mcus + keep_x_mcus;
335. // Same approach for the columns
336. const int skip_y_mcus = JpegDec.MCUSPerCol - keep_y_mcus;
337. const int skip_start_y_mcus = skip_y_mcus / 2;
338. const int skip_end_y_mcu_index = skip_start_y_mcus + keep_y_mcus;
339.
340. int error_reporter;
341. int image_width;
342. int image_height;
343. int8_t image_data;
344.
345. switch (command)
346.
347. //A1-Turn camera 60° to the right -----
348. case 1:
349. desPos = curPos + 67; //sets desired pos to 60.3 degrees to right
```

```
350. break;
351.
352. //B2-Turn camera 60° to the left -----
353. case 2:
354. desPos = curPos - 67; //sets desired pos to 60.3 degrees to left
355. break;
356.
357. //C3-Take picture -----
358. case 3:
359. imageData = imageDataNext; 360. imageDataNext = myCAM.readByte(); 361.
362. if (headFlag == 1)
363. {
364. imageBuff[i++]=imageDataNext;
365.
366. if (i >= BUFFER_SIZE)
367. {
368. outFile.write(imageBuff, i);
369. i = 0;
370. }
371. }
372.
373. if (imageData == 0xff && imageDataNext ==0xd8)
374. {
375. headFlag = 1;
376. sprintf(name,"%d.jpg",count);
377. count++;
378.
379.         outFile = SD.open(name,FILE_WRITE|FILE_READ);
380.
381. if (! outFile)
382. {
383. Serial.println(F("File open failed"));
```



```
384. while (1);
385. }
386. imageBuff[i++]=imageData;
387. imageBuff[i++]=imageDataNext;
388. }
389.
390. if (imageData == 0xff && imageDataNext ==0xd9)
391. {
392. headFlag = 0;
393. outFile.write(imageBuff, i);
394. i = 0;
395. outFile.close();
396. Serial.println(F("Image save succeed"));
397. break;
398. }
399. break;
400.
401. //D4-Change camera mode from color to grayscale -----
402. case 4:
403. TF_LITE_REPORT_ERROR(error_reporter, 404. "Decoding JPEG and converting to
    greyscale");
405.
406.
407. // Pointer to the current pixel
408. uint16_t* pImg;
409. // Color of the current pixel
410. uint16_t color;
411.
412. // Loop over the MCUs
413. while (JpegDec.read()) {
414. // Skip over the initial set of rows
415. if (JpegDec.MCUy < skip_start_y_mcus) {
416. continue;
417. }
```

```
418. // Skip if we're on a column that we don't want
419. if (JpegDec.MCUx < skip_start_x_mcus ||
420.     JpegDec.MCUx >= skip_end_x_mcu_index) {
421.     continue;
422. }
423. // Skip if we've got all the rows we want
424. if (JpegDec.MCUy >= skip_end_y_mcu_index) {
425.     continue;
426. }
427. // Pointer to the current pixel
428. plmg = JpegDec.plmage;
429.
430. // The x and y indexes of the current MCU, ignoring the MCUs we skip
431. int relative_mcu_x = JpegDec.MCUx - skip_start_x_mcus;
432. int relative_mcu_y = JpegDec.MCUy - skip_start_y_mcus;
433.
434. // The coordinates of the top left of this MCU when applied to the output
435. // image
436. int x_origin = relative_mcu_x * JpegDec.MCUWidth;
437. int y_origin = relative_mcu_y * JpegDec.MCUHeight;
438.
439. // Loop through the MCU's rows and columns
440. for (int mcu_row = 0; mcu_row < JpegDec.MCUHeight; mcu_row++) {
441.     // The y coordinate of this pixel in the output index
442.     int current_y = y_origin + mcu_row;
443.     for (int mcu_col = 0; mcu_col < JpegDec.MCUWidth; mcu_col++) {
444.         // Read the color of the pixel as 16-bit integer
445.         color = *plmg++;
446.         // Extract the color values (5 red bits, 6 green, 5 blue)
447.         uint8_t r, g, b;
448.         r = ((color & 0xF800) >> 11) * 8;
449.         g = ((color & 0x07E0) >> 5) * 4;
450.         b = ((color & 0x001F) >> 0) * 8;
451.         // Convert to grayscale by calculating luminance
```

```
452.
453. float gray_value = (0.2126 * r) + (0.7152 * g) + (0.0722 * b);
454.
455. // Convert to signed 8-bit integer by subtracting 128.
456. gray_value -= 128;
457.
458. // The x coordinate of this pixel in the output image
459. int current_x = x_origin + mcu_col;
460. // The index of this pixel in our flat output buffer
461. int index = (current_y * image_width) + current_x;
462.     image_data[index] = static_cast<int8_t>(gray_value);
463.
464. /* Additional part needed for BLE image transfer */
465. index_test = index;
466. image_send[index] = static_cast<int8_t>(gray_value);
467. }
468. }
469. }
470. TF_LITE_REPORT_ERROR(error_reporter, "Image decoded and processed");
471. break;
472.
473. //E5-Change camera mode back from grayscale to color -----
474. case 5:
475. //Cam control
476. break;
477.
478. //F6-Rotate image 180° (upside down). -----
479. case 6:
480. h=3;
481. while(h!=0)
482. {
483. gpio_trig = myCAM.read_reg(ARDUCHIP_PIN); //Leggi il trigger da GPIO0~5 484.
485. if(gpio_trig & 0x01)
```

```
486.  {
487.  h=h-1;
488.  }
489.  else h=3;
490.  if(h==0) start_capture = 1;
491.  }
492.
493.  if(start_capture)
494.  {
495.  //Flush the FIFO
496.  myCAM.flush_fifo();
497.  //Start capture
498.  myCAM.start_capture();
499.  }
500.
501.  //Polling the capture done flag
502.  if(myCAM.read_reg(ARDUCHIP_TRIG) & CAP_DONE_MASK)
503.  {
504.
505.  k = k + 1;
506.  itoa(k, str, 10); strcat(str, ".bmp");
507.
508.
509.  outFile = SD.open(str, FILE_WRITE);
510.  if (! outFile)
511.  return;
512.
513.  for( i = 0; i < 54; i++)
514.  {
515.  char ch = pgm_read_byte(&bmp_header[i]);
516.  outFile.write((uint8_t*)&ch,1);
517.  }
518.
```

```
519. //Abilita FIFO
520. myCAM.enable_fifo();
521. //Read the first dummy byte from FIFO
522. temp = myCAM.read_fifo();
523. //Read 320x240x2 byte from FIFO
524. for(i = 0; i < 240; i++)
525. for(j = 0; j < 320; j++)
526. {
527. VH = myCAM.read_fifo();
528. VL = myCAM.read_fifo();
529. //RGB565 to RGB555 Conversion
530. VL = (VH << 7) | ((VL & 0xC0) >> 1) | (VL & 0x1f);
531. VH = VH >> 1;
532. //Write image data to file
533. outFile.write(VL);
534. outFile.write(VH);
535. }
536. //Disable FIFO when all the image data is saved to the file
537. myCAM.disable_fifo();
538. //Close the file
539. outFile.close();

541. //Clear the capture done flag
542. myCAM.clear_fifo_flag();
543. //Clear the start capture flag
544. start_capture = 0;
545. }
546. break;
547.

548. //G7-Special effects filter (Apply any filter or image distortion you want and state what
    filter or distortion was used).
549. case 7:
550. while (JpegDec.read()) {
551. // Skip over the initial set of rows
```

```
552.  if (JpegDec.MCUy < skip_start_y_mcus) {
553.  continue;
554.  }
555.  // Skip if we're on a column that we don't want
556.  if (JpegDec.MCUx < skip_start_x_mcus ||
557.  JpegDec.MCUx >= skip_end_x_mcu_index) {
558.  continue;
559.  }
560.  // Skip if we've got all the rows we want
561.  if (JpegDec.MCUy >= skip_end_y_mcu_index) {
562.  continue;
563.  }
564.  // Pointer to the current pixel
565.  plmg = JpegDec.plmage;
566.
567.  // The x and y indexes of the current MCU, ignoring the MCUs we skip
568.  int relative_mcu_x = JpegDec.MCUx - skip_start_x_mcus;
569.  int relative_mcu_y = JpegDec.MCUy - skip_start_y_mcus;
570.
571.  // The coordinates of the top left of this MCU when applied to the output
572.  // image
573.  int x_origin = relative_mcu_x * JpegDec.MCUWidth;
574.  int y_origin = relative_mcu_y * JpegDec.MCUHeight;
575.
576.  // Loop through the MCU's rows and columns
577.  for (int mcu_row = 0; mcu_row < JpegDec.MCUHeight; mcu_row++) {
578.  // The y coordinate of this pixel in the output index
579.  int current_y = y_origin + mcu_row;
580.  for (int mcu_col = 0; mcu_col < JpegDec.MCUWidth; mcu_col++) {
581.  // Read the color of the pixel as 16-bit integer
582.  color = *plmg++;
583.  // distort color values (5 red bits, 6 green, 5 blue)
584.  uint8_t r, g, b;
585.  r = ((color & 0xF800) >> 11) * 2;
```

```
586.  g = ((color & 0x07E0) >> 5) * 10;
587.  b = ((color & 0x001F) >> 0) * 2;
588.  // Convert to grayscale by calculating luminance
589.
590.  float gray_value = (0.2126 * r) + (0.7152 * g) + (0.0722 * b);
591.
592.  // Convert to signed 8-bit integer by subtracting 128.
593.  gray_value -= 128;
594.
595.  // The x coordinate of this pixel in the output image
596.  int current_x = x_origin + mcu_col;
597.  // The index of this pixel in our flat output buffer
598.  int index = (current_y * image_width) + current_x;
599.      image_data[index] = static_cast<int8_t>(gray_value);
600.
601.  /* Additional part needed for BLE image transfer */
602.  index_test = index;
603.  image_send[index] = static_cast<int8_t>(gray_value);
604.  }
605.  }
606.  }
607.  break;
608.
609.  //H8-Remove all filters. -----
610.  case 8:
611.    desPos = 0;
612.    myCAM.clear_fifo_flag();
613.    start_capture = 0;
614.    h=3;
615.
616.  break;
617.  //=====
=====
```

```
618.  //==                      Decoder Loop                      ==
619.  //=====
=====
620.
621.
622.
623.
624.  //=====
=====

625.  //==                      Motor Loop                      ==
626.  //=====
=====

627.  //runs until the motor is at the desired position
628.  while (curPos != desPos)
629.  {
630.
631.  //if current position is less than desired,
632.  if (curPos < desPos)
633.  {
634.  curPos++; //add 1 to curPos
635.  PORTA = halfSteps[curPos%24]; //sends to motor
636.
637.  delay(3);
638.  }
639.
640.  //if current position is more than desired,
641.  if (curPos > desPos)
642.  {
643.  curPos--; // subtract 1 from curPos
644.  PORTA = halfSteps[curPos%24]; //sends to motor
645.
646.  delay(3);
647.  }
```



```
648.  }
649.  //=====
=====

650.  //==          Motor Loop          ==
651.  //=====
=====

652.
653.
654.
655.
656.
657.
658.

659.

660.  //=====
=====

661.  //==          ArduCam Camera Loop          ==
662.  //=====
=====

663.  // This code takes a picture using the Arducam every 5 seconds and saves it to an SD
      card, independently of commands.
664.  myCAM.takePicture(CAM_IMAGE_MODE_QVGA,CAM_IMAGE_PIX_FMT_JPG);
665.  while (myCAM.getReceivedLength())
666.  {
667.  imageData = imageDataNext; 668.  imageDataNext = myCAM.readByte();
668.
669.
670.  if (headFlag == 1)
671.  {
672.  imageBuff[i++]=imageDataNext;
673.
674.  if (i >= BUFFER_SIZE)
675.  {
```

```
676.  outFile.write(imageBuff, i);
677.
678.  i = 0;
679.  }
680.  }
681.
682.  if (imageData == 0xff && imageDataNext ==0xd8)
683.  {
684.
685.  headFlag = 1;
686.  sprintf(name,"%d.jpg",count);
687.  count++;
688.
689.          outFile = SD.open(name,FILE_WRITE|FILE_READ);
690.
691.  if (! outFile)
692.  {
693.  Serial.println(F("File open failed"));
694.  while (1);
695.  }
696.  imageBuff[i++]=imageData;
697.  imageBuff[i++]=imageDataNext;
698.  }
699.
700.  if (imageData == 0xff && imageDataNext ==0xd9)
701.  {
702.  headFlag = 0;
703.  outFile.write(imageBuff, i);
704.  i = 0;
705.
706.  outFile.close();
707.  Serial.println(F("Image save succeed"));
```

```
708.  
709.  break;  
710.  }  
711.  }  
712.  
713.  arducamDelayMs(5000);  
714.  //=====  
=====  
715.  //==          ArduCam Camera Loop          ==  
716.  //=====  
=====  
717.  
718.  }  
719.  720.  
721.  //=====  
=====  
722.  //==          END OF PROGRAM          ==  
723.  //=====  
=====
```